การพัฒนาเกราะกันกระสุนจากเส้นใยเคฟลาร์และพอลิเบนซอกซาซีนคอมพอสิทที่เติมฟูมซิลิกา

นางสาว กนกวรรณ พันธ์สน

วิทยานิพนธ์นี้เป็นส่วนหนึ่งของการศึกษาตามหลักสูตรปริญญาวิศวกรรมศาสตรมหาบัณฑิต
สาขาวิชาวิศวกรรมเคมี   ภาควิชาวิศวกรรมเคมี
คณะวิศวกรรมศาสตร์   จุฬาลงกรณ์มหาวิทยาลัย
ปีการศึกษา 2550

DEVELOPMENT OF BALLISTIC ARMOR BASED ON KEVLAR™ FIBER AND FUMED

SILICA-FILLED POLYBENZOXAZINE COMPOSITES

Miss Kanokwan Punson

A Thesis Submitted in Partial Fulfillment of the Requirements

for the Degree of Master of Engineering Program in Chemical Engineering

Department of Chemical Engineering

Faculty of Engineering

Chulalongkorn University

Academic Year 2007

Thesis Title   DEVELOPMENT OF BALLISTIC ARMOR BASED ON KEVLAR™ FIBER
                    AND FUMED SILICA-FILLED POLYBENZOXAZINE COMPOSITES

By   Miss. Kanokwan Punson
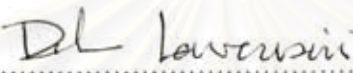
Field of Study   Chemical Engineering

Thesis Advisor   Assistant Professor Sarawut Rimdusit, Ph.D.

Thesis Co-advisor   Anongnat Somwangthanaroj, Ph.D.

Accepted by the Faculty of Engineering, Chulalongkorn University in Partial
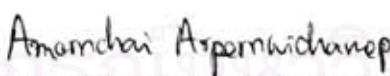Fulfillment of the Requirements for the Master's Degree

.... Dean of the Faculty of Engineering

(Professor Direk Lavansiri, Ph.D.)

THESIS COMMITTEE

.... Chairman

(Associate Professor Siriporn Damrongsakkul, Ph.D.)

.... Thesis Advisor

(Assistant Professor Sarawut Rimdusit, Ph.D.)

.... Thesis Co-advisor

(Anongnat Somwangthanaroj, Ph.D)

.... Member

(Amornchai Arpornwichanop, D.Eng.)

.... Member

(Somboon Sahasithiwat, Ph.D.)

iv

กนกวรรณ พันธ์สน : การพัฒนาเกราะกันกระสุนจากเส้นใยเคฟลาร์และพอลิเบนซอกซาซีนคอมพอสิทที่เติมฟูมซิลิกา (DEVELOPMENT OF BALLISTIC ARMOR BASED ON KEVLAR[TM] FIBER AND FUMED SILICA-FILLED POLYBENZOXAZINE COMPOSITES) อ. ที่ปรึกษา : ผศ. ดร. ศราวุธ ริมดุสิต, อ. ที่ปรึกษาร่วม : อ. ดร. อนงค์นาฏ สมหวังธนโรจน์, 111 หน้า.

งานวิจัยนี้มีจุดประสงค์เพื่อทำการพัฒนาเกราะกันกระสุนจากเส้นใยเคฟลาร์โดยมีพอลิเบนซอกซาซีน (PBZ) ที่มีการเติมฟูมซิลิกา (nano-SiO$_2$) เป็นเมตริกเรซินและเสริมแรงด้วยเส้นใยเคฟลาร์ จากงานวิจัยที่ผ่านมาพบว่าพอลิเบนซอกซาซีนเป็นพอลิเมอร์ที่มีความสามารถในการดัดแปลงให้เหมาะสมกับการใช้งานได้หลากหลาย โดยพอลิเบนซอกซาซีนเป็นพอลิเมอร์ที่มีคุณสมบัติทางกลและทางความร้อนที่โดดเด่น อีกทั้งยังมีความหนืดก่อนการขึ้นรูปต่ำ นอกจากนี้คุณสมบัติเด่นอีกประการของพอลิเบนซอกซาซีนคือสามารถเข้ากันได้ดีกับสารตัวเติมชนิดต่างๆ ดังนั้นในงานวิจัยนี้จึงเลือกใช้ฟูมซิลิกาในการปรับปรุงสภาพแข็งเกร็งของพอลิเบนซอกซาซีนซึ่งเป็นค่าที่สัมพันธ์กับความสามารถในการกระจายแรงซึ่งแสดงด้วยค่าความเร็วเสียง โดยคุณสมบัติดังกล่าวเป็นคุณสมบัติที่สำคัญของกลไกการด้านทานแรงปะทะของกระสุน โดยสภาวะที่เหมาะสมที่ใช้ในการขึ้นรูปพอลิเบนซอกซาซีนที่เติมฟูมซิลิกา และวัสดุคอมพอสิทในงานวิจัยนี้ คือ การบ่มด้วยเครื่องอัดรีดแบบอัตโนมัติที่ความดัน 25 MPa ที่อุณหภูมิ 160 องศาเซลเซียสเป็นเวลา 2 ชั่วโมง และ 180 องศาเซลเซียสเป็นเวลา 2 ชั่วโมง จากนั้นบ่มให้สมบูรณ์ภายในตู้อบที่อุณหภูมิ 200 องศาเซลเซียสเป็นเวลา 4 ชั่วโมง จากผลการศึกษาพบว่าที่อัตราส่วน 7wt% nano-SiO$_2$/PBZ เป็นอัตราส่วนที่เหมาะสมที่ใช้เป็นพอลิเมอร์เมตริกในวัสดุคอมพอสิทที่มีผลต่อความสามารถในการป้องกันกระสุนได้สูงสุด นอกจากนี้พบว่าค่ามอดูลัสของการดัดโค้งของพอลิเบนซอกซาซีนที่เติมฟูมซิลิกาในปริมาณ 7 เปอร์เซ็นต์โดยน้ำหนักจะมีค่าเพิ่มสูงขึ้นจาก 5.98 GPa ในพอลิเบนซอกซาซีนเป็น 7.52 GPa อีกทั้งค่าของคุณสมบัติทางความร้อนของพอลิเบนซอกซาซีนที่เติมฟูมซิลิกาจะเพิ่มขึ้นเมื่อปริมาณของฟูมซิลิกาเพิ่มขึ้นซึ่งในงานวิจัยนี้อัตราส่วนของเส้นใยเสริมแรงและเมตริกเรซินที่เหมาะสม คือ 75:25 ทั้งนี้จากการศึกษาพบว่าสำหรับวัสดุคอมพอสิตที่ใช้ 7wt% nano-SiO$_2$/PBZ เป็นเมตริกเรซินในวัสดุคอมพอสิตสามารถป้องกันแรงปะทะของกระสุนได้ในระดับ IIIA และจากการศึกษาผลกระทบจากจำนวนชั้น และ การจัดเรียงตัวที่เหมาะสมของวัสดุคอมพอสิตเพื่อให้สามารถป้องกันแรงปะทะของกระสุนได้ในระดับ IIIA ต้องใช้วัสดุคอมพอสิตอย่างน้อย 30 ชั้น และ วัสดุคอมพอสิตในส่วนแรกที่ปะทะกับหัวกระสุนจะต้องมีความหนาอย่างน้อย 15 ชั้น เพื่อให้วัสดุคอมพอสิตมีความสามารถในการทรงรูปมากเพียงพอที่จะทำให้หัวกระสุนเสียรูปได้ ซึ่งถือเป็นกลไกหนึ่งในการดูดซับพลังงานจากหัวกระสุนของวัสดุคอมพอสิต

ภาควิชา...วิศวกรรมเคมี......................... ลายมือชื่อนิสิต.............................
สาขาวิชา....วิศวกรรมเคมี....................... ลายมือชื่ออาจารย์ที่ปรึกษา......................
ปีการศึกษา....2550.......................... ลายมือชื่ออาจารย์ที่ปรึกษาร่วม...................

4770565521 : MAJOR CHEMICAL ENGINEERING

KEY WORD: POLYBENZOXAZINE COMPOSITES/BALLISTIC ARMOR/FUMED SILICA/KEVLAR[TM]-REINFORCED COMPOSITE

KANOKWAN PUNSON: DEVELOPMENT OF BALLISTIC ARMOR BASED ON KEVLAR[TM] FIBER AND FUMED SILICA-FILLED POLYBENZOXAZINE COMPOSITES. THESIS ADVISOR: ASST. PROF. SARAWUT RIMDUSIT, Ph.D., THESIS COADVISOR: ANONGNAT SOMWANGTHANAROJ, Ph.D., 111 PP.

The aim of this study is to develop a ballistic armor produced from the matrix of polybenzoxazine (PBZ) modified with fumed silica (nano-SiO_2), and the reinforcing Kevlar[TM] fiber. From our previous research, polybenzoxazine has been reported to be a versatile polymer being tailor-made for many purposes. The outstanding properties of polybenzoxazine are its outstanding mechanical and thermal properties as well as its good processability. One of the unique properties of this polymer is its compatibility with many kinds of fillers. In this study, fumed silica was selected to mix with polybenzoxazine in order to modify its rigidity which is related to its sound propagation velocity. The property is important in ballistic impact resistant mechanism. The suitable condition for the preparation of the polybenzoxazine-fumed silica molding compounds and composites was investigated. The results revealed that the processing condition of the molding compounds to attain their fully cured stage was by heating at $160^\circ C$ for 2 hours, $180^\circ C$ for 2 hours (in the hydraulic hot-press machine, at 25 MPa), followed by post-curing at $200^\circ C$ for 4 hours (in an oven). The experimental results also revealed that the optimal nano-SiO_2 content in the polybenzoxazine was at 7wt% the Kevlar composite preparation. In addition, the polybenzoxazine matrix modified with 7wt% of the nano-SiO_2 was able to increase the flexural modulus from 5.98 GPa of the pure polybenzoxazine up to about 7.52 GPa in the composite. The thermal properties were found to increase with increasing the nano-SiO_2 contents. In the ballistic composite sample, the optimal weight ratio of fiber and modified polybenzoxazine matrix was approximately 75:25. The armor composite with 7wt% nano-SiO_2 at this composition ratio was able to render desirable ballistic performance up to NIJ standard of level IIIA. The thickness of the polybenzoxazine armor composite that can resist a ballistic impact of the NIJ standard at this level was 30 piles or higher. In addition, it was found that the first plate with the thickness of at least 15 piles was crucial to sufficiently destroy the projectiles of this high level.

Department......Chemical Engineering...   Student's signature....................................

Field of study....Chemical Engineering.....   Advisor's signature....................................

Academic year ......2007.....   Co-advisor's signature....................................

ACKNOWLEDGEMENTS

CONTENTS

LIST OF FIGURES

LIST OF TABLES

CHAPTER I

INTRODUCTION

1.1 General Introduction

In recent years, lightweight armors are increasingly necessary in the region that the terrorist problem is remained. These armors can be used as the protection of passenger in vehicles against handgun, or as a personal armor. (Nunes et al, 2004). Protective armors were traditionally made of metals in the old day. With the development of the thermoplastic polymers and synthetic fibers, hard armor systems have been developed that combine the use of metals, ceramics, fabrics and fiber-reinforced composites in recent years. Soft armors were prepared from woven fiber glass and nylon and used for ballistic protection.

The high strength fibers have been developed rapidly for armor structure. Fibers conventionally used include aramids (Kevlar or Twaron), polyethylene fiber (Spectra or Dyneema), nylon fiber, and glass fiber (Yang, 1993). The selection of fibers for application depends heavily on its mechanical property. Several factors must be considered i.e. sonic velocity and energy absorption of the specimens. Kevlar^{TM} aramid fibers are one of the best fibers used for protection human lives and vital equipment against ballistic threats. Kevlar^{TM} aramid fibers can be attributed to its excellent thermal properties, high crystallinity, high orientation fine structure, and high tensile properties. The high glass transition temperature and thermal stability of Kevlar^{TM} aramid fibers ensure the integrity of a ballistic structure at relatively high temperatures in a ballistic event. Hence, it renders the increase of dynamic modulus, which enhances the high rate of wave propagation and rapid response to longitudinal deformation. The high tenacity and moderate elongation of Kevlar^{TM} fibers provide high toughness and high loading to break for the transverse deformation.

The development of composite technology with fiber-reinforced composites had been known to improve the properties of the armor structure and the ballistic energy dissipation. The ballistic impact performance of composite laminates substantially depends on the mechanical characteristics of the reinforcement and the matrix and the physical characteristics of the target including the elastic modulus, tensile strength, fracture strain and laminate configuration (Yang, 1993). Absorption of kinetic energy of composite material composes of several mechanisms, including cone deformation on the back face, shear plugging of the projectile into the target, tensile failure of the primary yarns, elastic deformation of the secondary yarns, fiber/matrix de-bonding and inter-laminar delamination, and inertia effect due to impact (Naik and Shriraol, 2004, and Morye et al., 2000).

The armor system is the composite composed of two layers of different materials. One layer is quite rigid (high modulus), and another one is soft or tough (low modulus). The combination of these two layers is suitable to gain the mechanism to receive the ballistic impact and dissipation of energy. The first layer is arranged to receive an impact from a large projectile prior to the second layer and engages the projectile to slow its velocity. The second one is substantially coextensive with the first layer and dissipates the incoming energy of the impact to resist complete penetration of the second layer by the projectile, preferably by deforming and acting in response to the impact as shown in Figure 1.1 (David et al., 2001).
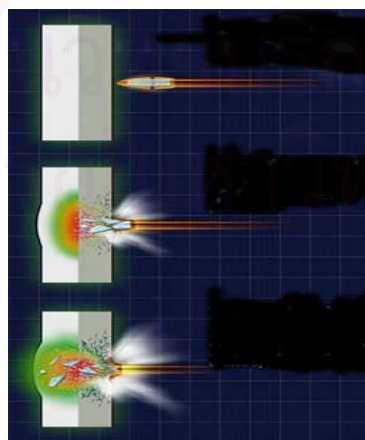
Figure 1.1: Mechanism of receiving and dissipating energy of ballistic armor.

In general, the selection of a resin have been used as matrices for ballistic armor depends on its required characteristics including cost, density, interfacial bonding, tensile, compressive and flexural properties, temperatures, compatibility of thermal expansion and processability. Resins are often selected on the basis of their modulus. Low modulus or soft resins generally offer relatively high breaking strain and good flexural properties. High modulus or rigid resins offer high compressive strength and brittleness (Morye et al., 2000). Benzoxazine resins provide a future class of preferred resins for composite the armor. Polybenzoxazine is a kind of polymer materials, which was developed for applications as a high performance polymer matrix. It can be synthesized from inexpensive raw material. A polymerization reaction of benzoxazine monomers is initiated by heat, without using a curing agent. As a consequence, there is no volatile by-product in the curing process, high thermal stability, easy processability, low water adsorption and near zero shrinkage after processing with excellent mechanical properties (Jang and Shin, 1995, and Ishida, 1996).

Inorganic nanoparticle filled polymer composite have been classified as materials with the potential to significantly improve properties over conventional mineral-filled micro- or macro- composites because the filler-matrix interface in these composites might constitute a much greater area and enhance the composites properties to a much greater extent at rather low filler concentration than another fillers (Wu et al., 2005). Filler-filled nanocomposites exhibit outstanding improvement on properties which include the increasing in modulus, strength, thermal stability, solvent resistance and the decreasing of gas permeability and flammability. In this work, fumed silica was used to improve matrix resin. Fumed silica is a useful reinforcement of thermoplastic and thermosetting polymer. Fumed silica is available as individual particles ranging from 10 - 20 nm and if dispersed well to the scale of 10 - 50 nm in matrix polymer, specific surface of fumed silica range from 50 to 400 m^2/g as shown in Figure 1.2. It has a potential to improve heat distortion temperature, decrease moisture uptake, increase stiffness and strength and increase flame resistance due to the nanometer size and high aspect ratio. It was able to improve thermal stability and thermo-mechanical properties for matrix resin that gives rise to receive the ballistic impact (Jana, 2001).
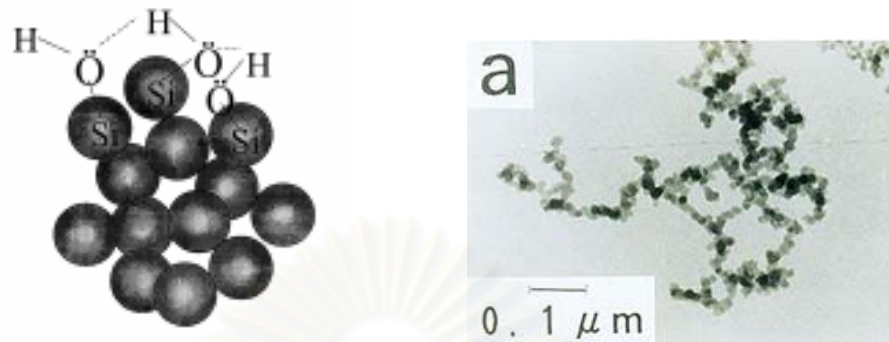
Figure 1.2: Scheme of aggregate formation between adjacent fumed silica particles (Jana, 2001).

The focus of this work is to determine the ballistic armor of fumed silica-filled polybenzoxazine matrix with Kevlar[TM] fibers and modifications on the formulation of the benzoxazine matrix material. This made it possible to fine tune and enhance the property of the ballistic armor.

1.2 Objectives

1. To develop a light weight ballistic armor based on Kevlar[TM] fiber-reinforced composites using unfilled and fumed silica-filled polybenzoxazine matrices for the protection of NIJ standard (level IIA or higher).
2. To evaluate the optimum of fumed silica loading and to investigate mechanical and thermal properties of fumed silica filled polybenzoxazine nanocomposite for use as ballistic armor composite matrices.

1.3 Scope of the study

1. Synthesis of benzoxazine resin by solventless technology.
2. Determination of the optimum composition of fumed silica filled benzoxazine with varied 0-10% by weight of fumed silica content.
3. Evaluation of the curing condition of the composites in item (2) by DSC.
4. Investigation of thermal properties, mechanical properties and morphology of nanocomposites in item (2).
5. Fabrication of the composite samples between the suitable matrices in item (2) and Kevlar^{TM} fiber (fumed silica loading 0-10% by weight) at 20-25 % by weight of resin contents.
6. Investigation of thermal properties, mechanical properties and some physical properties for the Kevlar^{TM} nanocomposites such as flexural modulus, flexural strength, degradation temperature.
7. Fire test based on NIJ standard (Level IIA or higher).

CHAPTER II

THEORY

2.1 Composites Materials

2.1.1. Aramid Fiber

Aramid fiber is the fundamental variety of organic high-strength high-modulus fibers used in soft armor. Kevlar^{TM} aramid fiber was introduced by the Du Pont Company in 1972. The word "aramid" is a generic term for a manufactured fiber in which the fiber-forming substance is a long chain synthetic polyamide in which at least 85% of the amide linkages are attached directly to two aromatic rings. This generic definition distinguishes aramids from the conventional polyamides such as nylon, which mostly contain aliphatic and cycloaliphatic units in the polymer main chain. By definition, therefore, the aramid family encompasses several other commercial fibers including Nomex, Teijinconex, Technora, and Twaron. Kevlar^{TM} is used as a reinforcing fiber for composites, thermoplastics, thermosets, tires, and mechanical rubber goods. Woven fabrics of Kevlar^{TM} aramid are used in protective apparel, parachute, ballistic body armor, and hard armor (Yang, 1993).

2.1.2 Manufacturing of Aramid Fiber

In 1970 Du pont scientist invented an ingenious dry-jet wet spinning process for spinning an anisotropic solution of aramid polymer to produce fibers. In this process, an anisotropic solution is extruded from spinneret holes through an air gap into a coagulation bath. The coagulated filaments are washed, neutralized and finally dried. It provided fibers almost twice as strong as the earlier fibers (Yang, 1993).

2.1.3 Processing of Kevlar[TM] Aramid fiber

Kevlar[TM] aramid fiber is based on poly (p-phenylene terephthalamide) (PPD-T), one of the para-oriented aromatic polyamides. The PPD-T synthesis involves the low temperature polycondensation of p-phenylene diamine (PPD) and terephthaloyl chloride (TCl) in a dialkyl amide solvent. The amide solvent includes hexamethylphosphoramide, N-methyl pyrrolidone and dimethyl acetamide.
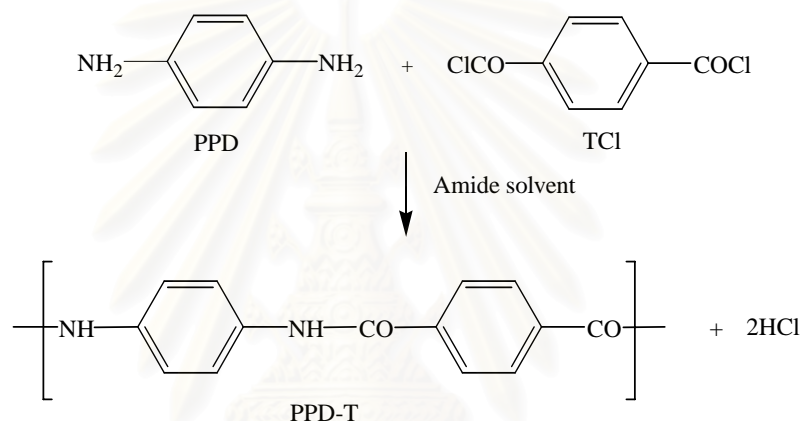
Figure 2.1: Preparation of Kevlar[TM] fiber (Yang, 1993).

2.1.4 Properties of Kevlar[TM] aramid yarns (Yang, 1993)

Kevlar[TM] fibers are widely used in composites, armor, aircraft cargo liners and marine applications. A variety of woven fabrics is also used in electrical wiring boards, coated fabrics and soft ballistic body armor. The use of Kevlar[TM] as tyre cord, Kevlar[TM] 29 as underwater cable, and Kevlar[TM] 49 as reinforcing fiber in aerospace composites emphasizes the fiber strength and stiffness, perhaps more than its toughness. Both Kevlar[TM] 49 and Kevlar[TM] 29 are used in ballistic protection for their toughness and ability to absorb energy (Machalaba, 2001).

Table 2.1 Properties of various grades of Kevlar[TM] fiber

Yarn properties	Kevlar and Kevlar 29	Kevlar 49	Kevlar 68	Kevlar 119	Kevlar 129	Kevlar 149
Tensile strength						
gpd	23.0	23.0	23.0	24.0	26.5	18.0
Kpsi	420	420	420	440	485	340
Initial modulus						
gpd	550	950	780	430	750	1100
Mpsi	10.3	17.4	14.4	8.0	14.0	21.0
% Elongation	3.6	2.8	3.0	4.4	3.3	1.5
Density (g/cm^3)	1.44	1.45	1.44	1.44	1.45	1.47
Moisture regain, % (25 $^\circ$C, 65% RH)	6	4.3	4.3	-	-	1.5

Note: Yarn properties determined on 10 in twisted yarns (ASTM D-885)

In general, Kevlar[TM] aramid fiber has a high breaking tenacity which is several times higher than that of steel wire, nylon and polyester yarns. It has much higher tensile modulus than steel wire, fiberglass, nylon and polyester fibers. The fiber has a low elongation at break, which is comparable to that of steel. Moreover, it has a low density, which make most Kevlar[TM] reinforced structures of a lighter weight for a given strength and stiffness (Yang, 1993).

The introduction of Kevlar[TM] aramid fiber in armor applications is extended because its superior mechanical properties which attribute to highly crystalline and highly oriented structure of the Kevlar. The high tensile strength and sufficient elongation of Kevlar fiber provide them high toughness and high work to break for the transverse deformation. Moreover, its high elastic modulus provides fast and effective spreading out kinetic energy from a projectile (Yang, 1993).

Table 2.2 Chemical and physical properties of Kevlar^{TM} aramid fiber (Yang, 1993)

Properties	Value
High melt temperature	530°C
Zero strength temperature	640°C
High glass transition temperature	375°C
Low density vs. glass (2.55) and steel (7.86)	1.44
Thermal stability	Relatively high
Combustibility	Low
Conductivity	Nonconductive
Specific strength and modulus	High

Besides the mechanical strength of fibers, sonic velocity and specific energy absorption are very important parameters affecting in kinetic energy lost from projectile at the impact point. The specific energy absorption evaluates capability to absorb energy locally and the sonic velocity evaluates capability to spread out energy. The fiber with high wave velocity will have greater volume of the fiber interacting with the projectile (Jacqueline, 1991). From these two parameters, it infers that the fiber which is appropriate in armor application should have high sonic velocity and specific energy absorption.

The performance of major ballistic fibers is shown in Figure 2.2. In this figure, the sonic velocities of the fibers are plotted against their specific energy absorptions (Jacob, 2001).
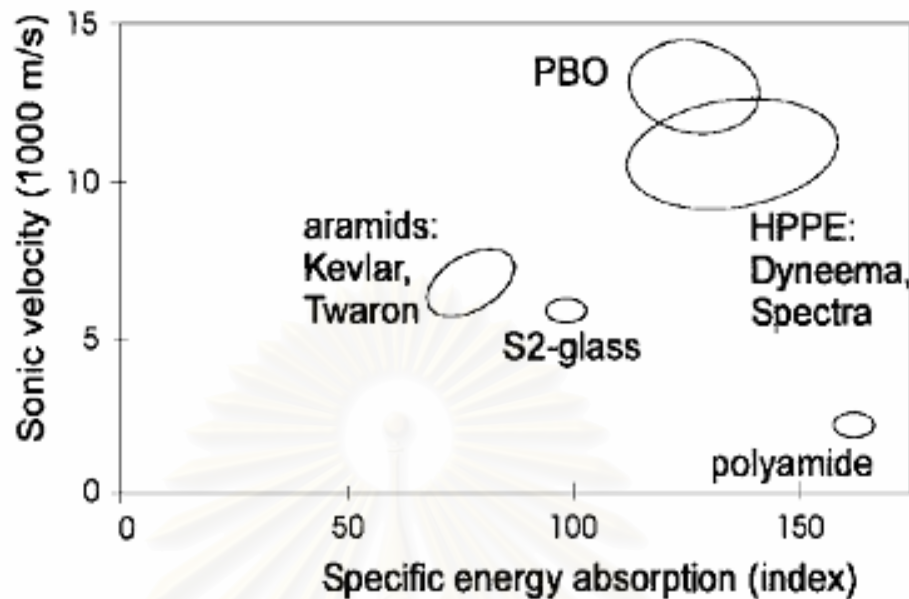
Figure 2.2 Sonic velocity and specific energy absorption of various
fibers (Jacob, 2001)

2.2 Matrix Resin

The matrix resin can be classified into two main categories based on their response to temperature: thermoplastics and thermosets. Thermosetting polymers differ from thermoplastics in that they become chemically crosslink during final molding and curing. For most practical purposes they can no longer be melted, reshaped or dissolved. A distinctive characteristic of a thermosetting polymer is that one giant macromolecule consisting of covalently bonded repeating units is formed during the polymerization process.

Polybenzoxazine is a newly developed class of thermosetting resin with interesting properties that are based on the ring opening polymerization of benzoxazine precursors. As a novel class of phenolic resin, it has been developed and studied to overcome several short comings of conventional Novolac and resole-type phenolic resin. Polybenzoxazine resins are expected to replace traditional phenolic, polyesters, vinyl esters, epoxies, BMI, cyanate esters and polyimides in many respects (Takeichi, 2002). The mechanical and physical properties can be tailored to various needs. The material can be synthesized using the patented solventless technology to

yield a relatively clean precursor without the need of solvent elimination or monomer purification (Ishida, U.S. Patent 5,543,516 1996).

Polybenzoxazine can be synthesized from inexpensive raw materials and can be cured without the use of strong acid or base catalyst. The crosslinking reaction of the resin is through thermally activated ring-opening reaction; therefore, it does not release by-products during the polymerization. The material has excellent properties commonly found in traditional phenolic resins such as high thermal stability, flame retardant, dimensional stability, low viscosity, near-zero shrinkage upon polymerization, low water absorption, excellent electrical properties, high mechanical integrity, glass transition temperatures much higher than cure temperature, fast mechanical property build-up as a function of degree of polymerization, high modulus and high char-yield. Furthermore, the ability of benzoxazine resin to be alloyed with other polymers renders the resin with even broader range of applications (Ishida, 1996, and Ishida, U.S. Patent 5,543,516 1996)

Benzoxazine resin based on bisphenol-A and aniline is synthesized according to the following reaction scheme as shown in Figure 2.3 (Ning, 2000).
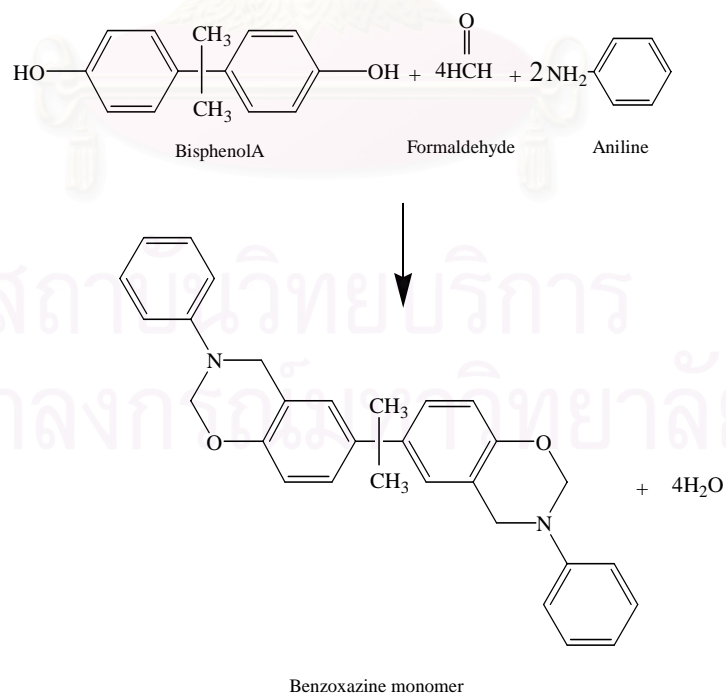
Figure 2.3: Synthesis of benzoxazine monomer

2.3 Classification of Nano-filler

In recent years, inorganic nanoparticles filled polymer composites have received increasing research interests of materials scientists because the filler-matrix interface in these composites might constitute a much greater area and hence influence the composites properties to a much greater extent at rather low filler concentration as compared to conventional micro-particulate composites. The property of nanoparticle filled polymer composites enhancements include increased stiffness and strength, decreased moisture uptake, decreased permeability of solvents and increased flame resistance due to the nanometer size and high aspect-ratio characteristics.

Recently, nanocomposites, which are nanometer-size particle filled polymer composites, have been developed to overcome limitations of traditional micrometer-scale polymer composites. Nanofillers are the filler that are less than 100 nm in at least one dimension. The small size of nanofillers leads to unique properties of the particles. For example, when polymer/clay nanocomposites and fiber reinforced composites are compared at the low filler content, nanocomposites exhibit better properties than conventional fiber composites. It was observed that nanocomposites exhibit higher Young's modulus than fiber composites. In addition, the small size of the nano fillers leads to exceptionally large interfacial area in the composites. As seen in figure 2.4, nanoscale fillers can be divided into three categories according to their shapes and sizes, i.e., disk, fiber and particle or sphere. Three dimensional (3D) nanofillers are relatively equi-axed particles less than 100 nm in their largest dimension. Fiber or tube filler have a diameter less than 100 nm and an aspect ratio of at least 100. The other shape is disk (plates, flakes), which includes mica, glass flakes, aluminum flakes and aluminum diboride, which are layered materials typically with a thickness in the order of 1 nm (Peter, 1998).
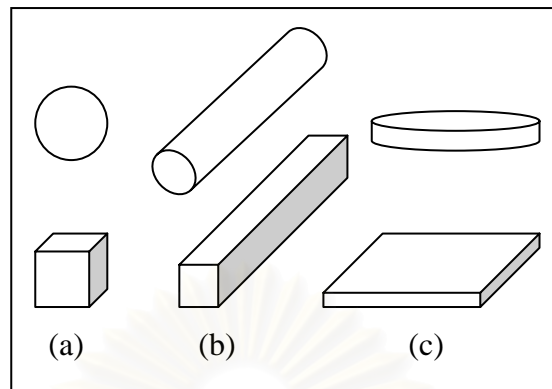
Figure 2.4 Shapes of reinforcing fillers (a) Particle, (b) Short fiber, (c) Disk

2.3.1 Disk Class

Fillers and reinforcements primarily in disk class include mica, glass flakes aluminum flakes and aluminum diboride. Flake composites also have strong resistance to puncturing by sharpy objects. Flake-filled polymer has unusually high moduli compared to most other particulate-filled composite. However, the most flake composite are brittle with low impact strength (Kojima, 1993)

2.3.2 Fiber Class

Fiber-reinforced materials, which consist of fibers in a matrix, contain reinforcements having lengths much greater than their cross-sectional dimensions. Such a composite is considered to be a discontinuous fiber or short fiber composite if its properties vary with fiber length. On the other hand, when the length of the fiber is such that any further increase in length does not, for example, further increase the elastic modulus of the composite, the composite is considered to be continuous fiber reinforced. Most continuous fiber (or continuous filament) composites, in fact, contain fibers that are comparable in length to the overall dimensions of the composite part. Fillers and reinforcements in the fiber class include glass fibers, carbon graphite fibers, metal fibers, asbestos, whiskers and polymeric fibers.

2.3.3 Particle Class

Particulate composites are composed of particles in a matrix. Reinforcement is considered to be a "particle" if all of its dimensions are roughly equal. Thus, particle-reinforced composites include those reinforced by spheres, rods, flaked, and many other shapes of roughly equal axes. There are also materials, usually polymers, which contain particles that extend rather than reinforce the material. These are generally referred as "filled" systems. Because filler particles are included for the purpose of cost reduction rather than reinforcement, these composites are not generally considered to be particulate composites. Nonetheless, in some cases the filler will also reinforce the matrix material. The same is possibly true for particles added for nonstructural purposes such as fire resistance, control of shrinkage, and enhanced thermal conductivity.

Nanosilica particles can be obtained from nanosilica powder, fumed silica and colloidal silica. They have been widely introduced into polymer to improve the heat resistance, mechanical and electrical properties of the polymer materials.

2.4 Synthesis of Fumed Silica

Fumed silica was first developed in 1941 by Dr. Harry Klopfer, as he was trying to develop a white reinforcing filler comparable to channel blacks in rubber properties. Fumed silica is widely used in industry as an active filler for reinforcement of elastomers, as a rheological additive in fluids and as a free flow agent in powders. Fumed silica is prepared by the hydrolysis of silicon tetrachloride vapor in flame of hydrogen at high fame temperatures of about 1200 to 1600 °C or higher (as shown in Figure 2.5). Figure 2.6 presents highly viscous droplets of amorphous silicon dioxide that are formed, so-called primary particles, which collide and are fused together to build up stable aggregates. After leaving the flame and cooling, these aggregates stick together to form loosely bonded agglomerates by surface interactions. Typical BET specific surface areas of fumed silica range from 50 to 400 m^2/g. Some specific properties of fumed silica are shown in Table 2.3 (Harry, 1987, and Barthel et al., 1999).

Fumed silica has been attracting attention as a reinforcing material for polymer because it exhibits a high transparency to light, outstanding electrical properties, and chemical resistance. Fumed silica has been used as a thixotropy or thickening agent in plastic, adhesives and paints. On these importance properties, fumed silica is widely used in many industries.

$$2H_2 \quad + \quad O_2 \quad \longrightarrow \quad 2H_2O$$
$$SiCl_4 \quad + \quad 2H_2O \longrightarrow \quad SiO_2 \quad + \quad 4HCl$$
$$2H_2 + O_2 + SiCl_4 \xrightarrow{\;>1000°C\;} SiO_2 \quad + \quad 4HCl$$
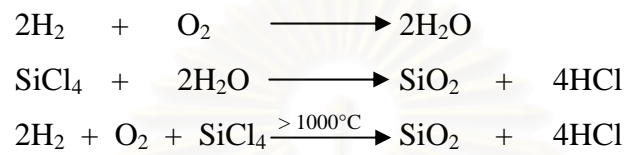
Figure 2.5 Synthesis method of fumed silica (Harry, 1987).

(a)   (b)
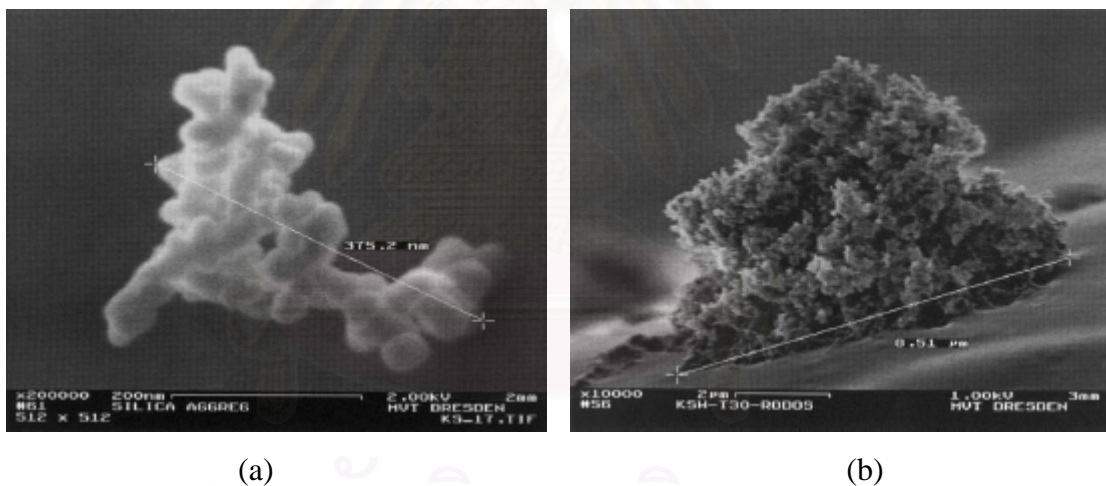
Figure 2.6 SEM images of fumed silica aggregates (a) and agglomerates (b) (Barthel et al., 1999).

Table 2.3 Properties of fumed silica (Harry, 1987).

Property	Value
Chemical formula	SiO_2
Density	2-2.2 g/cm^3
Decomposition temperature	> 2000 °C
Moisture content	
-hydrophilic	0.5-2.5 %
-hydrophobic	0.5%
Particle size primary	5-40 nm
Specific surface area	50-400 m^2/g
Refractive index	1.46

At present, fumed silica is evaluated as a reinforcement to improve materials properties including increase in mechanical strength, modulus, ductility and flame retardant.

2.5 Advanced Composite Technology for Ballistic Armor

The development of composite technology represents one of the most significant advances in material science since 1940s. A composite material can be defined as a macroscopic combination of two or more distinct materials, having a recognizable interface between them (Thornton, 2001). The definition can be restricted to include only those materials that contain a reinforcing material (fibers or particles) supported by a binder (matrix) material. Advanced composites reinforced with aramid fiber have received considerable attention in recent years due to their high strength and stiffness, high durability, desired flexibility and light weight over traditional materials (metallic, ceramic, steel or polymeric matrices). The matrix resins, thermoset and thermoplastic resin are used as matrices for Kevlar[TM]-reinforced composites. Thermoset composites are generally stiffer, more thermally stable, and more brittle than thermoplastic composites. Composites reinforced with Kevlar[TM] have been developed rapidly for many applications in advanced materials. The

applications make use of the high tensile strength and modulus, light weight, thermal and dimensional stability (Morye et al., 2000, and Hearle, 2000).

Table 2.4 Comparison properties of fiber-reinforced composites

Reinforcement	Glass fiber	Aramid UD roving	Carbon UD high modulus	Steel	Aluminium alloy
Specific Gravity	1.7	1.44	-	7.8	2.8
Tensile Strength (MPa)	220	1380	1260	450	300
Tensile Modulus (GPa)	14	76	200	207	70
Compression Strength (MPa)	230	276	840	-	-
Compression Modulus (GPa)	15	76	190	-	-
Flexural Strength(MPa)	270	620	1070	-	-
Flexural Modulus(GPa)	14	76	190	-	-
Shear Strength (MPa)	90	60	65	330	180
Shear Modulus (GPa)	3.3	2.1	5.5	80	26

2.5.1 Fiber-reinforce Matrix Systems

When developing a new part, designers of composites choose from a wide variety of fiber reinforcements and resin systems. Combining fiber and resin elements together to make a composite part can accomplish in numerous ways. One-step processes from the original labor-intensive wet lay-up, to highly automated method such as resin transfer molding (RTM) and pultrusion and filament winding (Kroschwitz, 1991). In many cases, the end user of the structure has fabricated the composite from prepregs. The three types of continuous fibers available as prepregs roving, tape, and woven fabric give the end user many options in terms of design and manufacture of a composite structure. Although the use of dry fibers and impregnation at the work (that is, filament-winding pultrusion or hand lay-up) is very advantageous in terms of costs, there are many advantages to the use of prepregs rather than wet impregnation, particularly for the manufacture of modern composites (Happer, 1992):

2.5.2 Prepregs

Prepregs are material forms consisting of continuous unidirectional or woven fibers pre-coated with a controlled quantity of an uncured catalyzed resin formulation. They are supplied in roll or sheet form, ready for immediate use at a composite manufacturing facility, and are widely used in the aerospace and other industries for high performance structural applications.

Prepregs offer several advantages to the composite parts manufacturer over other product forms (Jonas, 1994) (e.g., wet lay-up):

1: The resin matrix is formulated by the prepregs supplier to give specific end properties, such as hot/wet mechanicals, impact resistance, fire retardancy.

2: Resin formulation is consistent from batch to batch.

3: Prepregs resin content is controlled to limits, which translates to controlled weight in the finished part.

4: Physical characteristics resin such as flow, tack, drapeability, and gel time of the prepregs can be tailored to meet end-user requirements. Resin flow is a measure of resin movement during the cure process. Flow requirements are determined by the type of process used.

2.6 Ballistic standard of Composite Armor

Since the introduction of Kevlar^{TM} aramid fiber to ballistic applications in the early 1970, ballistic standard for body armor of aramid fiber have been established. There are presently two standards for various types of personal body armor in United States.

In December 1978, the National Bureau of Standards and National Institute of Law Enforcement and Criminal Justice (now National Institute of Justice) first classified the ballistic body armors into several catetories according to projectile size and velocity in its NILE/CJ report. The current NIJ classification for police body armor is shown in Table 2.5:

Table 2.5 NIJ standard of body armor

Protection Level	Caliber	Bullet Type, Weight	Velocity (m/s)
I	.38 Special	Round Nose Lead, 158 grain (10.2 grams)	259
	.22 Special	Long Rifle High Velocity Lead, 40 grain,(2.6 g)	320
II-A	9 mm	Full Metal Jacket , 124 grain,(8.0 g)	332
	.357 Magnum	Jacketed Soft point, 158 grain,(10.2 g)	381
II	9 mm	Full Metal Jacket , 124 grain,(8.0 g)	358
	.357 Magnum	Jacketed Soft point, 158 grain,(10.2 g)	425
III-A	9 mm	Full Metal Jacket , 124 grain,(8.0 g)	426
	.44 Magnum	Lead Semi-Wadcutter Gas Checked, 240grain, (15.5 g)	426
III	7.62 x 51 mm (.30 Winchester)	Full Metal Jacket , 150 grain,(9.7 g)	838
IV	.30 caliber	Armor Piercing, 166 grain,(10.8 g)	868

The first two types of body armor cover lightweight body armor for protection from common handguns. These protective garments are suitable for routine full-time wear. Type II armor is heavier and bulkier than Type II-A armor. Its wearing depends largely on the local climate. Type III-A armor provides protection from 9 mm submachine guns and .44 Magnum handguns. This is the highest level of protection for soft body armor. It is generally unsuitable for routine wearing except in circumstances under terrorist threats. Types III and IV armors cover no concealable vests for tactical projectiles. Type III armor provides protection from lead-core rifle bullets, while Type IV offers protection from steel-core armor-piercing rifle bullets. These body armors are intended for use in tactical situations only (Morye et al., 2000).

Figure 2.7 Typical deformable bullets.

2.7 Test Method for Composite Armor

The required test bullet for the armor type was selected as specified in Table 2.5. The test was begun with the threat round number one, by firing a minimum of three pretest rounds to ensure that the first test round fired will strike the target as aimed, and using a suitable targeting device (e.g., a pointing laser). These pretest rounds were also served to "warm" or stabilize the temperature of the barrel before further testing. Set up the test equipment as shown in figure 2.8. Use a test barrel appropriate for the ammunition required to test the armor (Table 2.5), mounted in an appropriate fixture with the barrel horizontal. Dimensions A and B shall be determined from the barrel muzzle. The backing material fixture will be rigidly held by a suitable (metal) test stand, which shall permit the entire armor and backing material assembly to be shifted vertically and horizontally such that the entire assembly can be targeted by the test barrel.
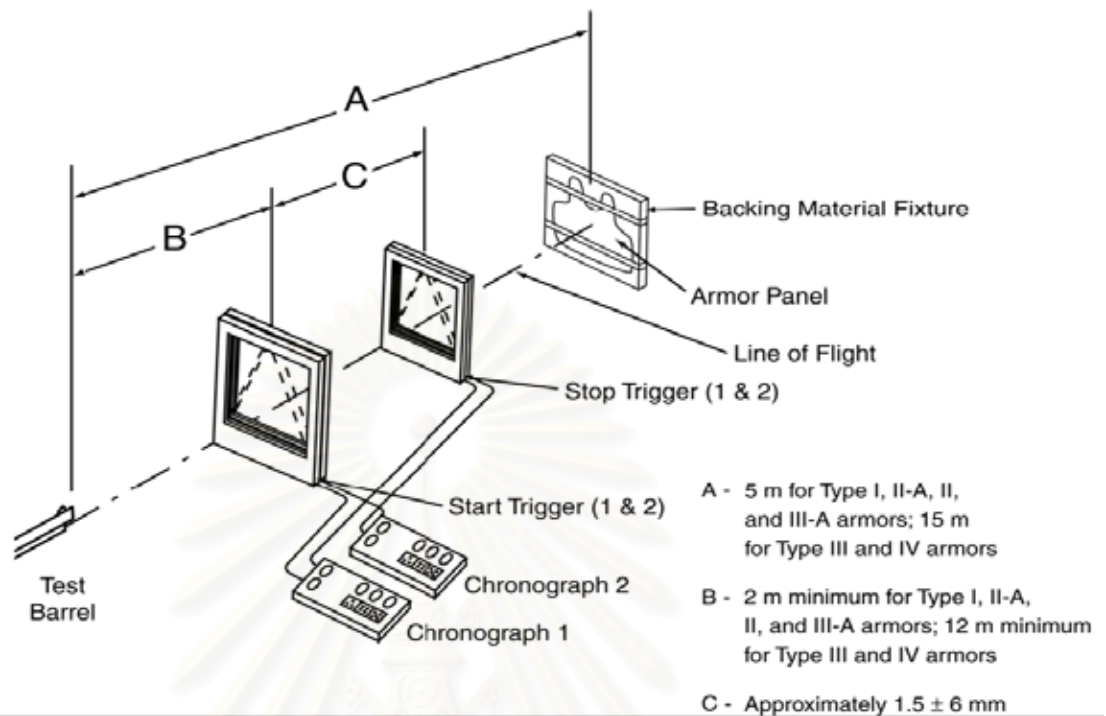
Figure 2.8: Test range configuration (National Institute of Justice [NIJ], 1997)

2.8 Mechanisms of Ballistic Impact

The soft armor system comprises a first pliable, cut resistant fibrous layer and a second pliable, impact/ballistic energy absorbing fibrous layer. The first layer is arranged to receive an impact from a large projectile prior to the second layer and engages the projectile to slow its velocity. The second layer is substantially coextensive with the first layer and dissipates the incoming energy of the impact to resist complete penetration of the second layer by the projectile, preferably by deforming and acting in response to the impact (David, 2001). Impact damage in composites has been noticed, First of all only plane stresses are considered in the criteria for fiber failure, matrix cracking and matrix crushing. Secondly, interlaminar shear stresses caused by matrix cracking and fiber failure are very important causes of delamination in impact events.

The ballistic resistance of a textile fabric to a projectile is generally attributed to its absorption of kinetic energy upon ballistic impact. This is analyzed by way of

simple ballistic impact in the longitudinal (axial) and transverse directions of a fiber. The mechanical strength, modulus of elasticity and specific energy absorption are unconditionally two of the most important technical and performance indexes of fiber. The specific energy absorption evaluates capability to absorb energy locally and the sonic velocity evaluates capability to spread out energy. Relationship between sonic velocity and specific energy absorption with the basic mechanical properties of material are shown in Equation. 2.4 to 2.6. The most of elasticity in turn determines the level of deformability of both transverse and axial directions when a longitudinal impact is applied to a fiber at velocity V, a longitudinal wave will be generated along the fiber at a velocity c. The fiber material behind the wave is subjected to a strain e as shown in the following equation.

$$e \ = \ V/c \qquad\qquad (2.4)$$

$$c \ = \ \sqrt{E/\rho} \qquad\qquad (2.5)$$

where c is the velocity of the longitudinal, E is modulus of elasticity of the initial polymer and the morphological structure of the wave and ρ is fiber density. Thus, the velocity of wave propagation increases with the square root of fiber modulus and inversely with the square root of fiber density. The higher the fiber modulus is the higher the wave velocity and the greater the volume of fiber that is capable of interacting with the projectile (Morye et al., 2000, and Barthel et al., 1999).

Specific energy absorption depends on rupture stress and rupture strain as shown in Equation. 2.6.

$$E_{sp} = \frac{0.5\sigma_{rupt} \times \varepsilon_{rupt}}{\rho} \qquad\qquad (2.6)$$

when

E_{sp} = specific energy absorption capability

σ_{rupt} = breaking strength

ε_{rupt} = strain of rupture

ρ = density

The ballistic dynamics is considerably more complicated when a fiber is impacted transversely than longitudinally.
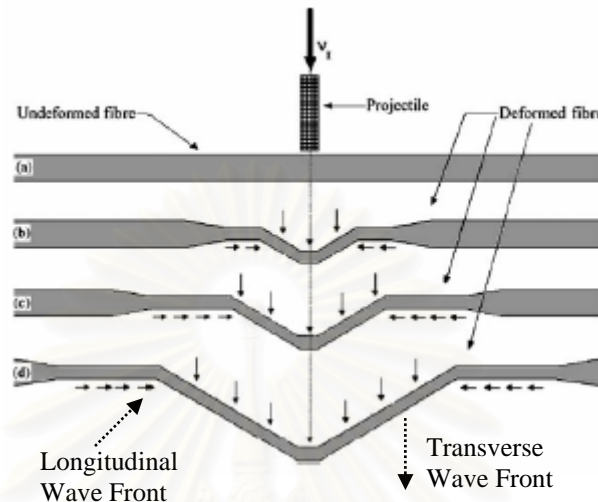
Figure 2.9: Configuration of a yarn/fiber before and after transverse impact (Naik, 2004).

2.9 Energy Absorption Mechanisms of Composite Armor

Upon ballistic impact, polymer composites retard the projectile by reducing its kinetic energy. Different damage and energy absorbing mechanisms of composite, possible energy absorbing mechanisms are shown as follows (Naik, 2004, and Scheirs, 2000).

1. Cone formation on the back face of the target
2. Deformation of secondary yarns
3. Fracture of primary yarns/fibres
4. Delamination
5. Matrix cracking
6. Shear plugging and friction between the projectile and the target.
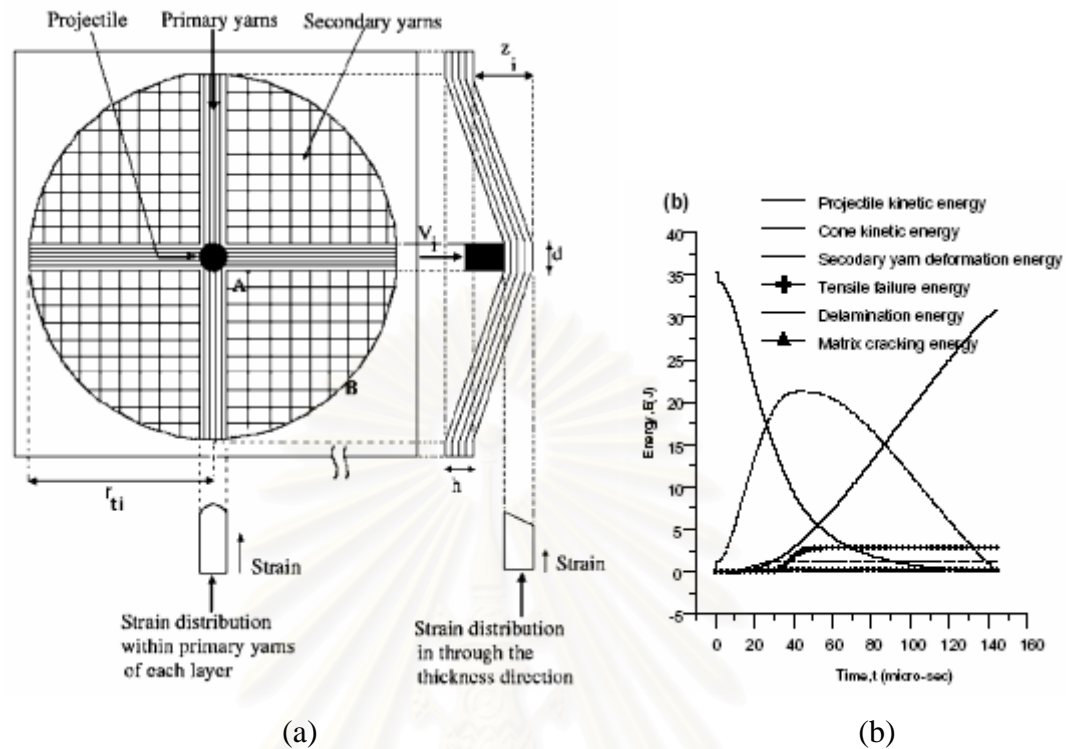
Figure 2.10: (a) Cone formation during ballistic impact on the back face of the composite target. (b) Energy absorbed by different mechanisms.

A cone is observed on the back face of the target as shown in Figure 2.9 when struck by a projectile. Shear plugging on the front face and cone formation on the back face start taking place depending on the target material properties during the ballistic impact event. The velocity of the cone is the same as the velocity of the projectile. Initially, the cone has velocity equal to that of the projectile and has zero mass. As the cone formation takes place, the yarns/fibers deform and absorb some energy. The primary yarns which provide the resistive force to the projectile motion deform the most, thus leading to their failure. When all the primary yarns fail the projectile exits the target. Tensile failure of the yarns thus absorbs some energy of the projectile. During the ballistic impact event, delamination and matrix cracking take place in the laminate area which forms the cone (Naik, 2004, and Ellis, 1996).
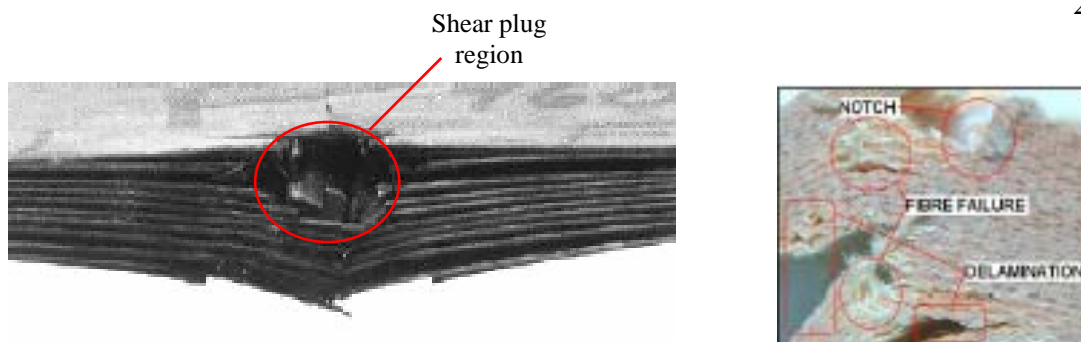
Figure 2.11: Illustration of a combination of shear plug, matrix cracking, delamination, and fiber failure (Ellis, 1996).

CHAPTER III

LITERATURE REVIEWS

3.1 Lightweight Armor and Fiber-Reinforced Composites

The lightweight armors are increasingly necessary in the region that the terrorist problem is remained. These armors can be used as the protection of passenger vehicles against handgun, or as a personal armor. Jacobs proposed high performance fiber used in ballistic products being characterized by low density, high strength, high energy absorption capability and high sonic velocity (Jacobs, 2001). The major fibers used include glass fibers, aramid (Kevlar^{TM}) and high performance polyethylene (UHMPE) fibers. Kevlar^{TM} was reported to be well suited to ballistic armor application because it combines a high specific strength and modulus with high thermal resistance and fire resistance. In the early 1970s, ballistic standards for body armor of aramid fiber have been established and improved over the years.

Park, 2003 patented a light weight soft armor product comprising at least one ballistic panel including an assembly of 50 plies woven aramid fabric, weighing between 600 and 850 denier. Its areal density was not greater than 0.66 g/cm^2 and can protect .22 caliber, 17 grains FSP (NIJ standard, Level IIA).

The development of composite technology represents the most significant advances in armor system. In the past, many combinations have been applied and found satisfactory, usually over a narrow range of applicability. Composite materials have one of the best stiffness to density and strength to density ratios among load bearing engineering materials. These characteristics are outstanding for ballistic protection, where the weight per protected area of a ballistic structure is of great interest. The reduction of weight, while maintaining the same level of protection, means more maneuverability for personal ballistic protection.

Morye et al., 2001 proposed that the use of aramid fiber with polymer matrix to produce the ballistic composites such as 50:50 mixture of phenol formaldehyde resin and polyvinyl butyral resin which its composites have 27 layers and 5.9 mm thickness and can protect the projectile 0.68 g at 512 m/s strike velocity.

Park, 1999 proposed the use of aramid fiber with polyethylene to produce the ballistic composites. The resin content is carefully controlled to achieve a balance of structure and ballistic properties. Therefore fabric is impregnated with resin applied to extent of about 20-25 percent by weight. If the amount of resin substantially increases above that desired level/weight, it will become a major part of the armor volume that weakens the materials. However if the amount of resin substantially less than that required, it will result in the composition material. The fibers are not properly consolidated and held in the proper position so that upon impact, the fiber tends to separate relatively easily allowing the projectile to pass through before the fiber absorbs force.

Coppage et al., 2000 patented composite fabric consist of aramid fiber combine with spectra fiber and at lest one flexible, rubbery resin used in making ballistic armor. The composite was able to pass the NIJ III-A (.44 magnum) and the products possessed an areal density of 0.48 g/cm^2.

Pathomsap, 2005 proposed the composite comprised at least 50 piles of the Kevlar^{TM} fiber and used 80:20 mixture of benzoxazine and urethane as the matrix resin to resist the ballistic impact at level III-A (9 mm). They also found that the 30-ply panel of the composite should be placed in the front face of the composite panel assembly to yield the best ballistic resistance. The products possessed an areal density of 0.24 g/cm^2 in the 10 piles/panel composites.

Tanoglu et al., 2001 proposed the properties of the interphase of various sizes of E-glass-fiber/epoxy-amine system. The composite performance such as strength, toughness, durability and impact/ballistic resistance, the balance of structural ballistic/impact and durability performance from the composite armor can be achieved

by tailoring the fiber/matrix interphase. It may affect the energy absorption in the composites used for lightweight armor applications. The damage mechanisms including interphase-related micro-mechanisms as well as macro-mechanisms are shown in Figure 3.1. The micro-mechanisms such as fiber/matrix debonding or frictional fiber sliding are more important energy-absorbing mechanisms than macro-mechanisms such as delamination or matrix cracking under certain conditions. The relative contribution of each energy-absorbing mechanism depends on the properties of the constituents (fiber, matrix and interface/interphase). The debonding of the fiber/matrix interface may initiate due to stress concentration at the free ends of the broken fiber. When the debonding is complete, pull-out of the fiber from the matrix may occur under further loading. The pull-out process is associated with frictional sliding because contact is maintained between the fully debonded fiber and the surrounding matrix.
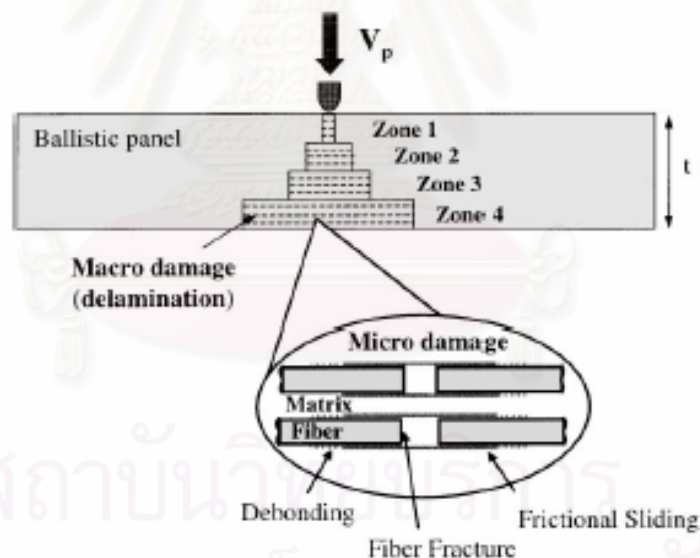
Figure 3.1: Schematic illustration of the composite ballistic panel and damage modes (macro and micro) occurred due to ballistic impact (Tanoglu et al., 2001).

Nunes et al., 2004 proposed that ballistic performance of glass-fiber-reinforced-epoxy matrix laminates was varied by modifying the properties of the constituent laminate or by changing the laminate assemblage. The laminates were obtained using 30 plies of glass-fiber-reinforced-epoxy matrix composite and using

alumina powder (20 μm) as filler for the epoxy resin in the front side plies of the laminate. The results showed that laminate fabricated with a tougher resin matrix exhibited the smallest delaminated area and a bullet before and after impact against one of the 30-ply laminates as shown in Figure 3.2. However the largest delamination were obtained for the composites where the matrix front side plies were blended to alumina. This behavior was explained by the mismatch of the elastic constants between the alumina filled region and the unfilled layers, which produces the change of the stiffness and the mechanical response of the laminate as the elastic shock waves propagate through it. This mismatch of elastic constant occurs at the middle plain of the laminate, where the shear stress attains its maximum value, favoring delamination. It showed that the ballistic behavior was modified by the presence of alumina powder rich resin layers.

Figure 3.2: Bullet before and after impact against a 30 ply laminate (Nunes et al., 2004).

3.2 Polymer Matrix

The application of fiber-reinforced composite armors consisted of multilayered fabrics combined with resin binder. The selection of resin for ballistic composite depends on its required characteristics; some important parameters needed to be considered including rigidity, adhesion, process ability, its velocity, curing temperature, cost and shelf-life.

Ning and Ishida, 1994 investigated the synthesis of bifunctional benzoxazine precursors. These benzoxazine resins were found to exhibit excellent mechanical and thermal properties with good handling capability for material processing and composite manufacturing, e.g., the higher glass transition temperature, tensile modulus and tensile strength than both phenolics and epoxies. They do not release by-product during cure and no solvent other than the solvency which the reactants may have for each other. The other outstanding property of benzoxazine resin is its ability to undergo hybrid network formation with several other resins for tailor-made properties.

Ishida and Allen, 1996 investigated the benzoxazine epoxy copolymer based on DGEBA. The addition of epoxy resin to the polybenzoxazine network greatly increases the crosslink density of the thermosetting matrix. Copolymerization leads to significant increase in the glass transition temperature, flexural stress, and flexural strain at break over those of the polybenzoxazine homopolymer.

Ishida and Rimdusit, 1998 investigated the thermal properties of the boron nitride-filled polybenzoxazine. The thermal conductivity of composite was found to increase with increasing boron nitride content. The high thermal conductivity of the composite was accomplished by using highly thermal conductive filler with a matrix resin which has low melt viscosity with good filler wetting and good adhesion to the filler. Boron nitride-filled polybenzoxazine has many outstanding properties which makes it suitable for an application as a molding compound for the electronic packaging industry and other applications with high thermal conductivity. The work revealed the ease of processing and good interfacial bonding of the matrix resin used in composite fabrication.

Rimdusit et al., 2006 investigated the effect to microwave cure and thermal cure in silicon carbide whisker (SiC_w) filled in polybenzoxazine (PBZ) composite on its corresponding thermal and mechanical behaviors. The result showed that the mechanical and thermal properties of polybenzoxazine composites tended to increase

with increasing SiC_w content. The flexural modulus and strength of the thermal cured composites were determined to be 5.3±0.48 GPa and 119±28 MPa at 4wt%. The neat polybenzoxazine and the SiC_w-filled polybenzoxazine composites possessed a glass transition temperature, ranging from 155 to 160°C. Moreover, the thermal and mechanical properties were increased with increasing the SiC_w contents.

Agag and Takeichi, 2000 prepared polybenzoxazine-clay hybrid nanocomposites. The results showed that the storage modulus of the hybrid materials increased with the increase in the clay contents.

In this work, polybenzoxazine as a ballistic composite was be selected becuase it is a new class of phenolic resins designed molecularly to overcome most problems encountered in traditional phenolics. Recently, various filler reinforcements i.e. whiskers, inorganic, and organic fillers are incorporated into polybenzoxazine matrix for high performance composite applications.

3.3 Development of Composites Matrix

Development of the composite matrix for ballistic armor with filled nano-particles might constitute a much greater area and hence influence the composites properties to much greater extent at the rather low filler concentration as compared to conventional micro-particulate composite.

Jana and Jain, 2001 found that epoxy-aided dispersion of nanosize fumed silica particles played an important role in modifying the barrier, thermal, and impact properties of PES. That means strong interaction between the polar group of epoxy and silanol groups on the surface of fumed silica particles helped dispersion of fumed silica particles into PES. Transmission Electron Microscope (TEM) images of stained samples confirmed coating of epoxy layers around fumed silica particles. The tensile strength of PES/epoxy/fumed silica composites was found to be almost as good as pure PES, while the impact strength increased due to strong interaction between filler and polymer matrix.

Chun et al., 2005 referred to the effect of silica nanoparticles (fumed silica) filled polypropylene on mechanical performance of the composites. It was shown that fumed silica was able to increase modulus of polypropylene composite about 13% at rather low filler concentration (1.75% by vol.). At low amount of nano-SiO_2, the energy absorption increased with increasing the nano-SiO_2 content as shown in Figure 3.3.
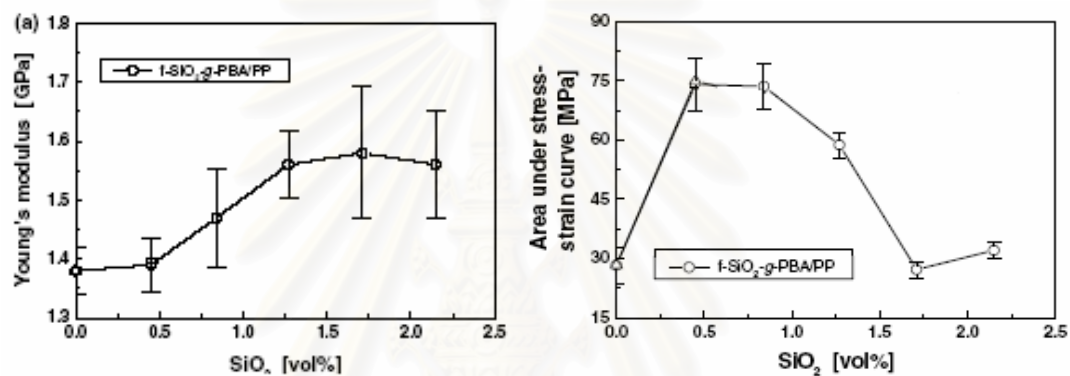
Figure 3.3: Modulus and area under stress-strain curve of polypropylene-filled fumed Silica (Chun et al., 2005).

Hui et al., 2006 referred to the relative improvements on mechanical properties of the nanosilica epoxy composites. The flexural modulus and microhardness of the nanocomposites were all enhanced with increasing silica content. The silica epoxy with 14 vol% nanosilica gave the highest improvement of about 19 and 37%, compared to neat epoxy, of microhardness and flexural modulus respectively. However, the flexural strength of these nanocomposites did not show an apparent effect.
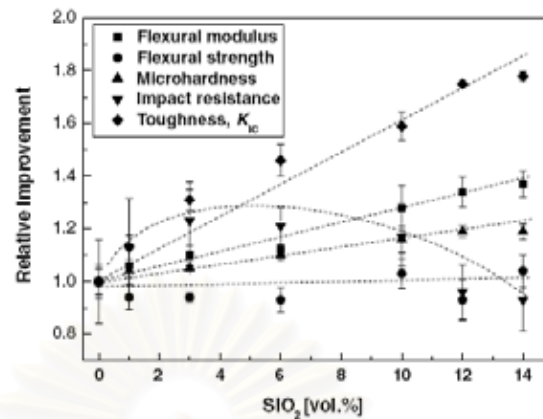
Figure 3.4: Relative improvements of various mechanical properties as a function of nanosilica volume fraction (Hui et al., 2006).

From the mentioned literatures, it can be referred that the SiO$_2$-filled benzoxazine has enormous potential to develop as a modified matrix in ballistic armor applications. In this study, the optimal composition ratios of the polymeric composites (between benzoxazine resin and fumed silica) including the number of the Kevlar layers to produce ballistic composite to meet the requirement of the NIJ standard (level IIA or higher) will be explored.

CHAPTER IV

EXPERIMENT

4.1 Materials

The materials in this research were benzoxazine resin, fumed silica, and Kevlar^{TM} fiber. Benzoxazine resin is based on bisphenol-A, aniline, and formaldehyde. Thai Polycarbonate Co., Ltd. (TPCC) supplied bisphenol-A (Commercial grade). Para-formaldehyde (AR grade) was purchased from Merck Company and aniline (AR grade) was obtained from Panreac Quimica SA Company. Fumed silica (Reolosil$^{®}$ QS-20), from Tokuyama Co., Tokyo, Japan was kindly supplied by Cobra International Co., Ltd. All chemicals were used without further purification. Kevlar^{TM} 29 fiber was used in the form of woven fabric.

4.2 Benzoxazine Resin Preparation

Benzoxazine resin is synthesized using bisphenol-A, formaldehyde, and aniline in the molar ratio of 1:4:2 respectively. This resin was prepared based on a patented solventless method (Ishida, US Patent 5,543,516, 1996). The preparation reaction is shown in Figure 4.1. The obtained benzoxazine monomer is clear-yellowish solid powder at room temperature and can be molten to yield a low viscosity resin at about 80°C. The product is then ground into fine powder and can be kept in a refrigerator for future-use.
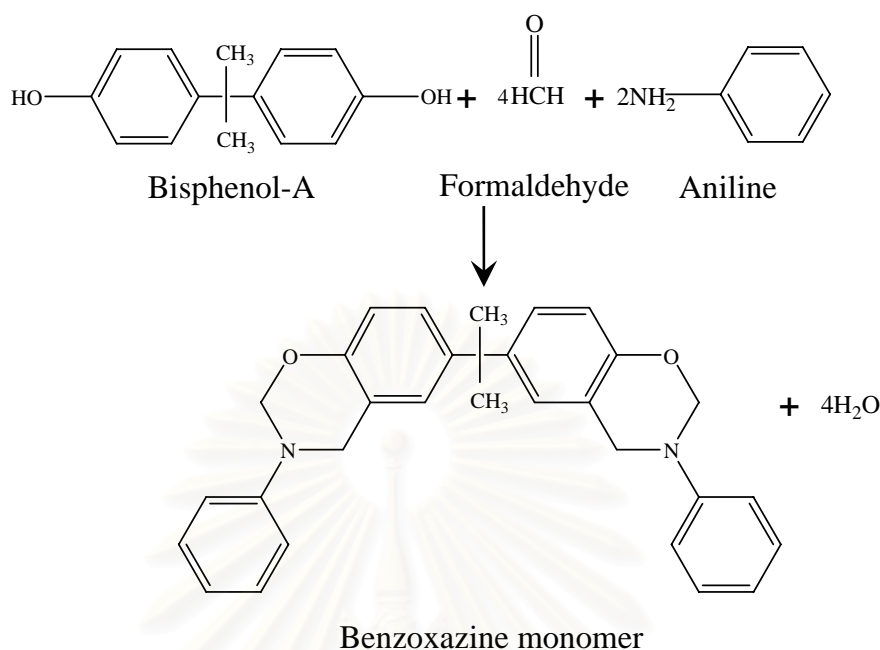
Figure 4.1: Preparation of bifunctional benzoxazine resin (BA-a).

4.3 Fumed Silica Characteristics

The used fumed silica (nano-SiO_2) was Reolosil® QS-20 with the density of 2.2 g/cm^3. It is fluffy and white powders of amorphous structure. The average diameter of the spherical primary particles was varied from 5 to 50 nm, with nominal surface area of about 200 m^2/g.

4.4 Fumed Silica filled Polybenzoxazine Nanocomposites Preparation

The samples were prepared with filler loadings of 0, 1, 3, 5, 7, and 10% by weight to yield molding compound. The fumed silica was firstly dried at 110°C for 24 hours in an air-circulated oven until a constant weight was achieved and was then kept in a desicator at room temperature. Fumed silica was thoroughly mixed by hand with benzoxazine resin in an aluminium container at about 120°C and mechanically stirred to achieve good dispersion of fumed silica in benzoxazine resin. For thermal-cured specimen, the compound was compression-molded by hot pressing. The thickness was

controlled by using a metal spacer. The hot-pressed temperature of 160°C was applied for 2 hr and 180°C was applied for 2 hr simultaneously with a hydraulic pressure of 25 MPa (Pathomsap, 2006). The specimens were then post cured in an air-circulated oven at 200°C for 4 hr. All samples were air-cooled to room temperature in the open mold before testing.

4.5 Composite Manufacturing

4.5.1 Matrices Preparation

Fumed silica was thoroughly mixed by hand with benzoxazine resin in an aluminium container at about 120°C and mechanically stirred to achieve good dispersion of fumed silica in benzoxazine resin. The filler contents were 0, 1, 3, 5, and 7% by weight to yield molding compounds. They were evaluated as potentially matrices for Kevlar^{TM}-reinforced composites as a ballistic armor.

4.5.2 Processing of Kevlar^{TM} Fiber Reinforced Prepreg

Kevlar^{TM} fiber reinforced prepreg were processed by the hand-lay up procedure at 120°C, brushing the matrix resin onto a Kevlar^{TM} fibrics. The weight fraction of resin was kept constant at 20-25%. Two experimental patterns of prepreg were applied.as follows.

Pattern 1) processing a composite samples with different fumed silica contents from 0% to 7% by weight

Pattern 2) alternating the layers of fumed silica-filled benzoxazine resin with the ones of benzoxazine resin.

After that, the prepregs were placed and heated in compression-molded at the temperature of 160°C for 2 hr and 180°C for 2 hr with the pressure of 25 MPa. The specimens were then post-curing in an air-circulated oven at 200°C for 4 hr. All samples were air-cooled to room temperature and were taken for further characterization.

4.6 Characterization Methods

4.6.1 Differential Scanning Calorimetry (DSC)

Curing temperature of fumed silica-filled polybenzoxazine composites were examined using a differential scanning calorimeter (DSC, model 2910) from TA Instuments. A sample mass of 5-10 mg was placed in a 50 μl aluminum pans provided with venting holes. The experiment was performed at a heating rate of $10^{o}C/min$ in the temperature range from $30^{o}C$ to $300^{o}C$ under nitrogen flux (50 ml/min). Curing temperatures and glass transition temperatures were obtained from the thermograms.

4.6.2 Thermogravimetric Analysis (TGA)

Thermal stability, degradation temperature (T_d) and char yield of fumed silica-filled polybenzoxazine composites were studied using a thermogravimetric analyzer (TG/DTA thermogravimetric analyzer model SII Diamond) from Perkin Elmer. The scans were performed at heating rate of $20^{o}C/min$ under oxygen flow (100 ml/min) in the temperature from 30 to $900^{o}C$. The initial mass of a tested sample, which was 15-20 mg, was placed in a 70 μL ceramic cup with cover provided with venting holes. The degradation temperature at 5% weight loss and the char yield at $800^{o}C$ were recorded for each specimen.

4.6.3 Density Measurement

A density of each specimen was determined by water displacement method according to ASTM D 792-91 (Method A). All specimens were prepared in a rectangular shape with the dimension of 50 mm x 25 mm x 2 mm. The density was calculated by the following equation:

The average value from at least three specimens was calculated.

$$\rho = \left(\frac{A}{A - B}\right) \times \rho_o \qquad (4.1)$$

where ρ = Density of the specimen (g/cm^3)

   A = Weight of the specimen in air (g)

   B = Weight of the specimen in liquid (g)

   ρ_o = Density of the liquid at the given temperature (g/cm^3)

4.6.4 Flexural Property Measurement

Flexural modulus and flexural strength of composite specimens were determined utilizing a Universal Testing Machine (model 5567) from Instron Instrument with a 1 kN static load cell. The test method used was a three-point bending mode with a support span of 32 mm at the crosshead speed of 1.2 mm/min. The dimension of the specimens was 50 mm x 25 mm x 2 mm. The flexural modulus and flexural strength from 5 samples were averaged and determined using ASTM D 790M-93 according to the following equations:

$$E_B = \frac{L^3 m}{4bd^3} \qquad (4.2)$$

$$S = \frac{3PL}{2bd^2} \qquad (4.3)$$

where E_B = Flexural modulus (MPa)

   S = Flexural strength (MPa)

   P = Load at a given point on the load-deflection curve (N)

   L = Support span (mm)

   b = Width of beam tested (mm)

   d = Depth of beam tested (mm)

   m = Slope of the tangent to the initial straight-line portion of the load-deflection curve (N/mm)

4.6.5 Dynamic Mechanical Analysis

Dynamic mechanical analyzer (DMA) model DMA242 from NETZSCH was used to investigate the dynamic mechanical properties of the specimens, i.e. storage modulus (G'), loss modulus (G''), loss tangent (tan δ) and glass transition temperature (T_g). The dimension of each specimen was 50 mm×10 mm×2 mm. The test was performed under bending mode. The strain was applied sinusoidally with a frequency of 1 Hz, and the specimen was heated at a rate of 5^oC/min from 30 to 270^oC. The glass transition temperature was reported as the maximum point on the loss modulus curves in the temperature sweep test.

4.6.6 Microhardness Testing

Microhardness of compressed specimens was measured utilizing a Vickers microhardness tester (model FM-700C) from Future-Tech. A pyramidal diamond was applied to the surface of the composite under a load of 4.90 N for 15 s. Diagonal length of the indentation was measured through a micrometric eyepiece with an objective lens (50x magnification). The tests were repeated ten times for each sample.

4.6.7 Rheological Properties Measurements

Rheological properties of each alloy were examined using a Rheometer (Haake Rheo Stress 600, Thermo Electron Cooperation) equipped with parallel plate geometry. The measuring gap was set at 0.5 mm. The pre-heated upper plate was then lowered to a set gap of 0.5 mm. The melt viscosity of the molding compound was performed under shear sweep mode at 120^oC, with the shear rate range of 1-500 (s^{-1}).

Processing window of the resin mixture was determined under an oscillatory shear mode. The composite waveform was obtained by the superposition of mechanical waves with frequencies 0.5 rad/s. A sample mass about 3 g was used in each test. The testing temperature program was ramped from room temperature at a

heating rate of 2°C/min to a temperature beyond the gel point of each resin and the dynamic viscosity was recorded.

4.6.8 Morphological Observation

The fractured surface of the composite specimen was observed with a scanning electron microscopy (SEM) from JEOL Ltd model JEOL JSM-6480 LV at an acceleration voltage of 15 kV. All specimens were coated with a thin layer of gold using a JEOL ion sputtering device model JFC-1100E for 4 min to obtain a thickness of approximately 300 Å. The micrograph was used to investigate the surface of the nano-SiO2 fillers and the interaction between the fillers and the polybenzoxazine matrix.

4.6.9 Fire Test

The ballistic tests were performed to evaluate the most appropriate composition of the matrix used for ballistic composite. The tested composite panel was approximately 13 cm × 13 cm with varied thickness depending on the number of layers of Kevlar^{TM} cloth used. Each plate was impacted with only one projectile. The Kevlar^{TM}–reinforced fumed silica-filled polybenzoxazine plates were about 2.0 mm thickness corresponding to 5 plies of the laminated composite. The composites used in this experiment consisted of two panels of 5 piles composites were listed in Table 4.1. The laminates were tested using a 9 mm handgun as shown in Figure 4.2 and were impacted by a standard grain of a round lead projectile with lead outer coating. The first experiment was aimed to evaluate the most suitable composition of the matrix resin for ballistic protection.

Figure 4.2: 9 mm handgun for the fire test

Table 4.1 Description of composites laminates used for ballistic evaluation.

Fire test	Type of matrix	Number of piles
Low impact	Kevlar fiber Epoxy 200 Epoxy 400 PBZ 1%SiO_2-filled PBZ 3%SiO_2-filled PBZ 5%SiO_2-filled PBZ 7%SiO_2-filled PBZ 7%SiO_2-filled PBZ/PBZ	5+5

The laminates with a combined thickness of 25, 30, and 35 plies were tested with a standard 240 grain of .44 Magnum Semi Jacketed Hollow Point (SJHP) bullets, with nominal masses of 15.6 g impacting at a minimum velocity of 426 m/s. The impact velocity obtained from this projectile was complied by the NIJ standard of level III-A. The velocity of each shot was recorded using a triggered timer system, as shown in Figure 4.3. The descriptions of all composites used in these experiments were listed in Table 4.2. This experiment was aimed to evaluate the most suitable

number of thickness of composite and the arrangement of the composite panel for ballistic protection.
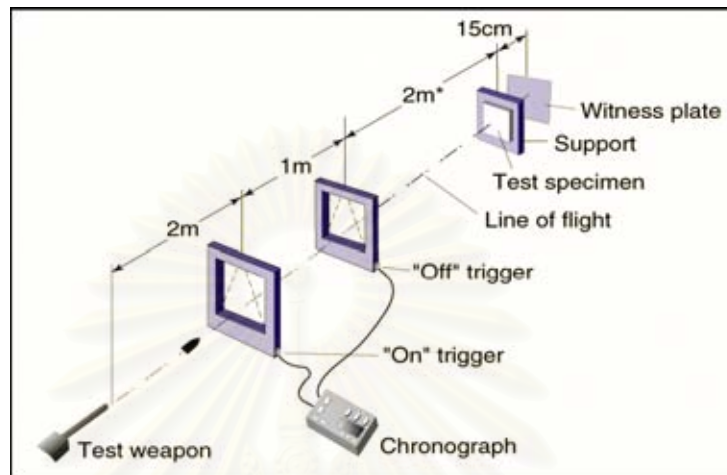
Figure 4.3 Testing scheme used for the NIJ standard ballistic test

Table 4.2 Description of composites laminates used for ballistic evaluation
(as level III-A of NIJ standard).

Number of piles	Number of piles	Type of matrix
25	15+5+5 15+10	7% SiO_2-filled PBZ
30	15+5+5+5 15+10+5	7% SiO_2-filled PBZ
35	10+10+5+5+5 15+5+5+5+5 15+10+5+5	7% SiO_2-filled PBZ

CHAPTER V

RESULTS AND DISCUSSION

5.1 Fumed Silica-filled Benzoxazine Resin Characterization

5.1.1 Investigation of Benzoxazine Resin Filled with Fumed Silica Curing Condition

The investigation of the curing condition of benzoxazine resin filled with different fumed silica (nano-SiO_2) contents in DSC experiment with a temperature range of 30 to 300°C was performed using a heating rate of 10°C/min. Figure 5.1 shows the curing exotherms of the neat benzoxazine resin (BA-a) and the benzoxazine molding compounds at different nano-SiO_2 contents. It reveals that the onset of curing reaction was at about 150^oC. A maximum exothermic peak of all these composition was observed at about 225^oC, which is the same peak maxima of the as-synthesized benzoxazine resin (Rimdusit, 2000). The curing exotherms of all these benzoxazine compounds exhibit thermally curability without adding initiator or catalyst the benzoxazine monomer. The unchanged exothermic peak position to of the benzoxazine molding compounds indicates that nano-SiO_2 had no effect on the curing reaction of the benzoxazine monomer. This is because the nano-SiO_2 filler is relatively inert to the benzoxazine curing reaction. Furthermore, the area under the curing peaks was found to decrease with increasing the nano-SiO_2 content. This phenomenon is related to the decreasing amount of benzoxazine resin in the molding compounds with an increasing of the nano-SiO_2 content.

Figure 5.2 presents the DSC thermograms of the benzoxazine molding compound at 10% by weight of the nano-SiO_2 at various curing conditions to determine its fully cured condition. The minimum curing temperature of these composites was selected at 160°C because this temperature was high enough to initiate the ring-opening reaction of the benzoxazine monomer. From the experiment,

the uncured benzoxazine molding compound possesses a heat of reaction determined from the area under the exothermic peak of about 254.1 J/g. The value decreases to 19.03 J/g after curing 160°C for 2 hrs, 180°C for 2 hrs, and post-curing at 200°C for 1 hr. The area under the peak was further reduced to 11.03 J/g and 4.41 J/g when the post-curing was changed to be at 200°C for 2 hrs and 3 hrs respectively. The exothermic peak almost disappears i.e. corresponding to 99% conversion of the composite, when the post-curing was at 200°C for 4 hrs. The disappearance of the exothermic peak suggested that suitable step-curing program to complete the polymerization of benzoxazine molding compound was at 160°C for 2 hrs, 180°C for 2 hrs, followed by post-curing at 200°C for 4 hrs. The degree of conversion of the sample was determined according to the following relationship:

$$\% \text{ conversion} = (1 - \frac{H_{rxn}}{H_0}) \times 100 \qquad (5.1)$$

Where: H_{rxn} is the heat of reaction of the partially cured specimens.

H_0 is the heat of reaction of the uncured resin.

5.1.2 Rheological Behavior

The relationships between apparent shear viscosity and apparent shear rate of nano-SiO_2 filled benzoxazine molding compound at various filler contents are shown in Figures 5.3 and 5.4. The shear viscosity of the molding compounds measured at 120°C as a function of shear rate having various nano-SiO_2 contents in comparison with that of neat benzoxazine resin is presented in Figure 5.3. The measurement was performed under shear rate sweep mode with the shear rate range of 0.001-500 1/s. From the curves, the values of shear viscosity of nano-SiO_2 filled benzoxazine molding compounds increase with increasing the amount of nano-SiO_2. In general, nano-SiO_2 is a common rheological filler used in many applications such as in the paint industry. The addition of nano-SiO_2 clearly increases the viscosity of benzoxazine compounds and in general can impart pseudoplasticity and thixotropy (Perez-Liminana et. al., 2003). Furthermore, the flow curves of the benzoxazine molding compounds exhibit two distinct regions. The first region at lower shear rate

(lower than 300 s^{-1}) was observed as a Newtonian zone, exhibiting a solid-like behavior with a high value of viscosity. The viscosity was increased from the aggregation of nano-SiO$_2$ particles to form clusters, which is due to the particle-particle interaction. At higher shear rate (higher than 300 s^{-1}), the viscosity of all nano-SiO$_2$ filled benzoxazine molding compounds decreases linearly with increasing shear rates. This mechanism is mainly attributed to the breakage of the silica agglomerates (Shirono, 2001 and Reynaud, 2001). As observed in many filled systems, the steady shear viscosity of nano-SiO$_2$ composites depends on interactions between the silica particles and nano-SiO$_2$ content. At low nano-SiO$_2$ content a silica-silica agglomerated structure is difficult to form clusters (Michael, 1998). The relationship between nano-SiO$_2$ content and viscosity of benzoxazine molding compounds is presented in Figure 5.4. The values of viscosity at low content of nano-SiO$_2$ is quite low, and shows increased at high content of nano-SiO$_2$ i.e. 1.9 Pa.s of 1wt% to 29.6 Pa.s of 10wt%. nano-SiO$_2$ has the effect on the viscosity of the benzoxazine molding compounds.

Figure 5.5 reveals the processing windows of nano-SiO$_2$ filled benzoxazine molding compounds. The complex viscosity of these molding compounds at various nano-SiO$_2$ contents was recorded as a function of temperature. At room temperature, all uncured molding compounds are solid at room temperature. They change to soft solid when the temperature was raised to their softening points. At this point, the dynamic viscosity of all nano-SiO$_2$ filled benzoxazine molding compounds rapidly decreases. Beyond the softening point, all molding compounds became liquid, which possess the lowest viscosity at this stage. This temperature range is highly useful for each molding compound because it is a processing window of each compound. In the last stage at higher temperature, all nano-SiO$_2$ filled benzoxazine molding compounds underwent crosslinking reaction past their gel points thus resulting in a rapid increase in the viscosity beyond this transition.

From the figure, the dynamic viscosity of the nano-SiO$_2$ filled benzoxazine molding compounds expectedly increases with increasing the amount of the nano-SiO$_2$. The liquefying temperature of these molding compounds was also found to increase with increasing amount of the nano-SiO$_2$. The liquefying temperature of

70°C was obtained for 1wt% of nano-SiO$_2$ filled system, while the value of 90°C was focused in the compound with 10wt% of nano-SiO$_2$. On the other hand, the gel points of all molding compounds were observed to be the same at a temperature of 180°C, even though the amount of nano-SiO$_2$ was increased from 1wt% to 10wt%. Therefore, it can be concluded that the nano-SiO$_2$ content has no effect on the gel point temperature of the molding compounds but significantly affects their liquefying temperature. This characteristic confirms the DSC result (Figures 5.1), which suggests that nano-SiO$_2$ has no effect on the curing reaction of the benzoxazine monomer.

5.1.3 Thermal Characterizations of Fumed Silica Filled Polybenzoxazine

5.1.3.1 Differential Scanning Calorimetry (DSC)

Figure 5.6 demonstrates the glass transition temperatures (T$_g$) of the neat polybenzoxazine (PBZ) and nano-SiO$_2$ filled polybenzoxazine composites. The T$_g$ corresponds to the temperature at which mobility of chain segments of polymer begins. From the thermogram, the glass transition temperature of the polybenzoxazine was determined to be 160 °C and those of the nano-SiO$_2$ filled polybenzoxazine composites were found to systematically increase from 160 to 165°C when the nano-SiO$_2$ content was increased from 1% to 10% by weight. The effect of nano-SiO$_2$ content on T$_g$ of the polybenzoxazine is illustrated in Figure 5.7. The T$_g$ of nano-SiO$_2$ filled polybenzoxazine composites tend to increase with increasing the filler content possibly due to the reinforcing effect of the SiO$_2$ nanoparticle. The nano-SiO$_2$ filler was known as a high stiffness material thus, the mobility of the polybenzoxazine may be highly restricted with this filler when adhering on the filler surface. In some reports, the decrease of T$_g$ was observed with the increasing amount of the nano-SiO$_2$ i.e. epoxy mounding compound (Preghenella et al, 2005 and Zhang et al, 2006).

5.1.3.2 Thermogravimetric Analysis (TGA)

In practice, the degradation temperature (T$_d$) is one of the key parameters used to determine temperature stability of polymer matrix. Figure 5.8

exhibits the TGA thermograms of the neat polybenzoxazine and nano-SiO_2 filled polybenzoxazine composites at various nano-SiO_2 contents. The decomposition temperature, in this case, is defined as the temperature at 5% weight loss of the specimen. From the thermograms, the degradation temperatures at 5% weight loss of the composites were found to slightly increase when the content of nano-SiO_2 increased. This is possibly due to the barrier effect of the inert nano-SiO_2 filler. From TGA curves, it can be seen that all composite compositions demonstrate an improvement in their thermal stability over the unfilled polybenzoxazine. As seen in the inset of Figure 5.8, the decomposition temperatures at 5 % weight loss of the composites are in the range of 352-360°C comparing with that 348°C of the polybenzoxazine. In addition, the effect of nano-SiO_2 content on the degradation temperature at 5% weight loss and 10% weight loss of nano-SiO_2 filled polybenzoxazine composites is also summarized in Table 5.1.

The relationship between the nano-SiO_2 contents and the solid residue of nano-SiO_2 filled polybenzoxazine composites is depicted in Figure 5.8 and Table 5.1. From the plot, the amount of residual weight at 800 °C of the nano-SiO_2 filled polybenzoxazine composites under oxygen is close to the actual amount of the nano-SiO_2 loading in composite. That is because nano-SiO_2 filler, which has very high thermal stability from its ceramic nature, starts to decompose at more than 2000°C (Wypych, 1999). Thus nano-SiO_2 filler does not experience any weight loss in the temperatures of 30-900°C under the TGA investigation. When the temperature is raised to 800°C, only the polybenzoxazine fraction was decomposed thermally. Therefore, the amounts of solid residue in this case directly correspond to that of the nano-SiO_2 filler presented in the composites.

5.1.4 Density Measurement

Figure 5.9 shows the density of neat polybenzoxazine and nano-SiO_2 filled polybenzoxazine composite at 1, 3, 5, 7, and 10wt% of nano-SiO_2 contents. The density measurements of all composite were applied to investigate the presence of void in composite specimens. One outstanding property of polybenzoxazine matrix is its low melt viscosity in which the highly filled composite can easily be obtained.

This figure exhibits the theoretical density of the composite in comparison with actual density. The theoretical density of the composites was calculated from Equation (5.2) and the actual density was calculated by using Equation (4.1). The calculated is base on the basis that the density of the nano-SiO$_2$ and of polybenzoxazine are 2.22 g/cm^3 (Wypych, 1999) and 1.20 g/cm^3 (Harper, 2004), respectively. Due to the higher density of nano-SiO$_2$, the results reveal that the theoretical and actual density of the polybenzoxazine composites was increase with the nano-SiO$_2$ content following the rule of mixture. Furthermore, it can be observed that the theoretical and actual density values are about the same. That means void content in the composite specimens was relatively negligible. The theoretical density by mass of polybenzoxazine filled with nano-SiO$_2$ can be calculated as follow (Piyawan, 1998):

$$\rho_c = \frac{1}{\dfrac{W_f}{\rho_f} + \dfrac{(1-W_f)}{\rho_m}} \tag{5.2}$$

where

W_f = filler weight fraction

$(1-W_f)$ = matrix weight fraction

ρ_f = filler density, g/cm^3

ρ_c = matrix density, g/cm^3.

5.1.5 Mechanical and Physical Property Characterizations

5.1.5.1 Flexural Property Measurement

Flexural modulus and flexural strength of neat polybenzoxazine and nano-SiO$_2$ filled polybenzoxazine composite are illustrated as a function of nano-SiO$_2$ content in Figures 5.10 and 5.11. The flexural modulus of the nano-SiO$_2$ filled polybenzoxazine composites is slightly higher than those of polybenzoxazine. As shown in Figure 5.10, the modulus values of the composites were found to be substantially improved by the presence of the nano-SiO$_2$ up to 10% by weight of the filler in our investigation. The flexural modulus of the neat polybenzoxazine was determined to be 5.98 GPa. At 1% to 10% by weight of nano-SiO$_2$ content, the

modulus of the nano-SiO_2 filled polybenzoxazine composites increases from 6.47 to 7.52 GPa. The phenomenon was due to the fact that with substantial interfacial interaction between the filler and the matrix, the addition of rigid particulate filler into the polymer matrix was able to improve the stiffness of the polymer composite. In addition, it is also found that the modulus of the composites following the rule of mixture. In this work, the flexural modulus of nano-SiO_2 filled composite at 10wt% was 26% higher than that of neat polybenzoxazine. The increase of the flexural modulus was found in the study of Zhang et al., 2006, who studied the mechanical properties in the system of epoxy and nano-SiO_2. He reported that the flexural modulus of the composite at 23% by weight of nano-SiO_2 was 30% increased from that of neat epoxy. However, as shown in Figure 5.11, nano-SiO_2 filled polybenzoxazine composites with 1% to 10% by weight of nano-SiO_2 tend to render slightly lower flexural strength than the neat polybenzoxazine. The flexural strength of the filled polybenzoxazine was found to be relatively unchanged with the nano-SiO_2 loading in the range of 1% to 10% by weight. It is postulated that the aggregation and agglomeration that may present in the nano-SiO_2 may cause the defects in the composites thus lowering the strength values. These observed phenomena are similar to those in the system of epoxy-silica nanoparticle (Zhang et al., 2006).

5.1.5.2 Dynamics Mechanical Measurement

Since all polymers are viscoelastic in nature, dynamic mechanical analysis method is suitable to evaluate the phenomena of the complex array when polymeric materials are presented. Figures 5.12 to 5.14 illustrate the dynamic mechanical properties of the nano-SiO_2 filled polybenzoxazine composites with the nano-SiO_2 ranging from 0 to 10wt%. At room temperature, the storage modulus (G') of the nano-SiO_2 filled polybenzoxazine composites increased with increasing nano-SiO_2 content as seen in Figure 5.12. Additionally, the storage modulus of the composites at its glassy state were raised from 4.8 GPa of the neat polybenzoxazine to 5.2, 5.8, 6.6, 7.2, and 7.4 GPa of the 1, 3, 5, 7, and 10% by weight of nano-SiO_2 composite respectively. The modulus of the nano-SiO_2 filled polybenzoxazine in the

rubbery plateau region was also found to increase significantly as a result of the addition of the nano-SiO_2. The influence is possibly attributed to the addition of rigid particulate filler into the polymer matrix was able to improve the stiffness of the polymer composite. The results indicate the substantial reinforcing effect of the nano-SiO_2 filler on both in the rubbery and the glassy state modulus, which imply strong interfacial bonding between the polymer and the reinforcing filler.

Figure 5.13 shows the loss modulus (G") curves of the nano-SiO_2 filled polybenzoxazine as a function of temperature. The maximum peak temperature in the loss modulus curve is assigned as a glass transition temperature (T_g) of the specimen. As seen in this figure, the linear relationship between the glass transition temperature and the filler content was observed. The glass transition temperature of the neat polybenzoxazine was determined to be 157°C whereas the glass transition temperature of the 10% by weight of nano-SiO_2 filled polybenzoxazine is about 167°C. The increasing of the T_g with an addition of the nano-SiO_2 is possibly due to the good interfacial bonding between the two phases that the more rigid filler can effectively restrict the mobility of the polybenzoxazine and cause the T_g enhancement. In this study, it can be noticed that the glass transition temperature observed from DMA thermograms exhibited the same trend as those obtained by DSC. Figure 5.14., exhibit the α-relaxation peaks of the loss tangent (tan δ) of nano-SiO_2 filled polybenzoxazine composites. It was found that the peak maxima were shifted to higher temperature. The glass transition temperatures from the loss tangent were in agreement with the ones from loss modulus.

5.1.5.3 Microhardness Evaluation

Surface hardness is generally investigated as one of the most important factors that are related to the wear resistance of materials. Figure 5.15 exhibits the Vickers microhardness (HV) values of the neat polybenzoxazine and nano-SiO_2 filled polybenzoxazine composite at different nano-SiO_2 content. The surface hardness of the nano-SiO_2 composite expectedly increased with increasing nano-SiO_2 filler content. The HV value of the nano-SiO_2 filled polybenzoxazine composites with the

nano-SiO$_2$ contents ranging from of 0 to 10% by weight (0% to 4.5% by volume) were 368 to 481 MPa. That is because the addition of nano-SiO$_2$ to polybenzoxazine was found to enhance the resistance of the polybenzoxazine deformation. From the results of the other nano-SiO$_2$ polymer composite system (Zhang et al., 2006), it was reported that the nano-SiO$_2$ filled into epoxy matrix (at 6% by volume of nano-SiO$_2$ content) showed the Vickers microhardness value of 222 MPa compared with 201 MPa of the neat epoxy matrix. Moreover, the value of our nano-SiO$_2$ filled polybenzoxazine composite had more significant change than that of nano-SiO$_2$ filled epoxy composite. The enhancing effect is relatively similar to our nano-SiO$_2$ filled polybenzoxazine. The wear resistant behaviors of these polybenzoxazine composites are under investigation for a potential use as a high wear resistant coating material.

5.1.6 Morphological Observations

The dispersion of filler particles in the polymer matrix is reported to have a significant impact on the mechanical properties of nanocomposite (Zheng, 2003). Therefore, the nano-SiO$_2$ dispersion in the composite was investigated using EDX-mapping. The EDX-mapping (1000 time magnifications) micrograph of the fracture surface at the nano-SiO$_2$ content at 10% by weight is shown in Figures 5.16. From the figure, the nano-SiO$_2$ is shown as light granules distributed all over the specimen. That means the filler was well dispersed, i.e. the nano-SiO$_2$ agglomeration was not found at any part of the specimens. The reason for this good dispersion behavior is attributed to the relatively low viscosity of the polybenzoxazine.

Figure 5.17 (a) to (d) shows the interfacial characteristics along the fracture surface at 500 times magnification of the nano-SiO$_2$ filled polybenzoxazine. The fracture surface of the neat polybenzoxazine is much smoother when compared to that of the nano-SiO$_2$ filled polybenzoxazine composite due to the adding of nano-SiO$_2$ filler are improve the loading area that enhance the polybenzoxazine matrix deformation. This suggested that the addition of nano-SiO$_2$ into polybenzoxazine matrix highly affect the fracture surface and brittle behavior of the composite matrix (Sipaut et. al., 2007).

5.2 Kevlar^{TM}-reinforced Composite Characterization

5.2.1 Differential Scanning Calorimetry for Curing Condition Observation

From the viscosity results (Figure 5.3) and the results of flexural properties and dynamic mechanical properties (Figures 5.10 to 5.14), the Fumed silica at 10wt% was not selected to process for ballistic armors because of too high viscosity.

Figure 5.18 illustrates the DSC thermograms of Kevlar^{TM}-reinforced 7wt% nano-SiO$_2$ filled polybenzoxazine prepregs. The composition was selected to represent all composite for determining the full cured condition as the ratio required the most thermal energy for curing. The Kevlar^{TM}-reinforced 7wt% nano-SiO$_2$ filled polybenzoxazine prepregs possessed curing exotherms with the same characteristic as the matrix in the previous experiment as shown in Figure 5.2. This characteristic indicated that Kevlar^{TM} fiber had no direct effect on chemical reaction during the curing process. From the result, there is no appearance of the exothermic peak in the DSC thermogram of the Kevlar^{TM} fiber. That means this condition provided the complete reaction. Therefore, the process curing condition temperature of Kevlar^{TM}-reinforced nano-SiO$_2$ filled polybenzoxazine prepregs at different nano-SiO$_2$ contents can be used in the same condition of the matrices. Hence, the condition used in this study was heating at 160°C for 2 hrs and 180 °C for 2 hrs with a hydraulic hot-press machine, and then further curing in an air-circulated oven at 200°C for 4 hrs. Furthermore, the disappearance of the exothermic peak between 170°C and 280°C suggested that suitable duration for complete cure of the Kevlar^{TM}-reinforced composite prepregs. Therefore, this curing condition can be used with their Kevlar^{TM}-reinforced composite prepregs in this work.

5.2.2 Determination of Polymer Matrix Content in the Composite

In general, the determination of the polymer matrix content in the armor composite is the most important factor related to the performance of the ballistic armor composites. The optimal range of the polymer matrix content for the best

ballistic efficiency of polymer composite was reported to be about 20 to 25% (Park, 2003). In this case, the polymer matrix content in the composites was calculated using the results from thermogravimetric analysis (TGA) thermograms of the nano-SiO_2 filled polybenzoxazine composite as polymer matrix and the Kevlar[TM]-reinforced nano-SiO_2 filled polybenzoxazine composite at different nano-SiO_2 content as exhibited in Figure 5.19. In this study, the percentage of polymer matrix content was found in the range of 20-25wt% in Kevlar[TM]-reinforced nano-SiO_2 filled polybenzoxazine composite at different nano-SiO_2 contents.

5.2.3 Thermal Stability Investigation of Kevlar[TM]-Reinforced Composite

Figure 5.20 exhibits TGA thermograms of Kevlar[TM]-reinforced nano-SiO_2 filled polybenzoxazine composites at different nano-SiO_2 content. The decomposition in all composites was found to be two stages. The first stage occurred at temperature between $350^{o}C$ and $490^{o}C$ corresponds to the decomposition temperature of polymer matrix, the second stage from the thermogram corresponds to the decomposition temperature of Kevlar fiber of all Kevlar[TM]-reinforced polybenzoxazine composites, which was approximately at $590^{o}C$. The degradation temperature at 5% weight loss of Kevlar[TM]-reinforced polybenzoxazine composites were found to increase with increasing the nano-SiO_2 in the matrix composites. In addition, the degradation temperature of the polymer matrix in the Kevlar-reinforced composite was similar to the degradation temperature of the pure matrices (as shown in Figure 5.8). Furthermore, the weight residue at $800^{o}C$ or the char yield of the composite which is related to the flammability of materials and is essential for some ballistic armor applications. The char yields of all composites were found to be 35.4% to 38.1% by weight (for an incorporation of the nano-SiO_2 at 0 to 7% by weight). This value was consisted of residual weight from the polymer matrix and Kevlar[TM] fiber.

5.2.4 Mechanical Property Investigation of Kevlar[TM]-Reinforced Composite

Figure 5.21 shows the flexural modulus of the Kevlar[TM]-reinforced nano-SiO_2 filled polybenzoxazine composite as a function of nano-SiO_2 contents. It can be seen

that the modulus of the composites was decreased with increasing nano-SiO_2 contents added into the polymer matrix. From the results, flexural modulus was slightly decreased from 17.9 GPa of neat polybenzoxazine to 15.2 GPa of the composite with 7wt% nano-SiO_2 filled polybenzoxazine composite as a matrix. From the observed flexural modulus, there are two reasonable explainable for this phenomenon. Firstly, the adhesion between the reinforcing fiber and the nano-SiO_2 filled polybenzoxazine matrix are decreased when increase the nano-SiO_2 content in the matrices. Secondly, the composite with nano-SiO_2 probably have more amounts of voids than the one without nano-SiO_2. This assumption can be proved from the difference between the actual density and theoretical density of both the composite with and without nano-SiO_2. Table 5.2 shows the comparison between theoretical densities and actual densities of Kevlar^{TM}-reinforced nano-SiO_2 filled polybenzoxazine. It can be observed that the actual density of the Kevlar^{TM}-reinforced deviated from the theoretical one at high nano-SiO_2 content. That is because the viscosity of the matrix with nano-SiO_2 was increased with increasing nano-SiO_2. That made it difficult to be wet throughout the fiber without void in the Kevlar-reinforced composite.

Figures 5.22 to 5.24 illustrate the dynamic mechanical properties of their Kevlar^{TM}-reinforced nano-SiO_2 filled polybenzoxazine composites at nano-SiO_2 in the range of 0 to 7% by weight. The storage modulus (G') of the nano-SiO_2filled composites at glassy state was decreased with increasing nano-SiO_2 contents as seen in Figure 5.22. The storage modulus of their composites at its glassy state of 15.3 GPa of neat polybenzoxazine as a matrix and were slightly decreased to 11.0 GPa of 7% by weight of nano-SiO_2 filled polybenzoxazine as a matrix. This phenomenon showed the same trend as the change in flexural modulus observed in the previous experiment. In addition, the storage modulus at glassy state of the composite without nano-SiO_2 was higher than that of the ones with nano-SiO_2. The phenomenon is attributed to the adhesion between fiber and the polymer matrix, and the voids in the composite.

Glass transition temperature (T_g) of Kevlar^{TM}-reinforced composite were also observed in the DMA thermogram based on the maximum peak of loss modulus. Figure 5.23 shows the loss modulus (G") curves of Kevlar^{TM}-reinforced nano-SiO_2 filled polybenzoxazine composites at nano-SiO_2 contents in the range of 0 to 7% by

weight as a function of temperature. This figure exhibits the glass transition temperature of all Kevlar[TM]-reinforced composite. It can be found that the T_g of the Kevlar[TM] reinforced polybenzoxazine composite was 183°C and shift to the high temperature when increasing nano-SiO$_2$ content in polymer matrix. Similarly, these glass transition temperatures exhibited the same trend as the ones obtained by the relaxation peaks of loss tangent thermograms as seen in Figure 5.24.

5.3 Fire Test of the Kevlar[TM]-reinforced Composite

5.3.1 Low Level Ballistic Impact Test

5.3.1.1 Specimen Characterization

This section exhibits low level of ballistic impact evaluation, which was performed on the composite laminates, which were made of Kevlar[TM] fabric impregnated with nano-SiO$_2$ filled polybenzoxazine resin at different nano-SiO$_2$ contents. The dimension of the laminated specimens was 130 mm x 130 mm x 2.0 mm corresponding to 5 piles of the Kevlar[TM]-reinforced composite with areal density of 0.24 g/cm^2. A Kevlar[TM]-reinforced composite consisting of 5 piles was fabricated using the hand-lay up procedure. The nominal weight fraction of polymer matrix was kept constant at 20% to 25%. The laminates were obtained by mechanically gripping two separated 5-ply laminates. From the previous research, we have already known that ballistic energy will be dissipated via the inertial effect when the projectile passes through the gap between two plates of the composite (Pathomsap, 2005).

5.3.1.2 Fire Test to Determine Optimum Fumed Silica Contents

The laminates fabricated with 10 piles of Kevlar[TM]panel i.e. 5/5 panel arrangement of Kevlar[TM]-reinforced nano-SiO$_2$ filled polybenzoxazine composite at various nano-SiO$_2$ contents (0 to 7wt%) were selected for the test. The 9 mm handgun with standard lead projectiles having lead outer coating is used to evaluate the most effective composition of the polymer matrix for ballistic protection.

In addition, the tested laminates were varied with different matrix materials such as bisphenol A-based flexible epoxy, hard epoxy (cured by amine hardener), at the same fiber content were also used to compare its ballistic impact performance with our nano-SiO_2 filled polybenzoxazine matrix composite as shown in Table 5.3. The fire test results of the 10-ply Kevlar[TM]-reinforced nano-SiO_2 filled polybenzoxazine as well as epoxy composites are listed. The results show that the laminates No.1 and No. 2 could not resist the projectiles in this test. While the laminates No. 3 and No. 4 had lower penetration resistance since their front plates were penetrated by the projectile. On the other hand, the firing results for the laminates No. 5, 6, and 7 (corresponding to 3%, 5%, and 7% by weight of nano-SiO2, respectively) exhibited outstanding ballistic impact resistance in comparison with the other composition of the Kevlar[TM]-reinforced polybenzoxazine composites as well as Kevlar[TM]-reinforced epoxy composites as seen in Table 5.3 and Figure 5.25 (a, b). From the results, this phenomenon may be attributed the rigidity of the polybenzoxazine when modified with fumed silica which is related to its wave propagation velocity. The velocity of wave propagation increases with increasing modulus of matrix. The wave velocities of the matrix of the composite using nano-SiO_2 filled polybenzoxazine as a matrix indicated that the composite has capability to spread out the ballistic energy. This capability of the composite led to property is important in ballistic impact resistant mechanism (Jacop, 2001). The value can be used to further clarify the impact failure of the samples. The ballistic impact performance of the Kevlar[TM]-reinforced nano-SiO_2 filled polybenzoxazine revealed relatively larger delaminated area than those of the epoxy and the polybenzoxazine matrix. The delaminated area has been known to be one major component of the energy absorption mechanisms in ballistic impact as discussion in next experimental.

Additionally, this work presents the ballistic impact resistance of the sample No. 8 were consisted of 10 ply Kevlar[TM]-reinforced nano-SiO_2 filled and unfilled polybenzoxazine composite. In each pile, it was consisted of one composite plate filled with nano-SiO_2 in the front layer alternated with one polybenzoxazine plate. The result shows that the samples were able to resist the projectiles in both front and rare faces. However, for this laminate can also be partially attributed to the

mismatch of the elastic constants between the layer of the laminate which produces an abrupt change of the stiffness, and consequently of the mechanical response of the laminate as the elastic shockwaves propagate through it. Moreover, this mismatch of elastic constants is occurring precisely at between the layers of the laminate, favoring delamination. In any respect, these results show that the ballistic behavior is being modified by the presence of fumed silica in polybenzoxazine matrix layers (Nunes et al., 2004)

The ballistic performance of the laminates of our fired composites was evaluated by measuring a diameter of the damage area of the composites and clay witness. The damage area (i.e. deformation depth and diameter) of the rear face and the clay witness after impacted with the projectiles were measured due to the impact energy absorption of the composite led to residual impact energy of the projectile transferred to the clay witness.

Table 5.4 and Figure 5.26 show the damage area of the rear side on the composite after ballistic impact at various matrix compositions. The results revealed that the composites with neat polybenzoxazine matrix (No. 3) gave a relatively larger damage area on the rear side (A^{RS}) than the laminate with the nano-SiO_2 filled polybenzoxazine matrix (No. 4 to 7). It can be seen that the damage area was found to be decreased with increasing nano-SiO_2 content in the matrices as shown in Table 5.4. In addition, the mismatch matrix between the piles of the laminate (No. 8) provided the damage area of rear side was less than that of the neat polybenzoxazine matrix but greater than that of the nano-SiO_2 filed polybenzoxazine matrix. Furthermore, in the ballistic impact test, the residual kinetic energy of the projectile absorbed by the clay witness was investigated with measuring damage area and damage volume of the clay. The lowest damage area of the clay was observed in the composite with nano-SiO_2 filled polybenzoxazine at 7wt% in the matrix were 21.6 mm of damage depth, 68.6 mm of damage diameter, and 26.5 ml of damage volume.

The delamination area is one of the important factors that related to the energy absorption of laminate, because it was a mechanism of energy absorption in composite materials. Comparing the ballistic performance of the nano-SiO_2 filled

polybenzoxazine and the polybenzoxazine composites, the nano-SiO_2 filled polybenzoxazine composite panel exhibited greater delaminated area compared to the much smaller delaminated area of the polybenzoxazine composites. It was obvious improvement in the energy absorption characteristics. Additionally, Figure 5.27 shows the delaminated area of both the front side (A^{FS}) and damage area or cone deformation of rear side (A^{RS}) of the composites with and without nano-SiO_2 filled at various nano-SiO_2 contents. From the figure, it can be seen that our composite without nano-SiO_2 had a small A^{FS}, and large A^{RS}. For the nano-SiO_2 filled composites at various nano-SiO_2 contents, it was found that the delaminated region generated on the A^{FS} was large, which led to small A^{RS}. This phenomenon of the composite with nano-SiO_2 was possibly due to the rigidity of polymer matrix was able to destroy the projectiles and reduced the impact energy that could transfer to the adjacent plate when compare with polybenzoxazine matrix. In addition, the adhesion between reinforced fiber and polymer matrix is one of the important factors that may be explained of this phenomenon, it was possible due to the strong adhesion between reinforcing fiber and polymer matrix, which resulted in low energy absorption of the composite. In addition, high adhesion between fiber and matrix made composite armor produced from the composite without nano-SiO_2 showed also high flexural modulus as seen in Figure 5.21. In case of the composites with nano-SiO_2, the weak adhesion between the Kevlar^{TM} fiber and all nano-SiO_2 filled polybenzoxazine matrices resulted in rather low modulus. This confirms the necessity of identifying optimal fiber-matrix interactions in order to yield a composite system of outstanding ballistic performance. The variation in the nano-SiO_2 filled polybenzoxazine compositions allowing an optimal interaction between the composite matrix and its reinforcing fiber was attributed to the outstanding ballistic performance obtained.

In general, the properties of the interphase and degree of adhesion between the fiber and the matrix govern load transfer between the composite constituents. Also, the properties of the interphase are critical to global composite performance such as impact and ballistic resistance. An optimum balance of ballistic impact and durability performance from the composite armor can be achieved by tailoring the fiber-matrix interphase (Tanoglu et al., 2001). From this result of the

delaminated area and the degree of adhesion of the composites after impacting with the projectile, it can be concluded that the polymer matrix should provide modulus suitable to both destroy the shape projectile as its structural integrity and absorb high energy. From the overall results, it is apparent that the Kevlar^{TM}-reinforced 7wt% nano-SiO$_2$ filled polybenzoxazine composite had the optimal ballistic performance because of the preferable adhesion between the Kevlar^{TM} fiber and matrix. That has suitable adhesion should provide optimal capability to spread out ballistic energy, its impact energy can be effectively transferred along the fiber. Consequently, the 7wt% nano-SiO$_2$ filled polybenzoxazine matrix was selected for the Kevlar^{TM}-reinforced composite system for our ballistic resistance composite in the next experiment.

5.3.2 High Level Ballistic Impact test of NIJ Level III-A

5.3.2.1 Specimen Characterization

In high level ballistic impact test, a projectile velocity is required to follow NIJ standard (level III-A). This evaluation was performed on the composite laminates which were made of Kevlar^{TM} fabric impregnated with nano-SiO$_2$ filled polybenzoxazine at 7wt% of nano-SiO$_2$ resin. The dimensions of the laminated specimens were 130 mm x 130 mm. A Kevlar^{TM}-reinforced composite consisting of 25 piles, 30 piles, and 35 piles were fabricated using the hand-lay up procedure. The nominal weight fraction of polymer matrix was kept constant in the range of 20% to 25%. Our composites sample with the combined thickness of 25 plies were arranged in two patterns i.e. 15/5/5 configuration and 15/10 configuration. The sample with the combined thickness of 30 plies were arranged in two patterns i.e. 15/5/5/5 configuration and 15/10/5 configuration. In the case of and the sample with thickness of 35 plies were arranged in three patterns i.e. 10/10/5/5/5 configuration, 15/5/5/5/5 configuration, and 15/10/5/5 configuration. The test outcomes are listed in Table 4.2.

From the previous research, we have already known that specimen's thickness and arrangement of the composite panel are important factors for the ballistic performance of ballistic composite. The composite having at least 50 piles of the Kevlar cloth with areal density 0.24 g/cm^2 in 10 piles/panel can protect the

ballistic impact at level III-A. They also found that the 30 piles panel of the composite should be placed in the front face of the composite panel assembly to yield the best ballistic resistance (Pathomsap, 2005).

5.3.2.2 Ballistic Impact Test of NIJ Level III-A

The ballistic impact velocities required by NIJ standard for level III-A was used to study the effect of the composite panel thickness and arrangement based on the Kevlar[TM]-reinforced 7wt% nano-SiO$_2$ filled polybenzoxazine composites. In this test, the dimensions of composite sample were approximately 2.1 mm in thickness of 5 piles/panel, 3.9 mm and 5.6 mm in thickness of 10 piles/panel, and 15 piles/panel of composite, respectively. All of the laminates were fired with a .44 Magnum 240 grains with impact velocity of 436 m/s as following NIJ standard for level III-A. It is noted that the level III-A is the maximum level observed in the polymer composite protection.

Table 5.5 shows the overall results of their ballistic performance, evaluated by the damage area. The results revealed that the laminates fabricated with 25 piles did not meet the requirement of the NIJ standard for level III-A of ballistic protection. It indicates that the composites possessed insufficient energy absorption to stop the level III-A projectile. For the laminates with thickness 30 and 35 piles exhibited outstanding ballistic impact resistance as seen the Figure 5.28. Therefore, the number of piles of the composites had an effect on impact energy absorption capability, i.e. the diameter and depth of clay were found to decrease with increasing number of piles of the composite. Figure 5.28 shows the image of delamination and damage areas of the laminate after the fire test. It can be seen that the composite was thickness at least 30 piles can stop the projectiles with only partial penetration without perforation.

Table 5.5 describes the effect of the arrangement of the laminates, the sample with combined thickness of 35 piles prepared with various types of arrangement, i.e. 10/10/5/5/5 configuration, 15/5/5/5/5 configuration, and 15/10/5/5 configuration. It can be indicated that the deformation depth and diameter of the clay

witness of composite sample with arrangement of 15/10/5/5 were less than those of the sample with the arrangement of 15/5/5/5/5 and 10/10/5/5/5 configuration respectively. Consequently, the composite with arrangement of 15/10/5/5 possessed greater ballistic performance than the other ones. This result is corresponded to our previous studies (Pathomsap, 2005 and Lorjai, 2006). In comparison of the deformation area of 30-pile composites for 15/5/5/5 configuration and 15/10/5 configuration, the composite with 15/10/5 configuration was able to meet the requirement for the level III-A of NIJ standard for ballistic protection, but the one with 15/5/5/5 configuration did not. Therefore, it can be confirmed that the configuration of composite panel in the fire test was an important factor on the ballistic performance of the composite.

In order to observe the effect of the number of ply in front of plate of the composite on the ballistic resistant efficiency, the composite of 35 piles were prepared with various types of arrangement, i.e. as 10/10/5/5/5 configuration, 15/5/5/5/5 configuration, and 15/10/5/5 configuration. Table 5.5 and Figure 5.29 shows the deformation area, which was represented to energy absorption of the composite. It is apparent that the sample (having the front plate of 15-ply panel and the next plate of 10-ply panel) rendered greater ballistic performance than the other two composites (the one having the front plate of 15-ply panel and the next plate of the 5-ply panel, and the one having the two front plates of 10-ply panel). Consequently, the diameter and the depth of the clay in the fire test were found to decrease with increasing the number of piles at the front plate and the second plate. As shown in Figure 5.29, the rear side picture was clearly demonstrated that the fiber failure of the composite with the front panel of 10 piles was more than that with the front panel of 15 piles. The front panel with at least 15 plies of Kevlar[TM] cloth was thus necessary for the level III-A resistance of perforation and was supposed to possess sufficient properties to destroy or deform the shape of the projectile. As a result, the kinetic energy was substantially reduced before piecing through the rear plate of 10 piles thick. Moreover, the energy might also be dissipated via the inertia effect when the projectile passed through the gap between the two plates.

Figure 5.30 shows the images of the projectile before and after impacting against of the armor composite for lower ballistic test and at high ballistic impact test, respectively. Figure 5.30 (a), shows the results of low ballistic test with the standard lead projectile having outer-coating was shot using a 9 mm handgun. In comparison between the Kevlar^{TM}-reinforced polybenzoxazine composite and the Kevlar^{TM}-reinforced nano-SiO$_2$filled polybenzoxazine composite, there were produce a huge damage on the projectile itself. For the Kevlar^{TM}-reinforced nano-SiO$_2$ filled polybenzoxazine composite had larger damage on the projectile shape after testing on the composite than without nano-SiO$_2$. Moreover a bigger cone of fragments (as revealed to larger rear side of cone deformation) was also found. This phenomenon is possibly due to the effect of nano-SiO$_2$ filled into polybenzoxazine resin. It is believed that the nano-SiO$_2$ in the composite was able to destroy the shape of the projectile and reduced the impact energy that could transfer to the adjacent plate. In the other word, this material could improve the impact performance of the composite. In general, the kinetic energy was absorbed and related to some basic factors, such as mechanical properties, matrix properties and interfacial strengths (Morye et al., 2000).

Figure 5.30 (b) shows the projectiles before and after the ballistic impact test according to NIJ standard (level III-A) of Kevlar^{TM}-reinforced with 7wt% nano-SiO$_2$ filled polybenzoxazine composite. The composites were prepared with varied types of arrangement as 10/10/5/5/5 configuration, and 15/10/5/5 configuration. This result was corresponded to that of the Figure 5.30 (a). It was clearly demonstrated the number of piles in front plate of composite resulted is consumed to destroy the shape of the projectile and yield the best ballistic efficiency.

From the overall results presented in this work, it is apparent that the suggested condition for best ballistic performance to destroy the projectile is that the laminates with 7wt% nano-SiO$_2$ filled-polybenzoxazine as a matrix in the Kevlar^{TM}-reinforced composite and the use of at least 15 piles as the front plate. Moreover, the arrangement of the composite panel had an effect to their ballistic resistance performance as well.
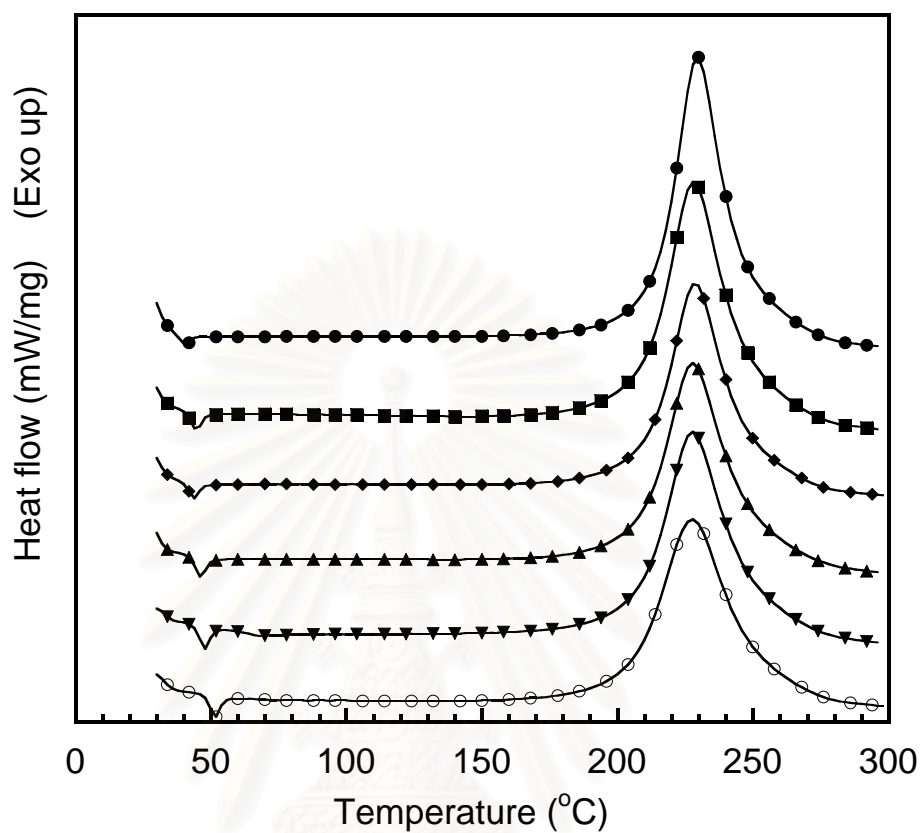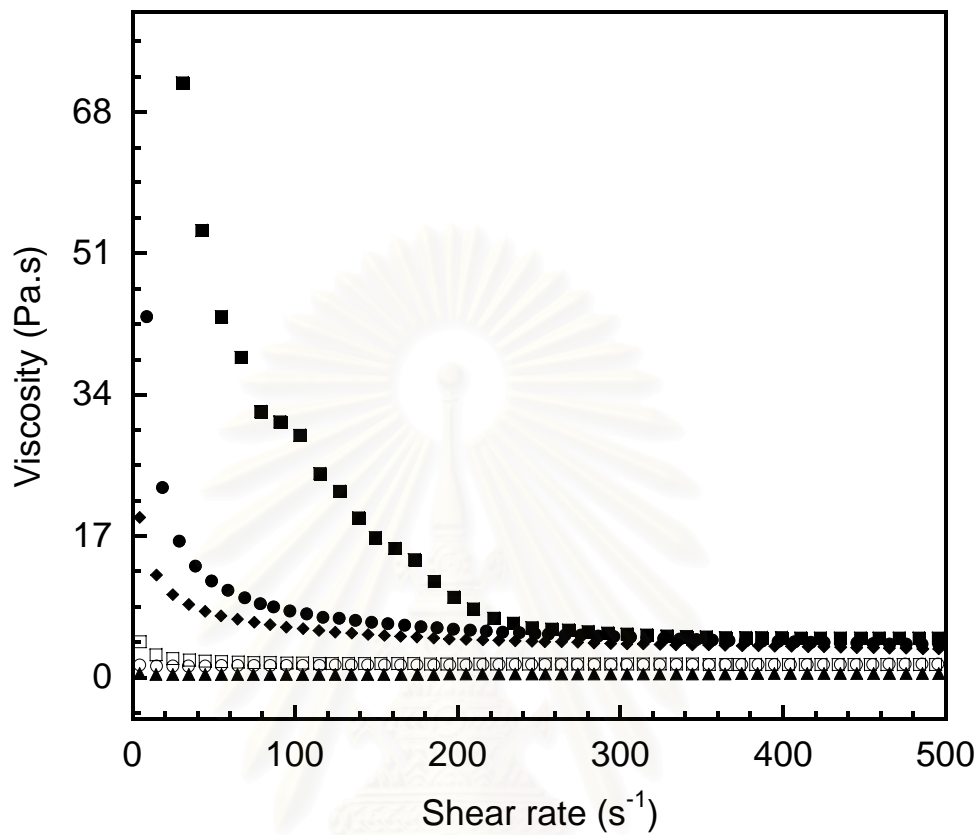
Figure 5.1: DSC thermograms of benzoxazine molding compound at different SiO_2
contents: (●) neat benzoxazine monomer, (■) 1wt%, (♦) 3wt%, (▲)
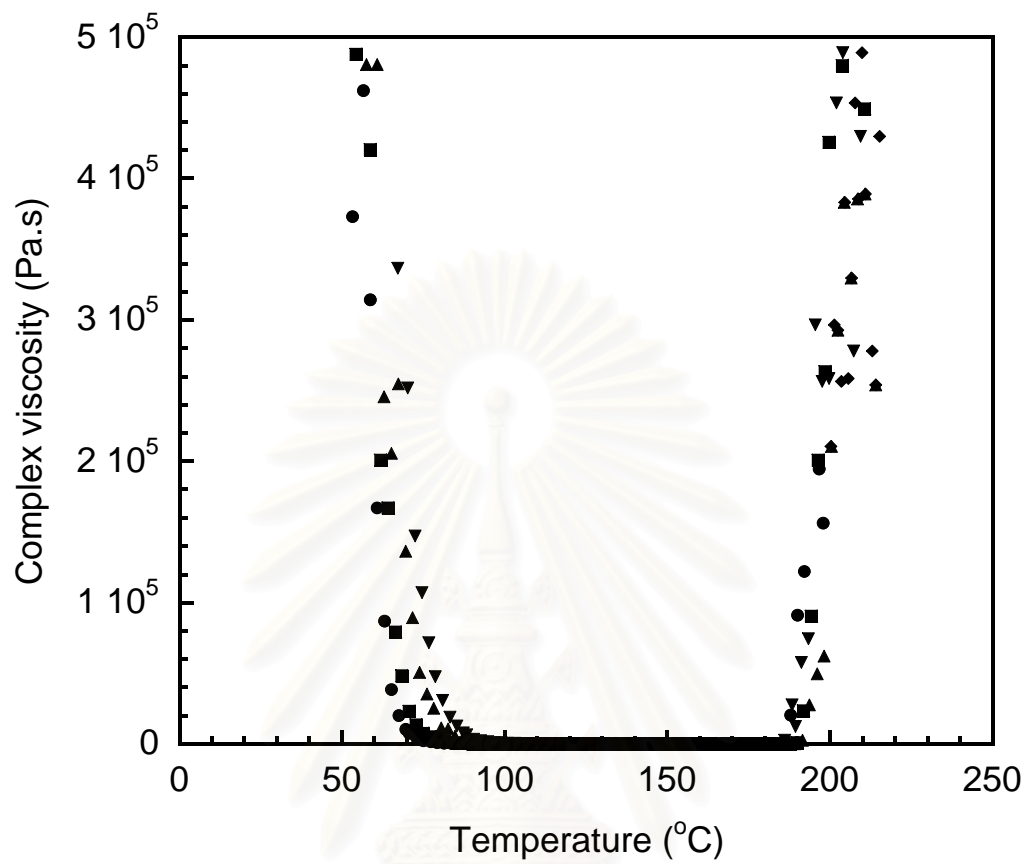5wt%, (▼) 7wt%, (○) 10wt%.
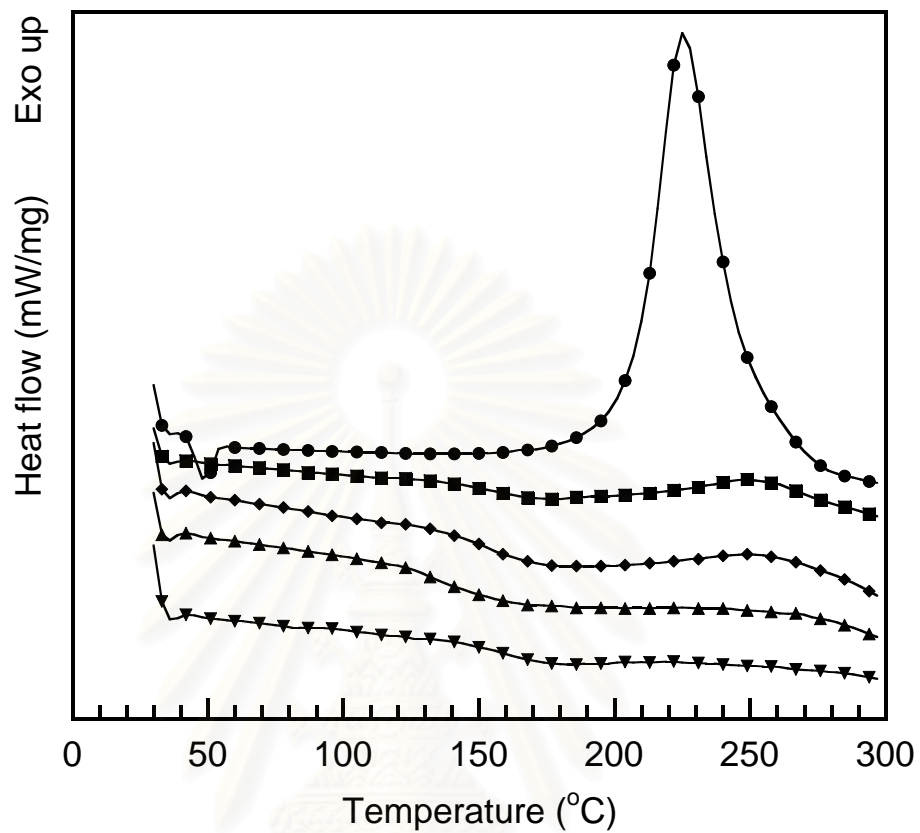
Figure 5.2: DSC thermograms of the composite (10wt% nano-SiO$_2$) at various post-
curing times at 200°C in an oven (after pressing in a hot-press machine
at 160°C for 2 h, and 180°C for 2 h): (●) Uncured molding compound,
(■) 1 hour, (♦) 2 hour, (▲) 3 hour, (▼) 4 hour.

Figure 5.3: Viscosity of benzoxazine molding compound at different SiO$_2$ contents at 120°C: (▲) neat benzoxazine monomer, (○) 1wt%, (□) 3wt%, (♦) 5wt%, (●) 7wt%, (■) 10wt%.
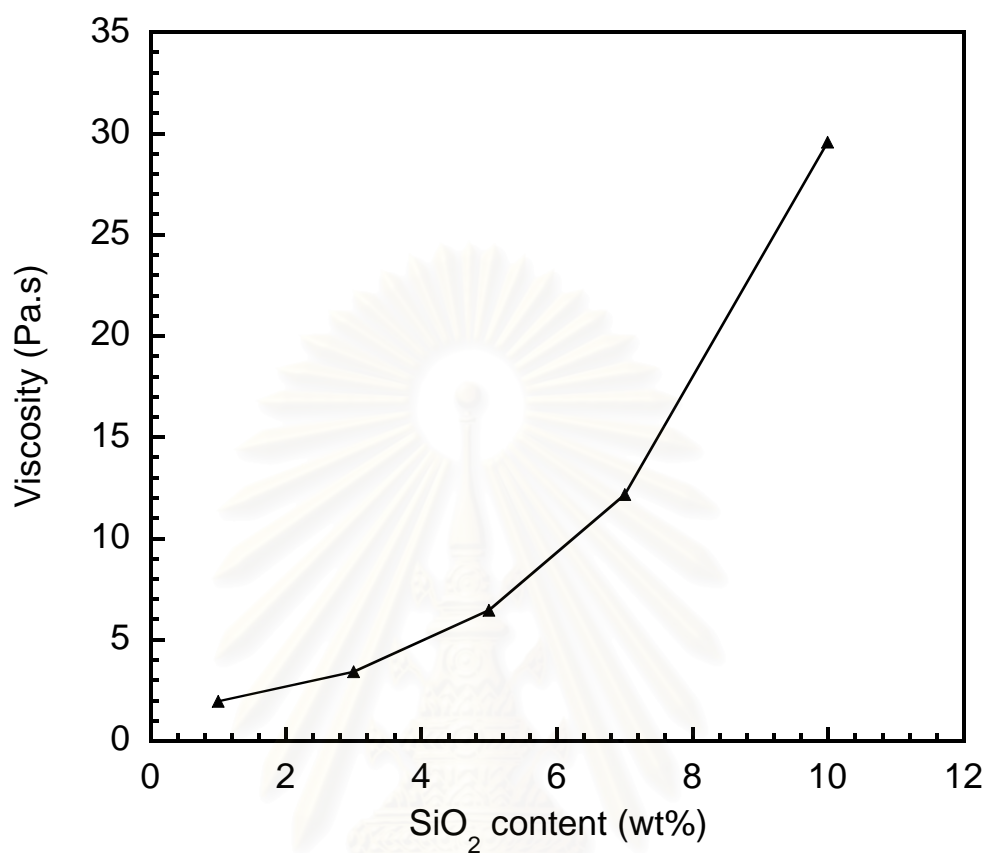
Figure 5.4: Relation between SiO_2 content and viscosity of benzoxazine molding
compound polybenzoxazine.

Figure 5.5: Processing window of benzoxazine molding compound at different SiO$_2$
contents: (●) 1 wt%, (■) 3wt%, (♦) 5wt%, (▲) 7wt%, (▼) 10wt%.
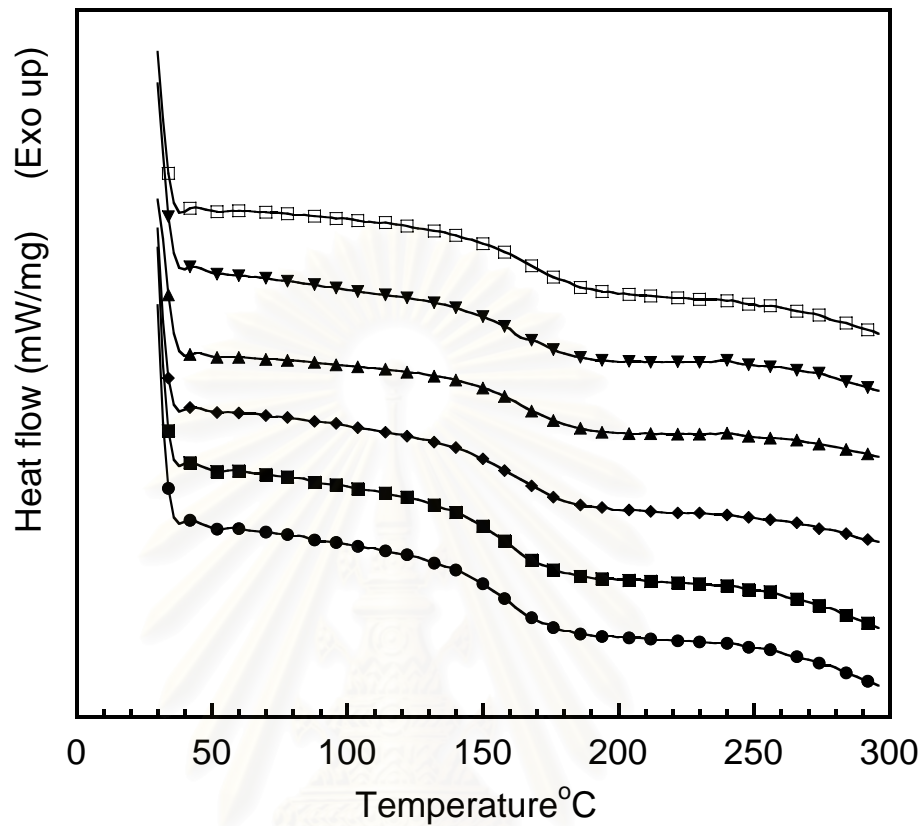
Figure 5.6: DSC thermograms showing glass-transition temperature of nano-SiO$_2$
filled polybenzoxazine composite: (●) neat polybenzoxazine (PBZ), (■)
1wt% nano-SiO$_2$ filled PBZ, (♦) 3wt% nano-SiO$_2$ filled PBZ, (▲) 5wt%
nano-SiO$_2$ filled PBZ, (▼) 7wt% nano-SiO$_2$ filled PBZ, (□) 10wt%
nano-SiO$_2$ filled PBZ.
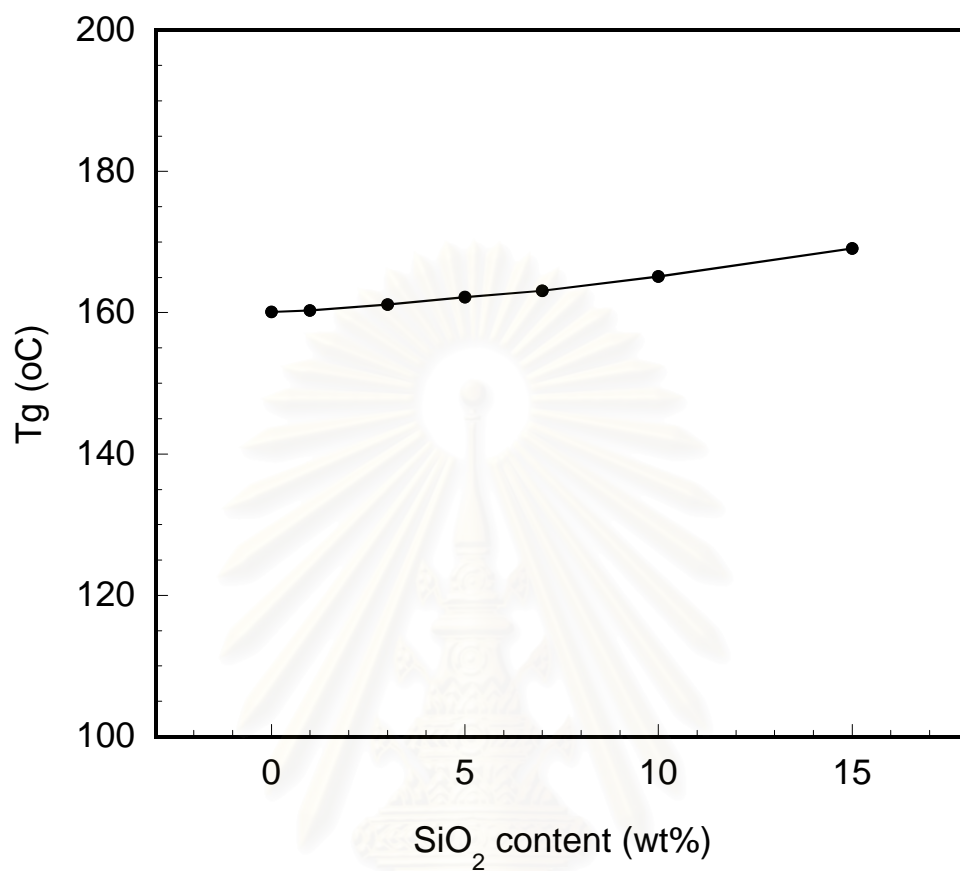
Figure 5.7: Relation between SiO₂ content and glass transition temperature of nano-SiO₂ filled polybenzoxazine composite.
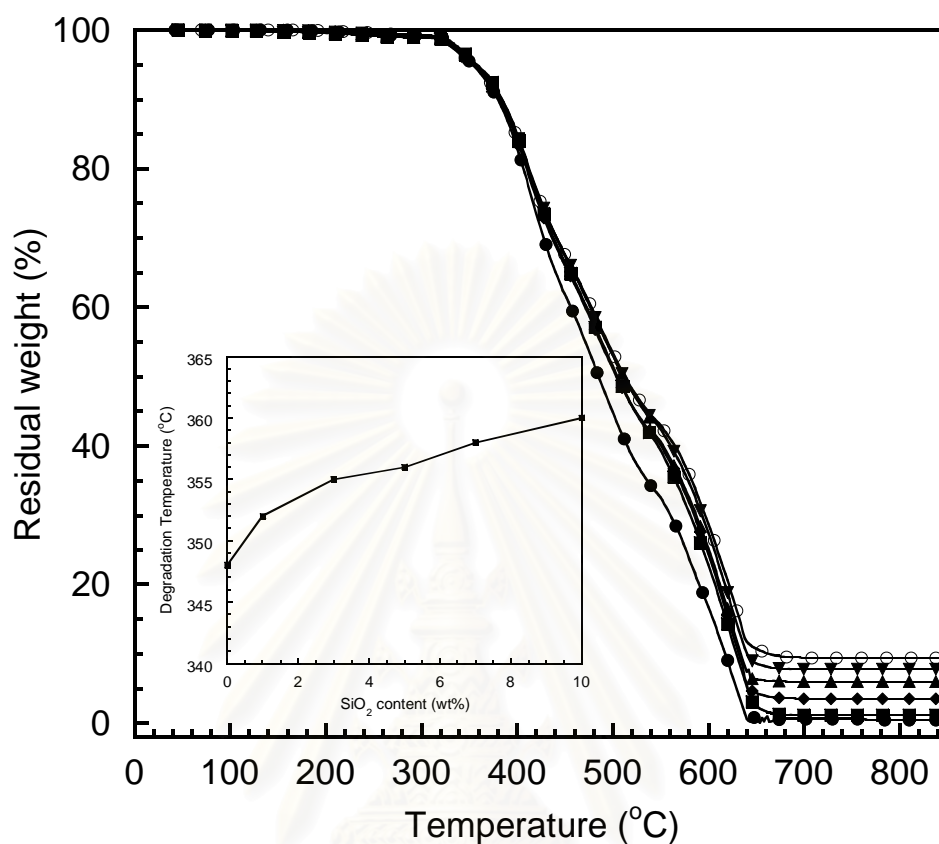
Figure 5.8: TGA thermograms of nano-SiO$_2$ filled polybenzoxazine composites (burned in oxygen): (●) neat polybenzoxazine (PBZ), (■) 1 wt% namo-SiO$_2$ filled PBZ, (♦) 3 wt% nano-SiO$_2$ filled PBZ, (▲) 5 wt% nano-SiO$_2$ filled PBZ, (▼) 7 wt% nano-SiO$_2$ filled PBZ, (○) 10 wt% nano-SiO$_2$ filled PBZ.

Table 5.1: Thermal characteristics of polybenzoxazine and nano-SiO$_2$ filled polybenzoxazine composites.

| Resins	Degradation Temperature (^{o}C)		Solid residue (%)
	5% weight loss	10% weight loss	
PBZ	348	376	0.4
1% SiO$_2$/PBZ	352	378	1.1
3% SiO$_2$/PBZ	355	380	3.5
5% SiO$_2$/PBZ	356	382	5.0
7% SiO$_2$/PBZ	358	383	7.7
10% SiO$_2$/PBZ	360	384	9.4
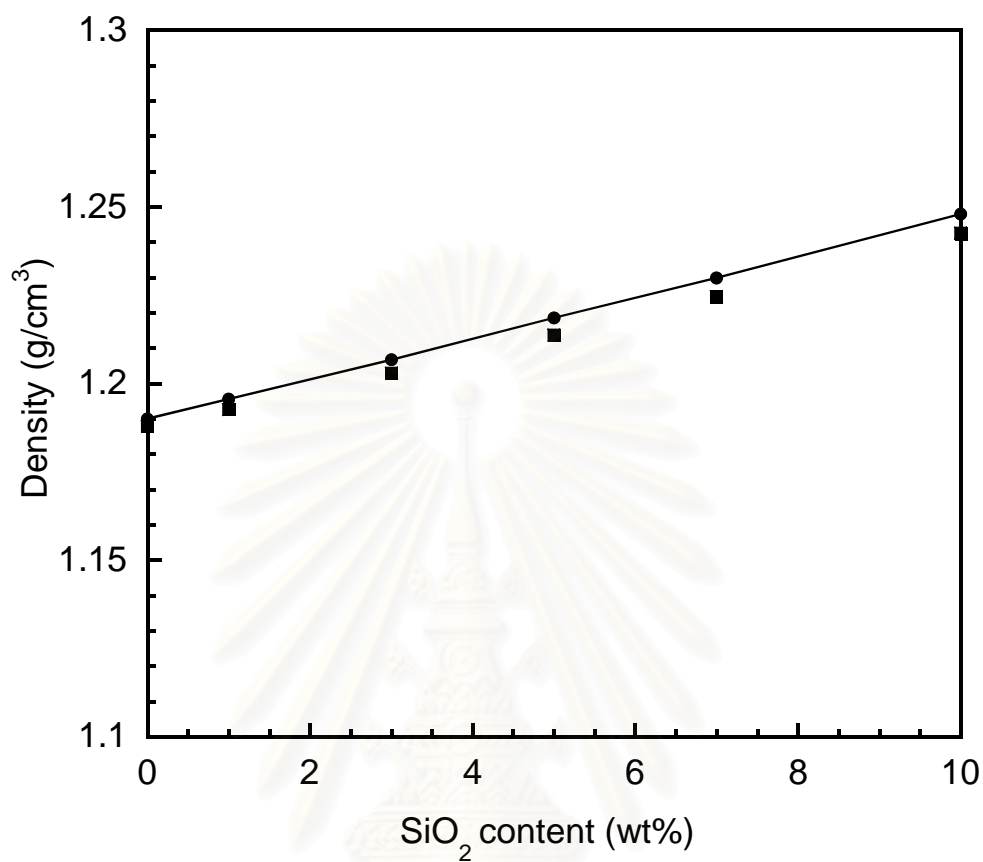
Figure 5.9: Theoretical and actual density of nano-SiO$_2$ filled polybenzoxazine
composites at different content of nano-SiO$_2$: (●) theoretical density,
(■) actual density.
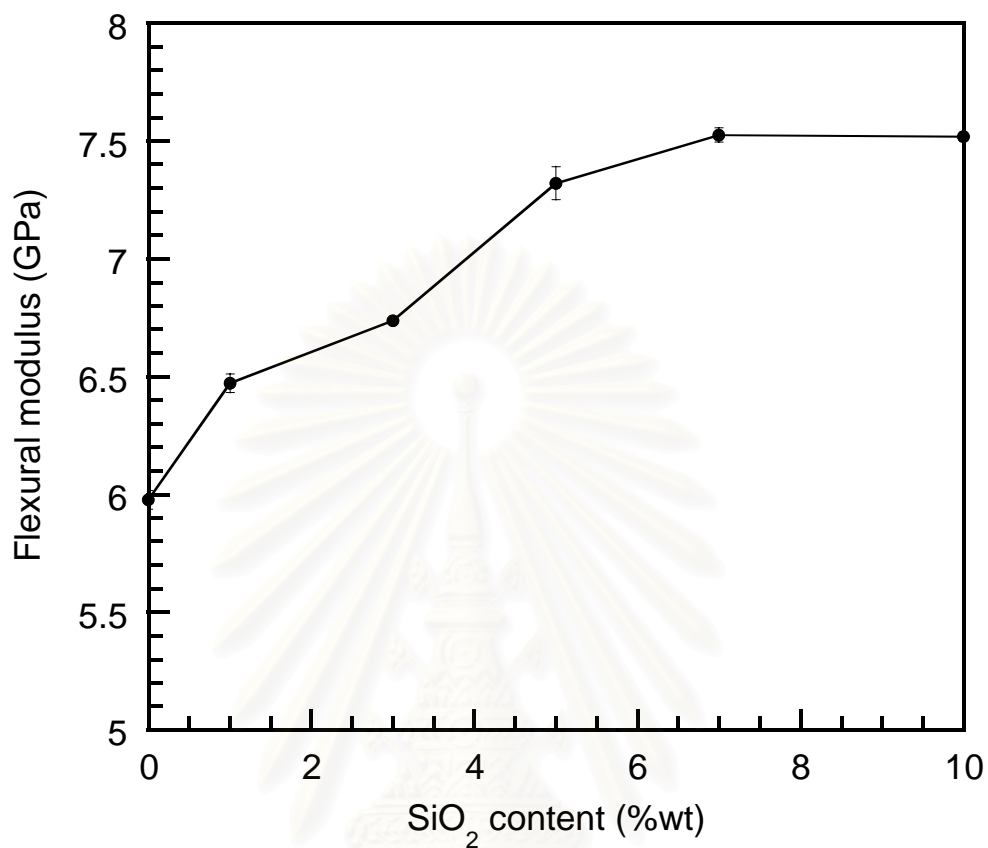
Figure 5.10: Relation between SiO₂ content and the flexural modulus of nano-SiO₂
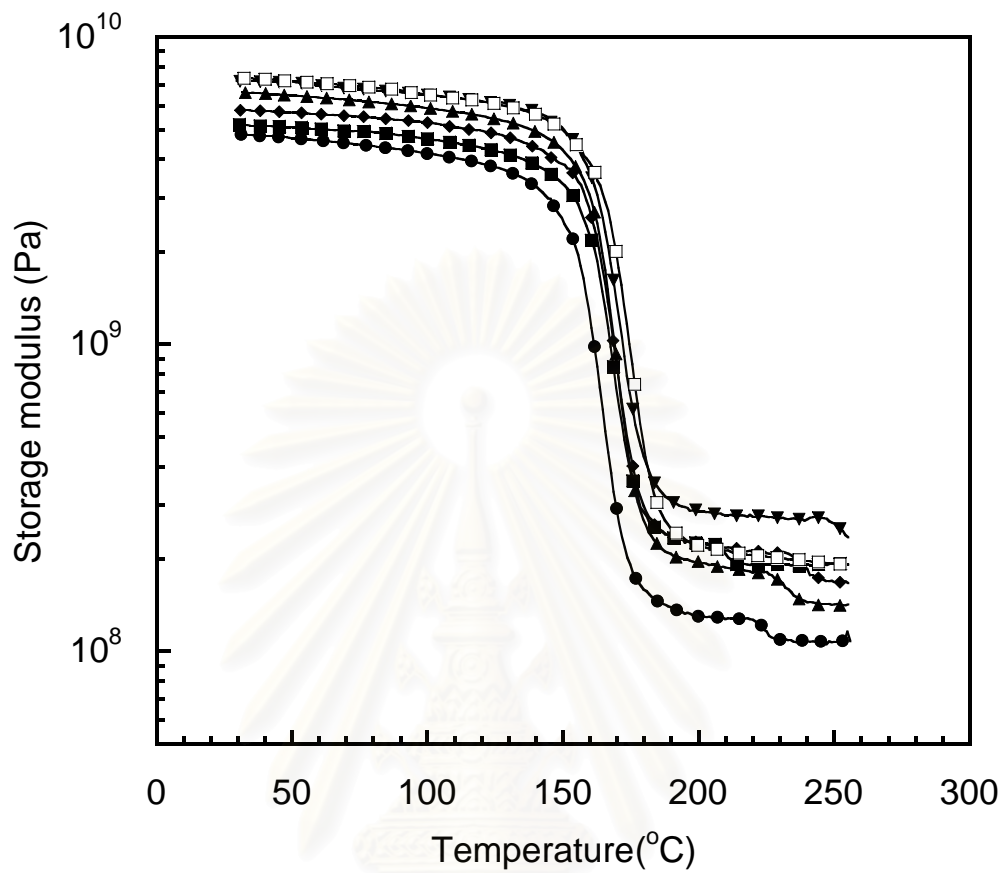filled polybenzoxazine composites.
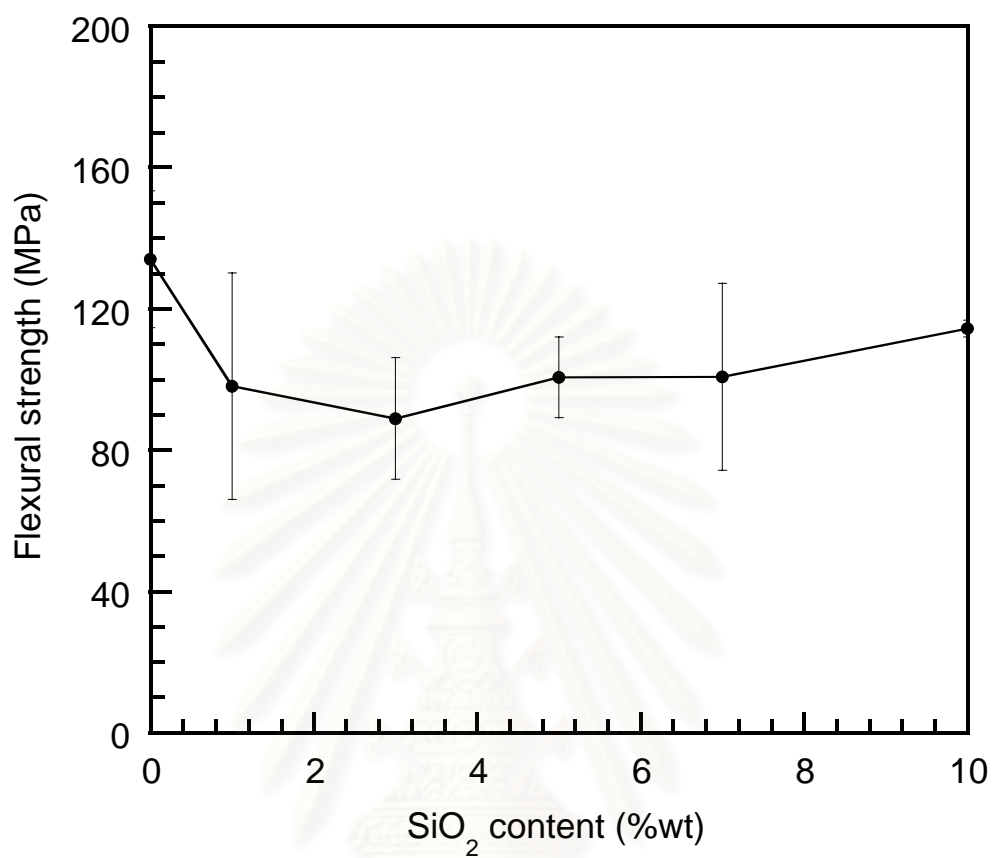
Figure 5.11: Relation between SiO_2 content and the flexural strength of nano-SiO_2 filled polybenzoxazine composites.

Figure 5.12: DMA thermograms of storage modulus of nano-SiO$_2$ filled polybenzoxazine composites: (●) neat polybenzoxazine (PBZ), (■) 1% nano-SiO$_2$ filled PBZ, (♦) 3% nano-SiO$_2$ filled PBZ, (▲) 5% nano-SiO$_2$ filled PBZ, (▼) 7% nano-SiO$_2$ filled PBZ, (□) 10% nano-SiO$_2$ filled PBZ.
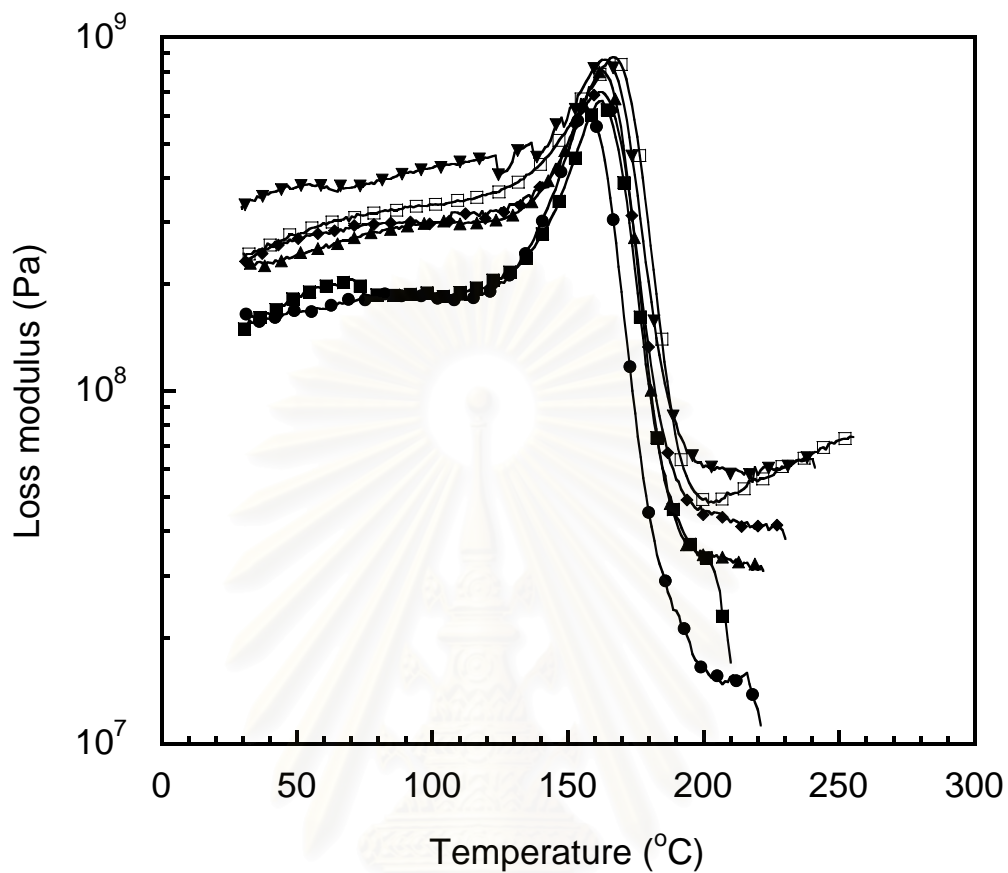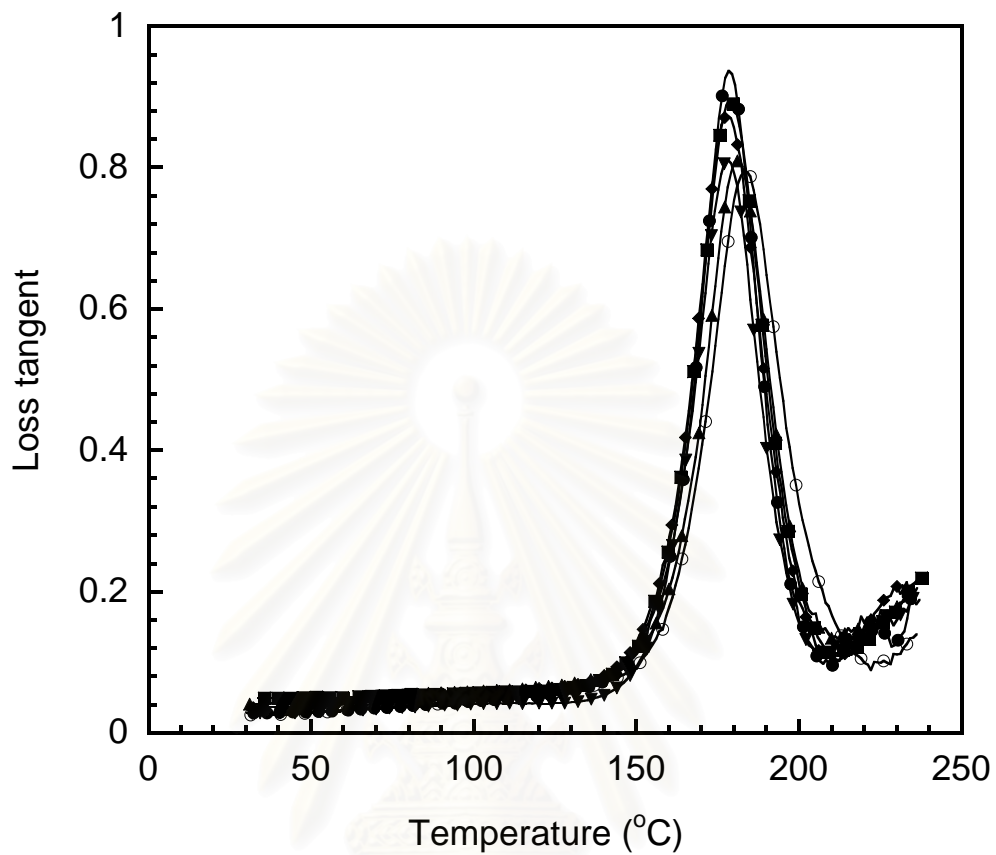
Figure 5.13: DMA thermograms of loss modulus of nano-SiO$_2$ filled polybenzoxazine composites: (●) neat polybenzoxazine (PBZ), (■) 1% nano-SiO$_2$ filled PBZ, (♦) 3% nano-SiO$_2$ filled PBZ, (▲) 5% nano-SiO$_2$ filled PBZ, (▼) 7% nano-SiO$_2$ filled PBZ, (□) 10% nano-SiO$_2$ filled PBZ.
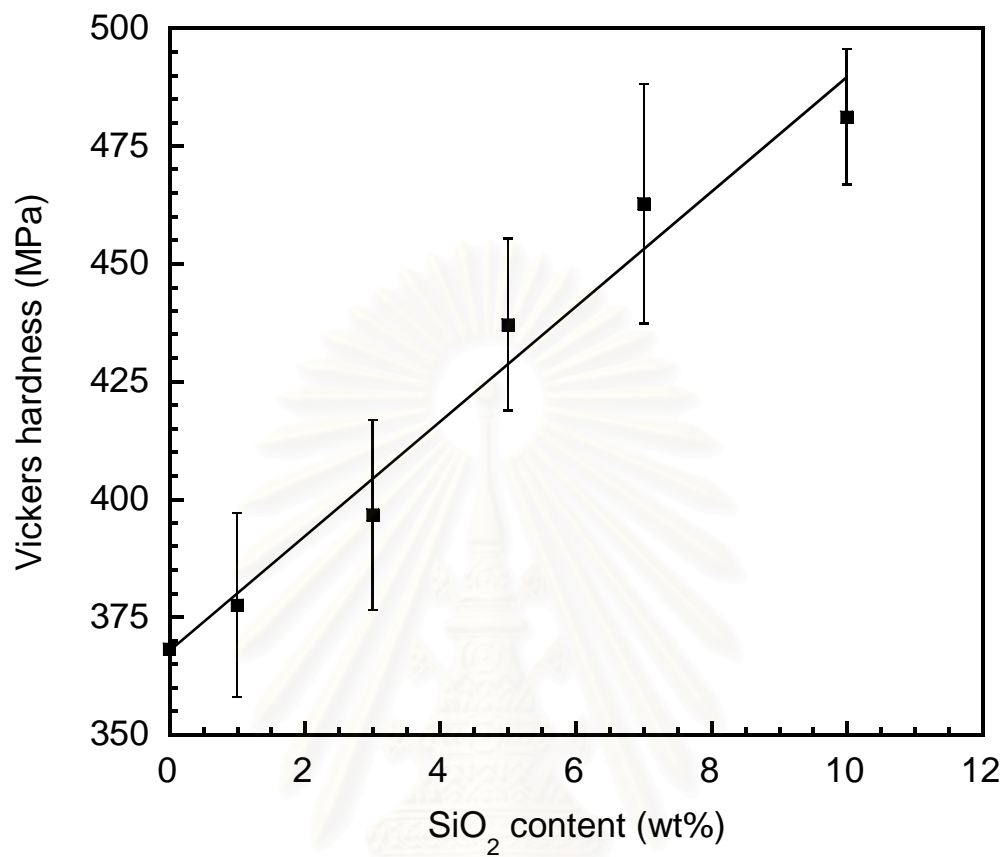
Figure 5.14: DMA thermograms of loss tangent of nano-SiO$_2$ filled polybenzoxazine composite: (●) neat polybenzoxazine (PBZ), (■) 1% nano-SiO$_2$ filled PBZ, (♦) 3% nano-SiO$_2$ filled PBZ, (▲) 5% nano-SiO$_2$ filled PBZ, (▼) 7% nano-SiO$_2$ filled PBZ, (□) 10% nano-SiO$_2$ filled PBZ.

Figure 5.15: Relation between SiO_2 content and micro Vickers hardness of nano-SiO_2 filled polybenzoxazine composites.
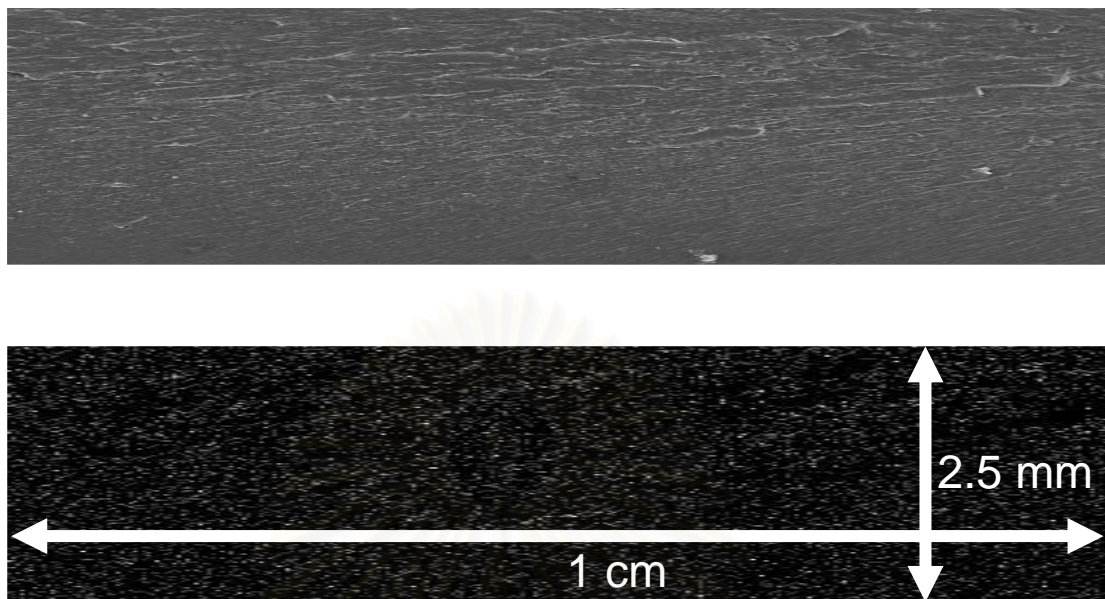
Figure 5.16: EDX mapping along fracture surface with the thickness of 2.5 mm at
1000 times magnification of 10 wt% nano-SiO$_2$ filled polybenzoxazine
composite.
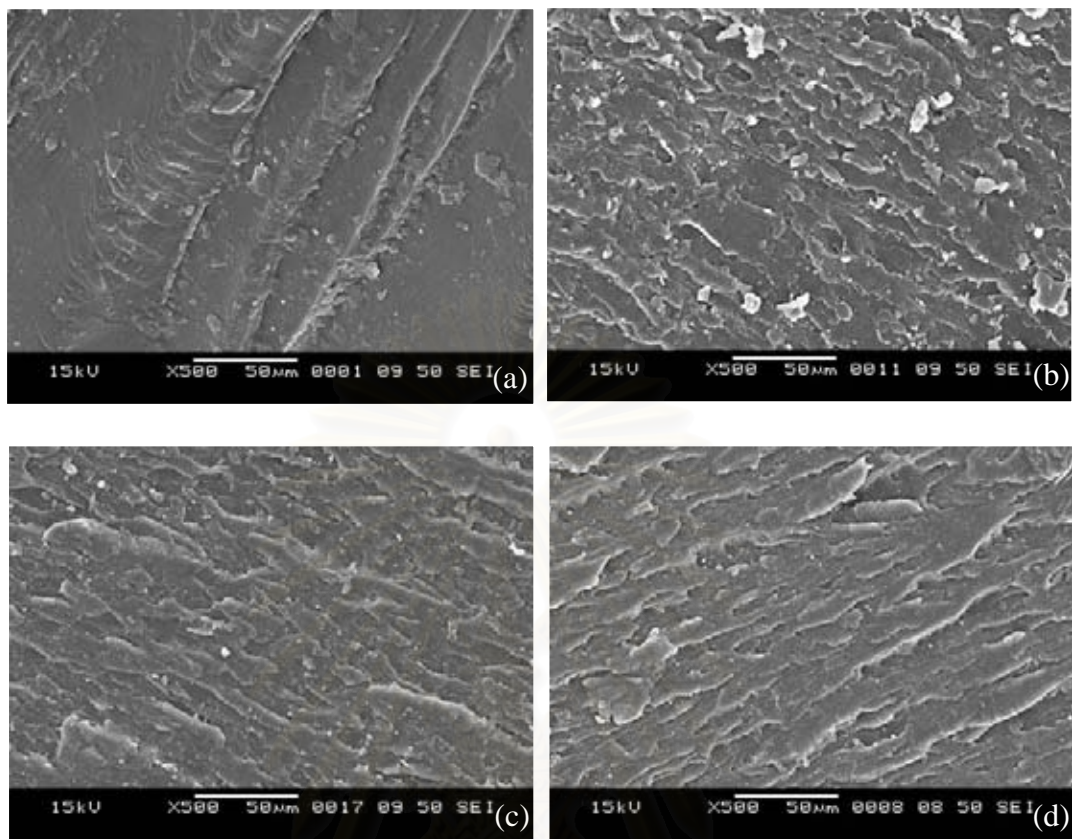
Figure 5.17: SEM micrographs of fracture surface of nano-SiO$_2$ filled
polybenzoxazine composites: (a) neat polybenzoxazine (PBZ), (b) 3
wt% nano-SiO$_2$ filled PBZ, (c) 7 wt% nano-SiO$_2$ filled PBZ, (d) 10wt%
nano-SiO$_2$ filled PBZ.
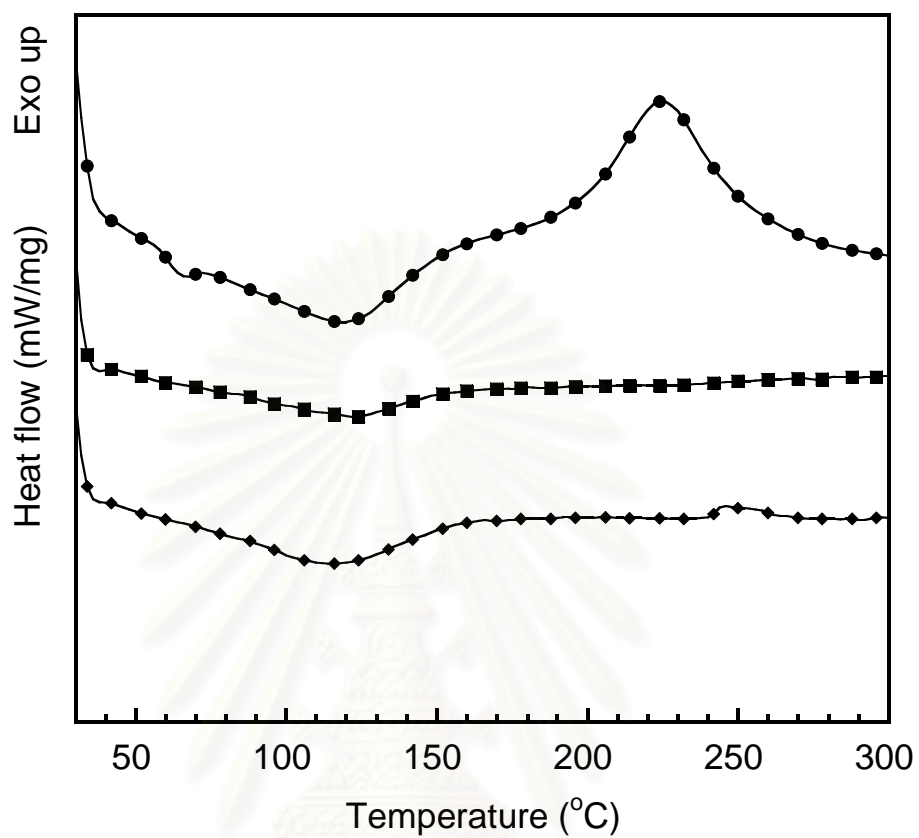
Figure 5.18: DSC thermograms of Kevlar[TM]-reinforced nano-SiO$_2$ filled
polybenzoxazine at 7 wt% SiO$_2$ contents: (♦) Kevlar[TM] fiber,
(●) Uncured composite, (■) 160°C/2 h, 180°C/2 h and 200°C/4 h.
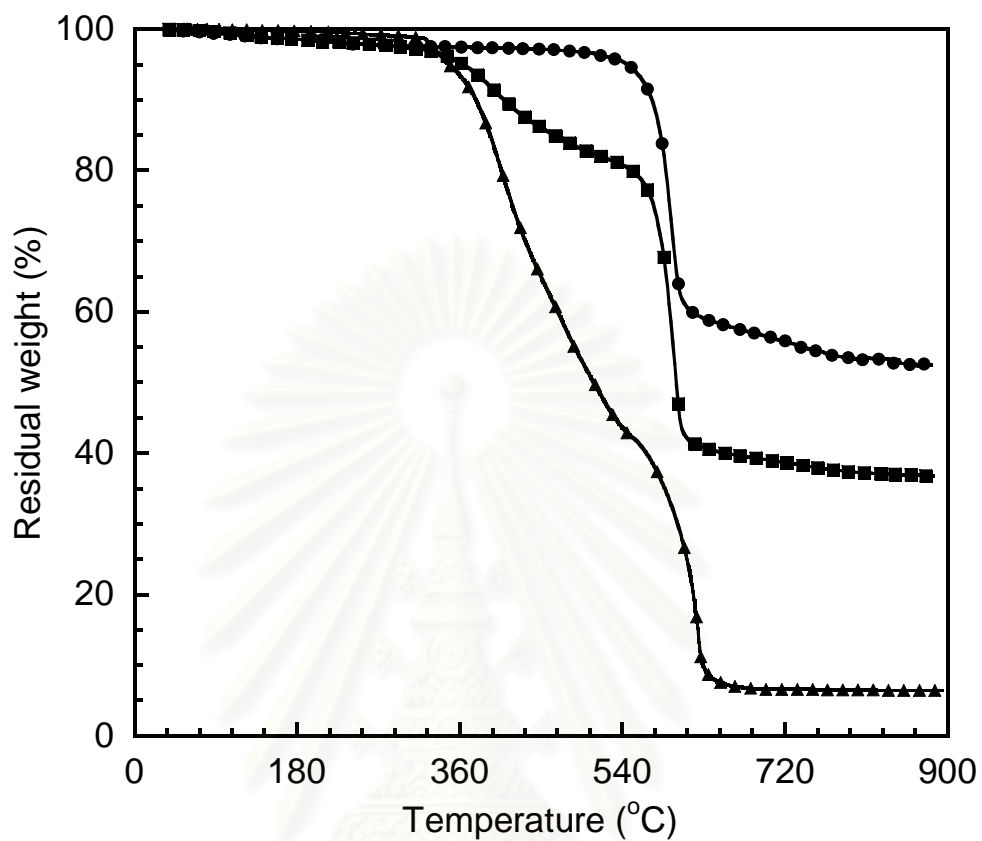
Figure 5.19: Composition determination of Kevlar^{TM}-reinforced nano-SiO$_2$ filled polybenzoxazine composites at 7 wt% SiO$_2$ contents: (●) Kevlar^{TM} fiber, (■) composite, (▲) matrix.
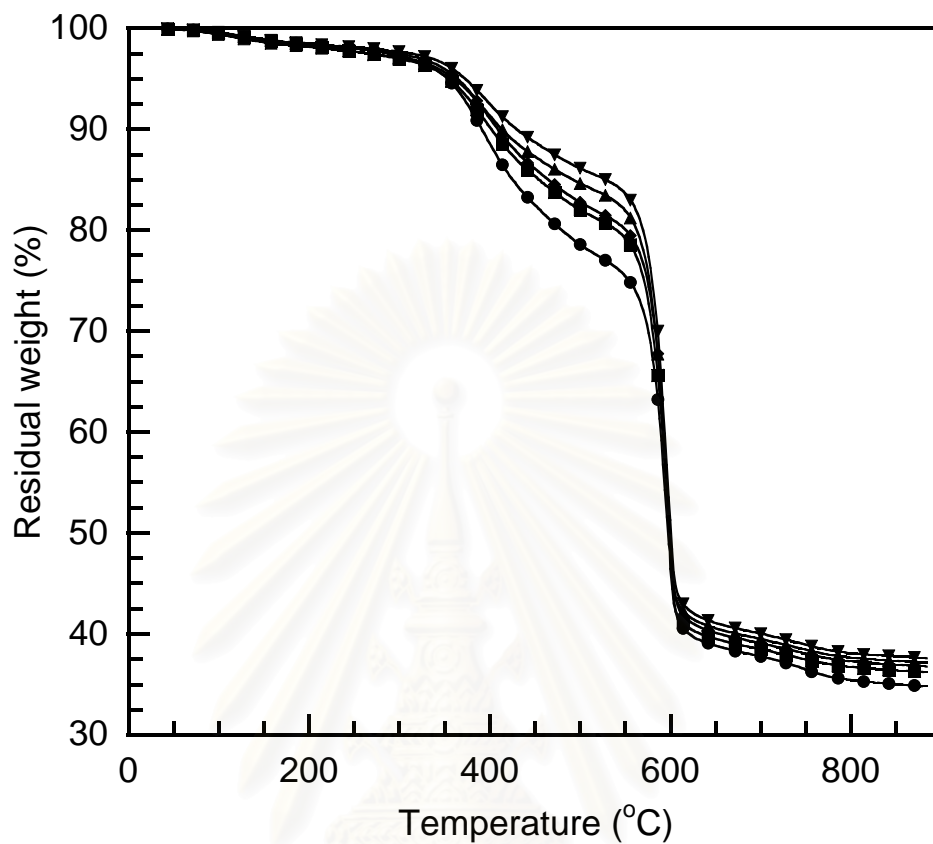
Figure 5.20: TGA thermograms of Kevlar^{TM}-reinforced nano-SiO$_2$ filled polybenzoxazine composites at different SiO$_2$ contents: (●) neat polybenzoxazine (PBZ), (■) 1 wt% nano-SiO$_2$, (♦) 3 wt% nano-SiO$_2$, (▲) 5 wt% nano-SiO$_2$, (▼) 7 wt% nano-SiO$_2$.
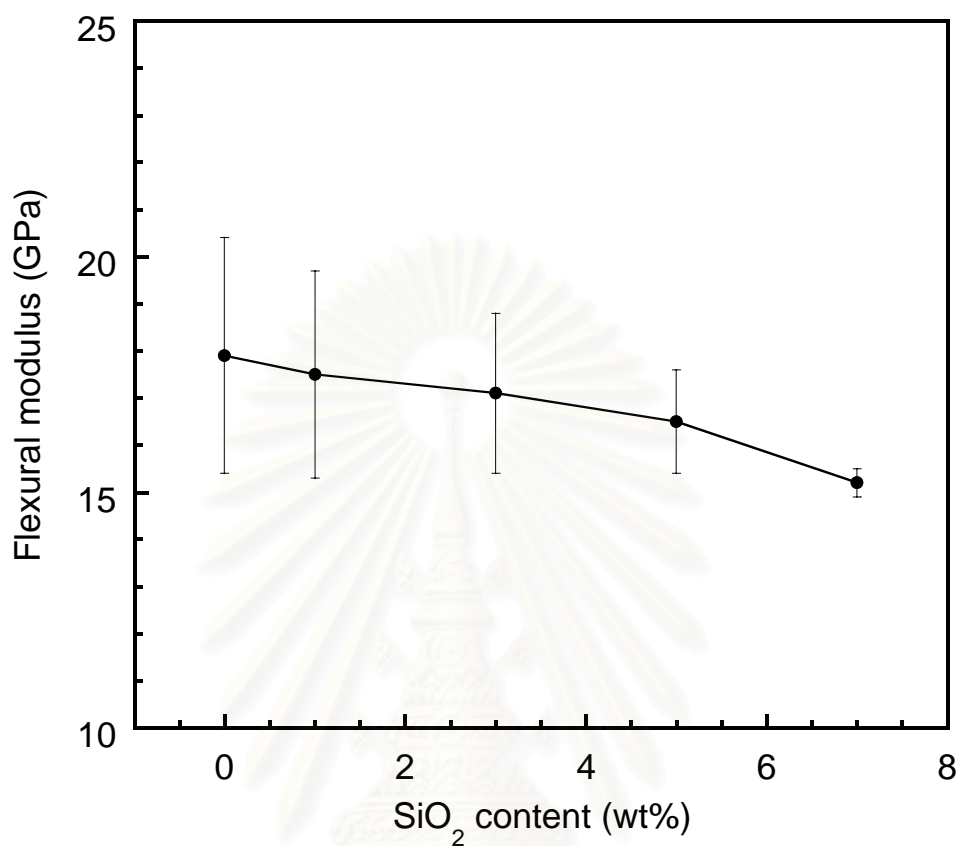
Figure 5.21: Relation between SiO_2 content and the flexural modulus of Kevlar[TM]-
reinforced nano-SiO_2 filled polybenzoxazine composites.

Table 5.2: Density of Kevlar[TM]-reinforced nano-SiO$_2$ filled polybenzoxazine
composites at various nano-SiO$_2$ contents.

SiO$_2$ Content (wt%)	Theoretical Density (g/cm^3)	Actual Density (g/cm^3)
0	1.37	1.31±0.002
1	1.38	1.30±0.010
3	1.38	1.29±0.007
5	1.39	1.28±0.014
7	1.40	1.26±0.005
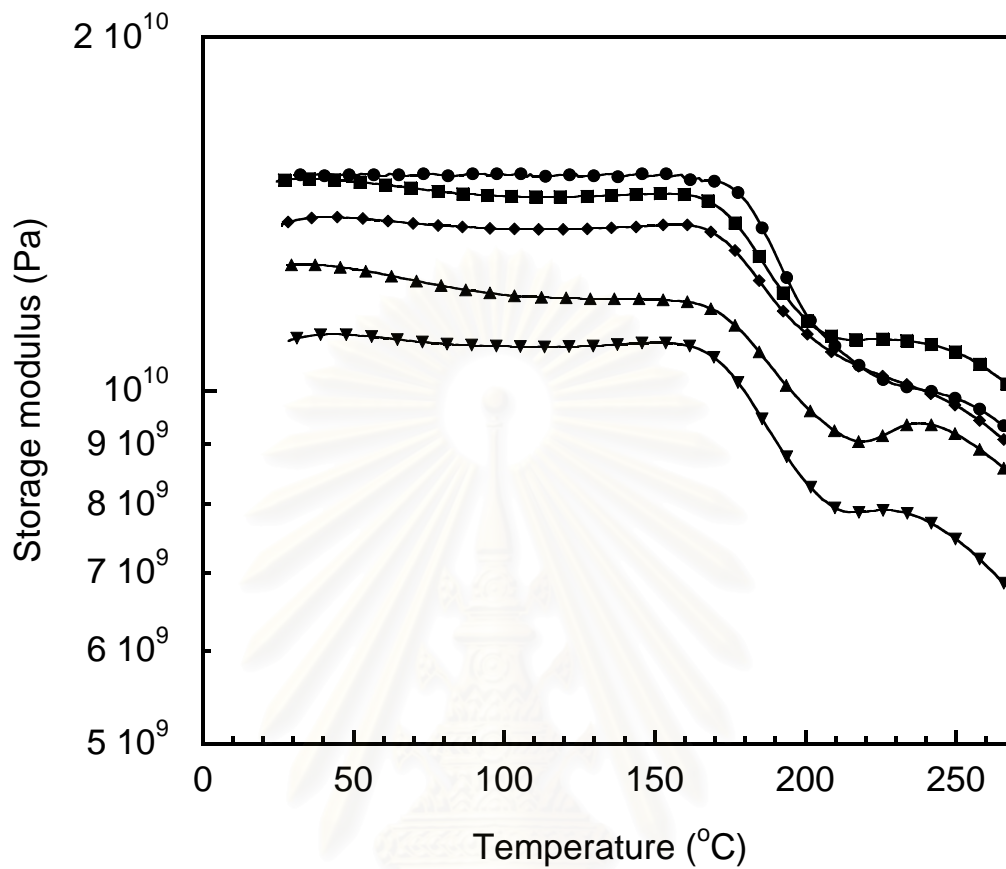
Figure 5.22: Storage modulus of Kevlar[TM]-reinforced nano-SiO$_2$ filled polybenzoxazine composites at different SiO$_2$ contents: (●) neat polybenzoxazine (PBZ), (■) 1% nano-SiO$_2$ filled PBZ, (♦) 3% nano-SiO$_2$ filled PBZ, (▲) 5% nano-SiO$_2$ filled PBZ, (▼) 7% nano-SiO$_2$ filled PBZ.
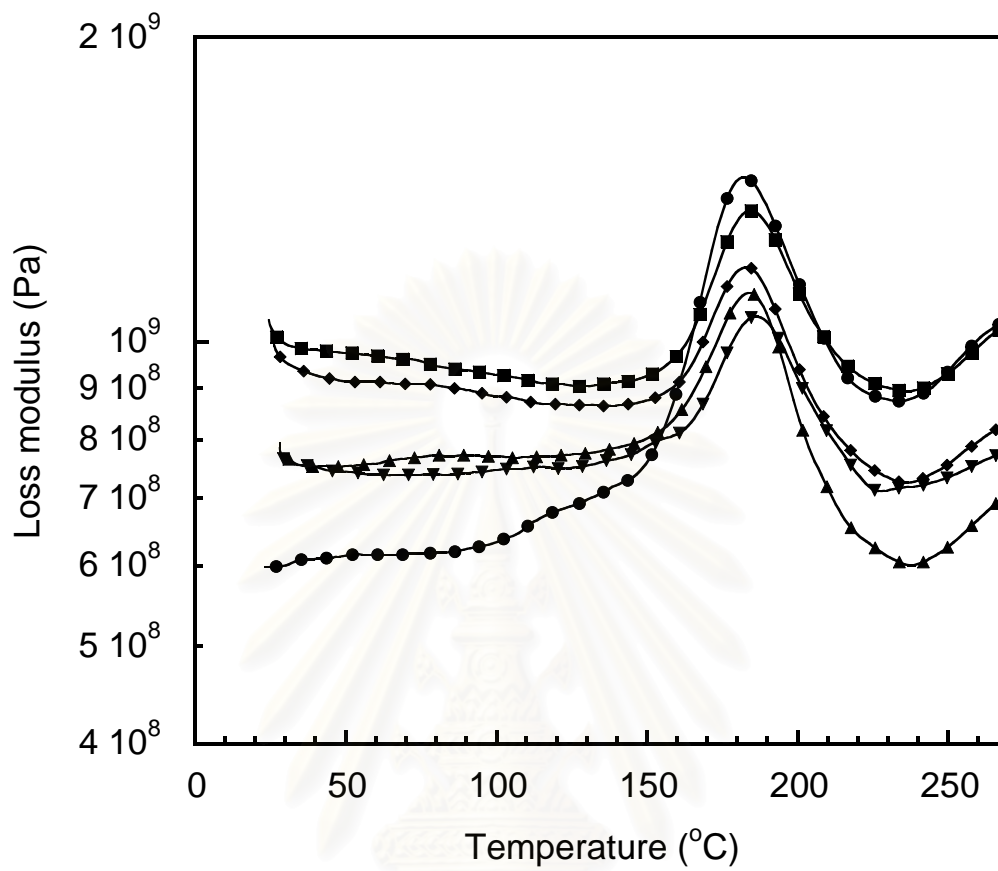
Figure 5.23: Loss modulus of Kevlar[TM]-reinforced nano-SiO$_2$ filled polybenzoxazine
composites at different SiO$_2$ contents: (●) neat polybenzoxazine
(PBZ), (■) 1% nano-SiO$_2$ filled PBZ, (♦) 3% nano-SiO$_2$ filled PBZ,
(▲) 5% nano-SiO$_2$ filled PBZ, (▼) 7% nano-SiO$_2$ filled PBZ.
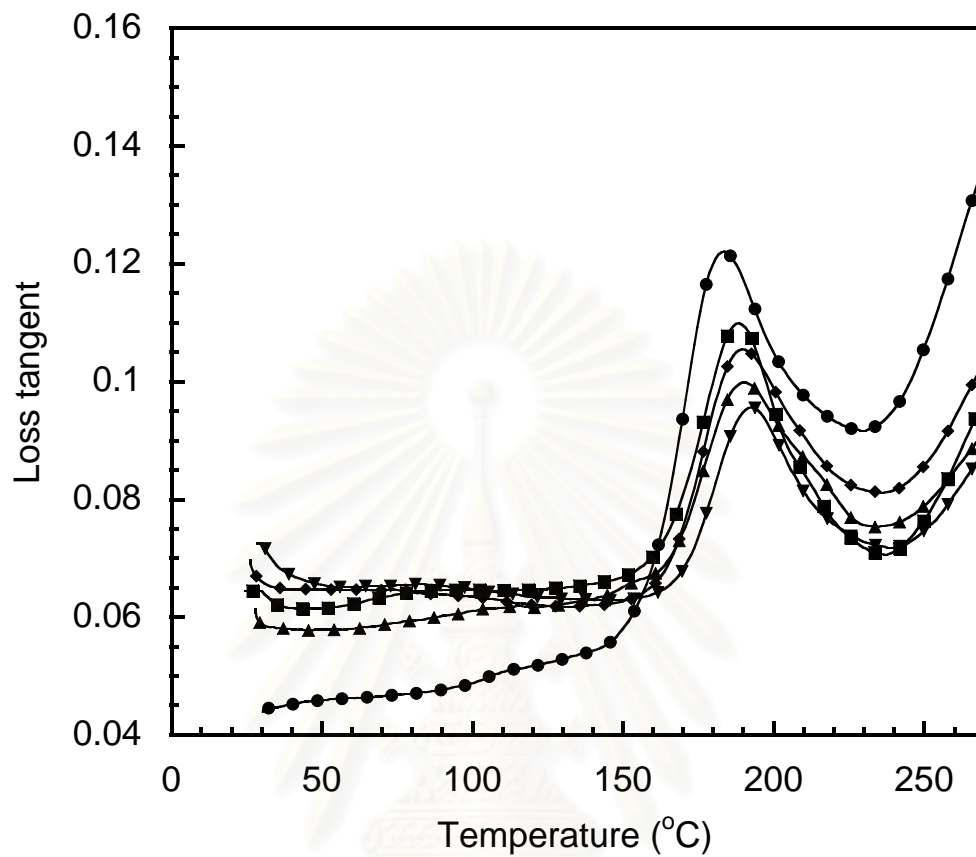
Figure 5.24: Loss tangent of Kevlar^{TM}-reinforced nano-SiO$_2$ filled polybenzoxazine composites at different SiO$_2$ contents: (●) neat polybenzoxazine (PBZ), (■) 1% nano-SiO$_2$ filled PBZ, (♦) 3% nano-SiO$_2$ filled PBZ, (▲) 5% nano-SiO$_2$ filled PBZ, (▼) 7% nano-SiO$_2$ filled PBZ.

Table 5.3: Low level ballistic impact test results of the composites at various matrix compositions

Number	Type of Matrix	Number of Plies Plate1+Plate2	Resistance to Penetration	
			Plate 1	Plate 2
1	Kevlar fiber	5+5	No	No
2	Epoxy 200	5+5	No	No
	Epoxy 400	5+5	No	No
3	Pure PBZ	5+5	No	Yes
	Pure PBZ	5+5	No	Yes
4	1%SiO$_2$/PBZ	5+5	No	Yes
	1%SiO$_2$/PBZ	5+5	No	Yes
5	3%SiO$_2$/PBZ	5+5	Yes	Yes
	3%SiO$_2$/PBZ	5+5	Yes	Yes
6	5%SiO$_2$/PBZ	5+5	Yes	Yes
	5%SiO$_2$/ PBZ	5+5	Yes	Yes
7	7%SiO$_2$/PBZ	5+5	Yes	Yes
	7%SiO$_2$/PBZ	5+5	Yes	Yes
8	7%SiO$_2$/PBZ / PBZ	5+5	Yes	Yes
	7%SiO$_2$/PBZ / PBZ	5+5	Yes	Yes
	7%SiO$_2$/PBZ / PBZ	5+5	Yes	Yes

Note: No = can not resist penetration
Yes = can resist penetration
PBZ = polybenzoxazine
SiO$_2$/PBZ = fumed silica filled-polybenzoxazine

Table 5.4: Damage properties of Kevlar^{TM}-reinforced composites with low level ballistic impact test

Type of Matrix	Damage Dimension of Rear Plate of the Composite		Damage Dimension of the Clay Witness		
	Depth (mm)	Diameter (mm)	Depth (mm)	Diameter (mm)	Volume (ml)
Kevlar fiber	-	-	-	-	-
Epoxy 200	-	-	-	-	-
Epoxy 400	-	-	-	-	-
BA-a pure	15.71	64.3	25.0	68.2	32.2
1%SiO$_2$/PBZ	14.98	63.5	26.9	66.1	30.0
3%SiO$_2$/PBZ	12.79	59.5	23.3	64.5	29.5
5%SiO$_2$/PBZ	11.41	57.5	22.8	67.0	31.2
7%SiO$_2$/PBZ	11.27	55.3	21.6	68.6	26.5
7%SiO$_2$/PBZ/PBZ	13.52	61.7	26.6	65.1	33.8

Note: No = can not resist penetration
Yes = can resist penetration
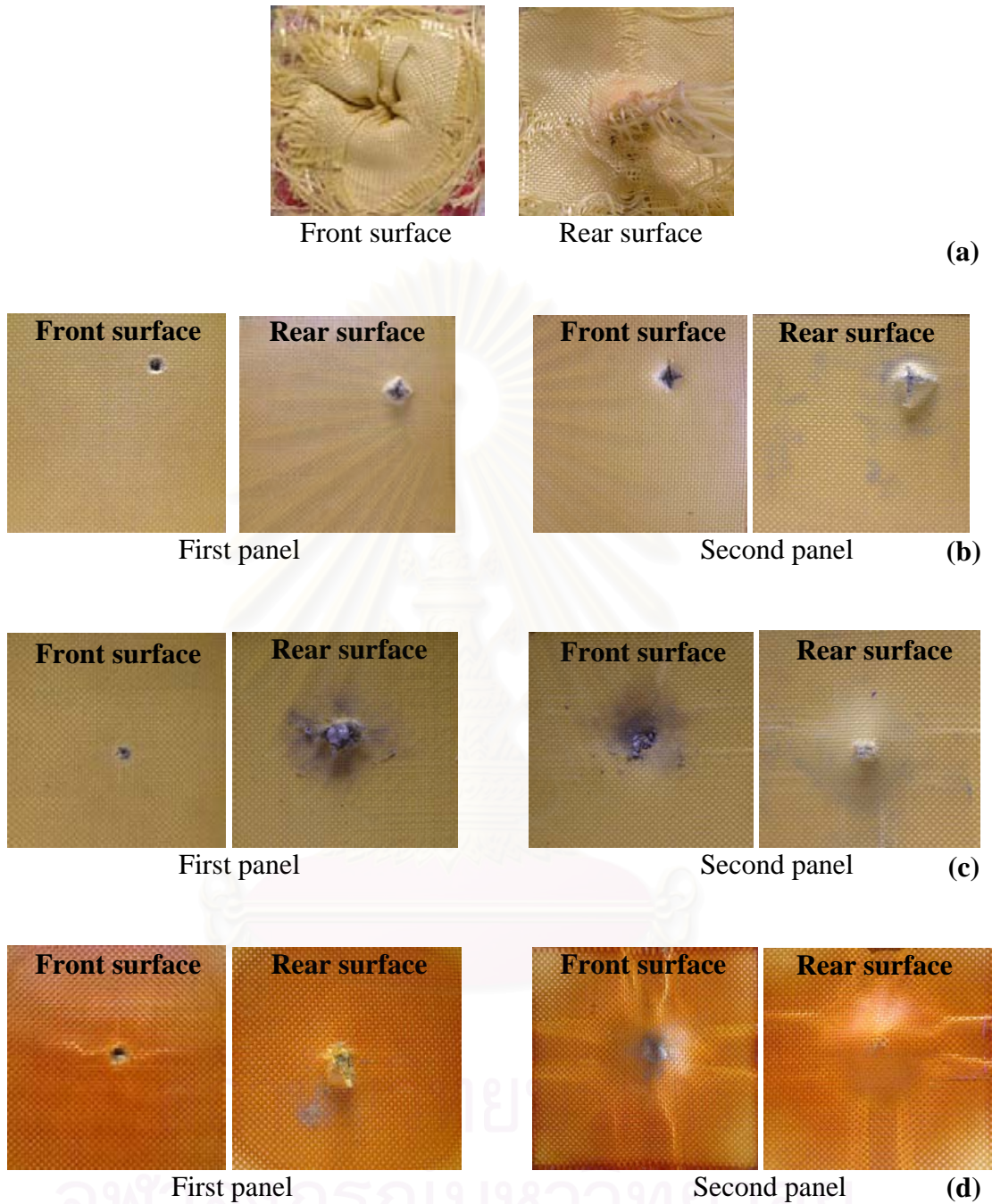
Figure 5.25 (a): Damaged and delaminated area of 5 piles/panel with the sample arrangement of 5/5 after impact with lead projectiles with lead outer-coating typically used in 9 mm: (a) Kevlar^{TM} fiber, (b) Kevlar^{TM}-reinforced flexible epoxy, (c) Kevlar^{TM}-reinforced hard epoxy, (d) Kevlar^{TM}-reinforced PBZ.
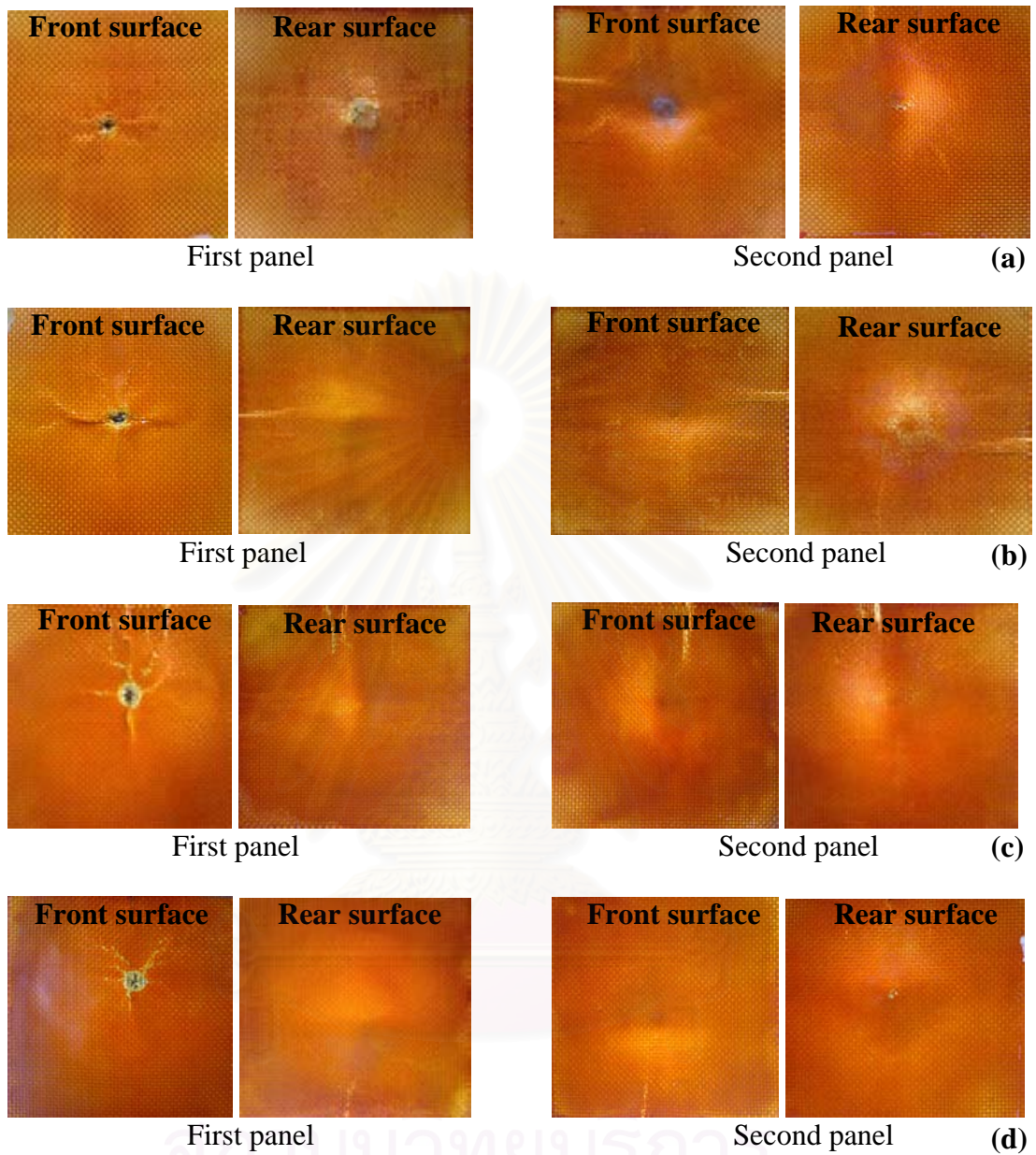
Figure 5.25 (b): Damaged and delaminated area of 5 piles/panel with the sample arrangement of 5/5 after impact with lead projectiles with lead outer-coating typically used in 9 mm: (a) Kevlar^{TM}-reinforced 1wt% nano-SiO2 filled PBZ, (b) Kevlar^{TM}-reinforced 3wt% nano-SiO2 filled PBZ, (c) Kevlar^{TM}-reinforced 5wt% nano-SiO2 filled PBZ, (d) Kevlar^{TM}-reinforced 7wt% nano-SiO2 filled PBZ.
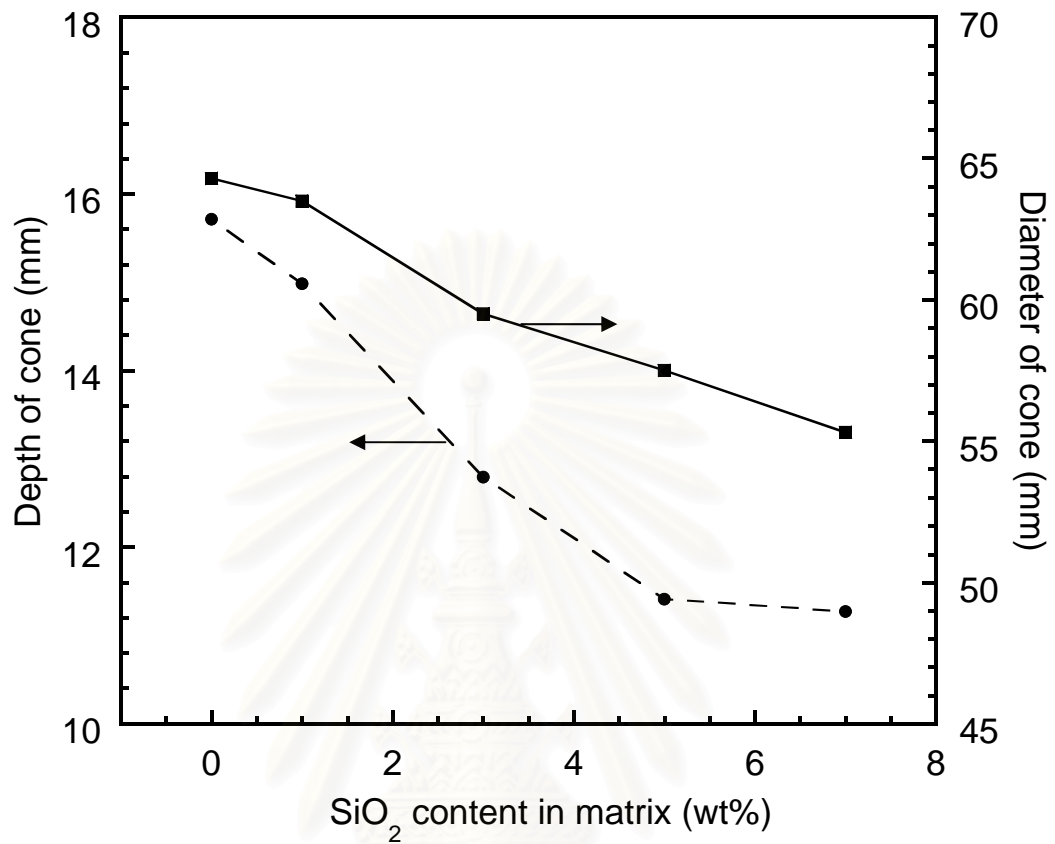
Figure 5.26: Depth and Diameter of after fired delamination area of the Kevlar[TM]-reinforced nano-SiO$_2$ filled polybenzoxazine composites at various matrix compositions (●) Depth of cone, and (■) Diameter of cone.

PBZ   1% SiO$_2$ 3% SiO$_2$

5% SiO$_2$ 7% SiO$_2$
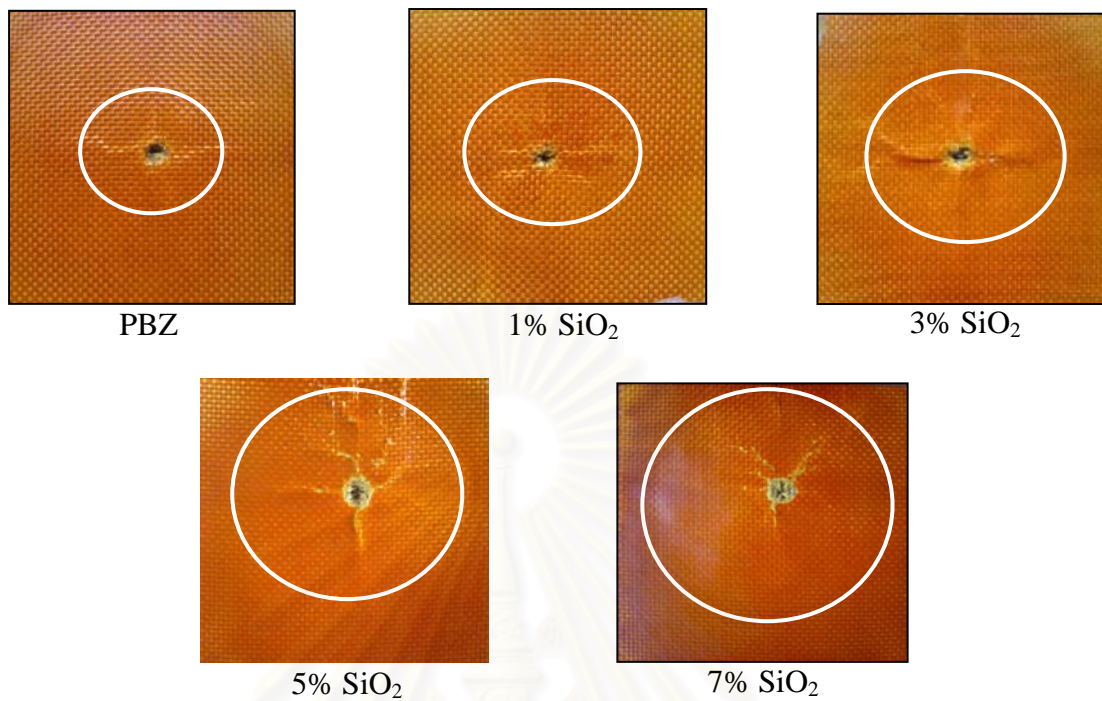
(a)
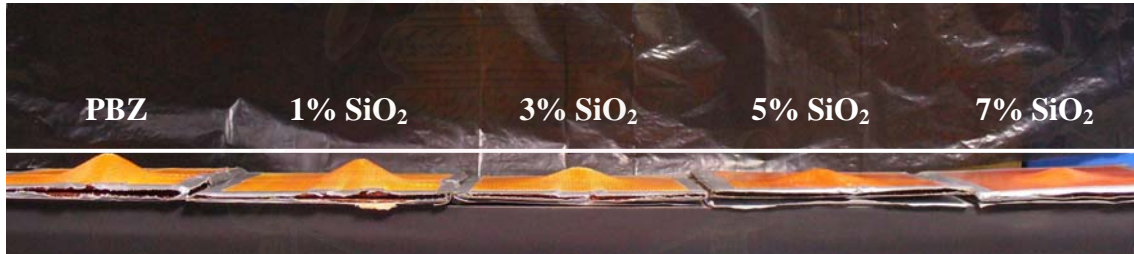
(b)

Figure 5.27: Comparison of damaged and delaminated area of 5 piles/panel with the sample arrangement of 5/5 after impact with lead projectiles with lead outer-coating typically used in 9 mm: (a) front surface of Kevlar[TM]-reinforced nano-SiO$_2$ filled polybenzoxazine composite, and (b) rear surface of Kevlar[TM]-reinforced nano-SiO$_2$ filled polybenzoxazine composite.

Table 5.5: Effect of number of piles and panel arrangement of Kevlar™-reinforced 7wt% nano-SiO2 filled polybenzoxazine composite after ballistic impact with NIJ standard, level IIIA.

Number of Layers of Composite	Impact Velocity (m/s)	Resistance to Penetration		Damage Dimension of the Clay Witness	
		1st	2nd	Diameter (mm)	Depth (mm)
15+5+5	453.64	No	No	-	-
15+10	448.53				
15+5+5+5	451.10	No	No	-	-
15+10+5	448.00	No	Yes	102.3	38.2
10+10+5+5+5	446.90	No	Yes	116.5	35.6
15+5+5+5+5	454.86	No	Yes	110.0	35.3
15+10+5+5	444.67	No	Yes	100.3	34.8

Note: No = can not resist penetration
       Yes = can resist penetration
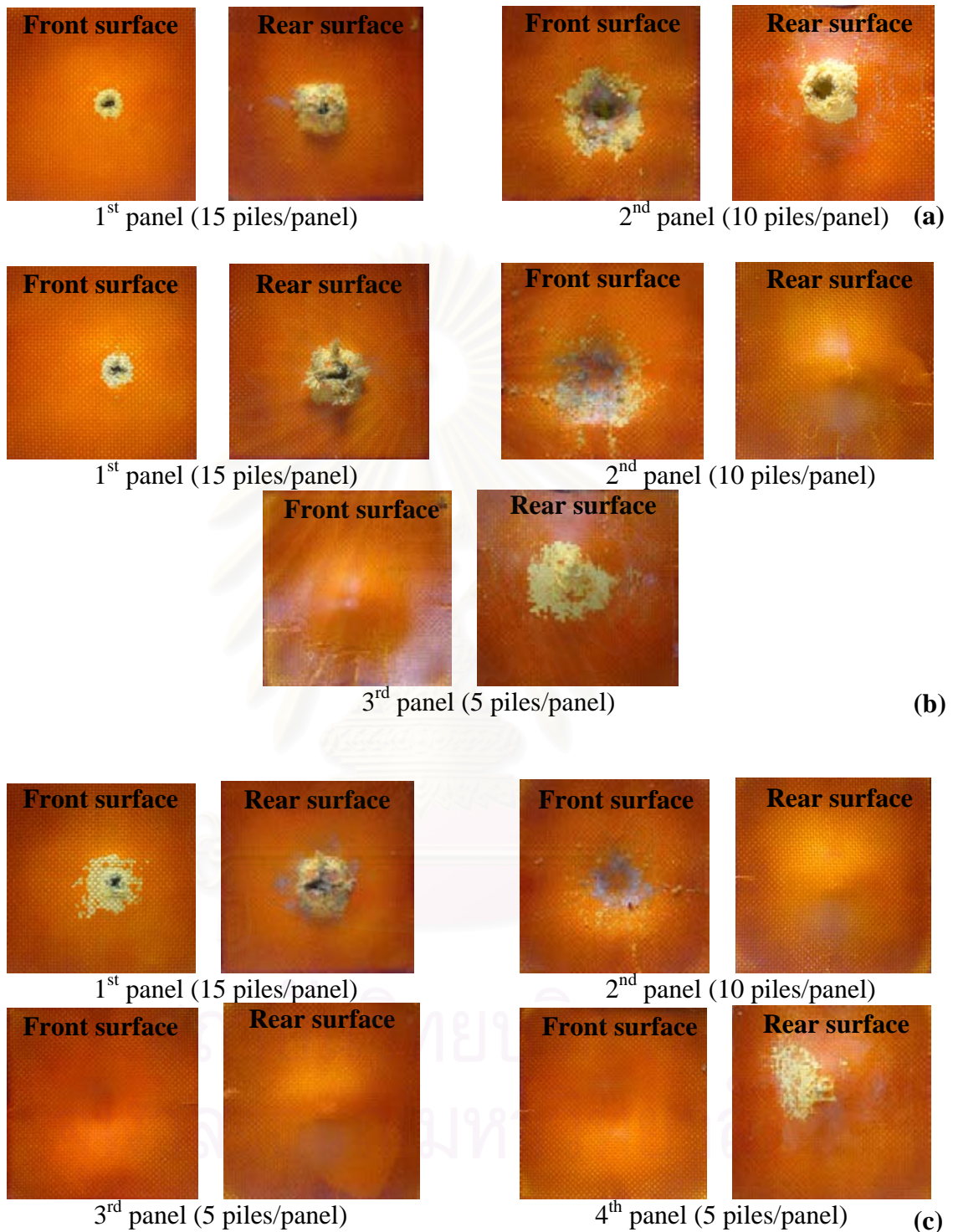
Figure 5.28: Damaged and delaminated area of sample after impact with projectiles velocities which required by NIJ standard, level III-A (.44 Magnum): (a) 30/20, (b) 30/20/10, (c) 30/20/10/10.
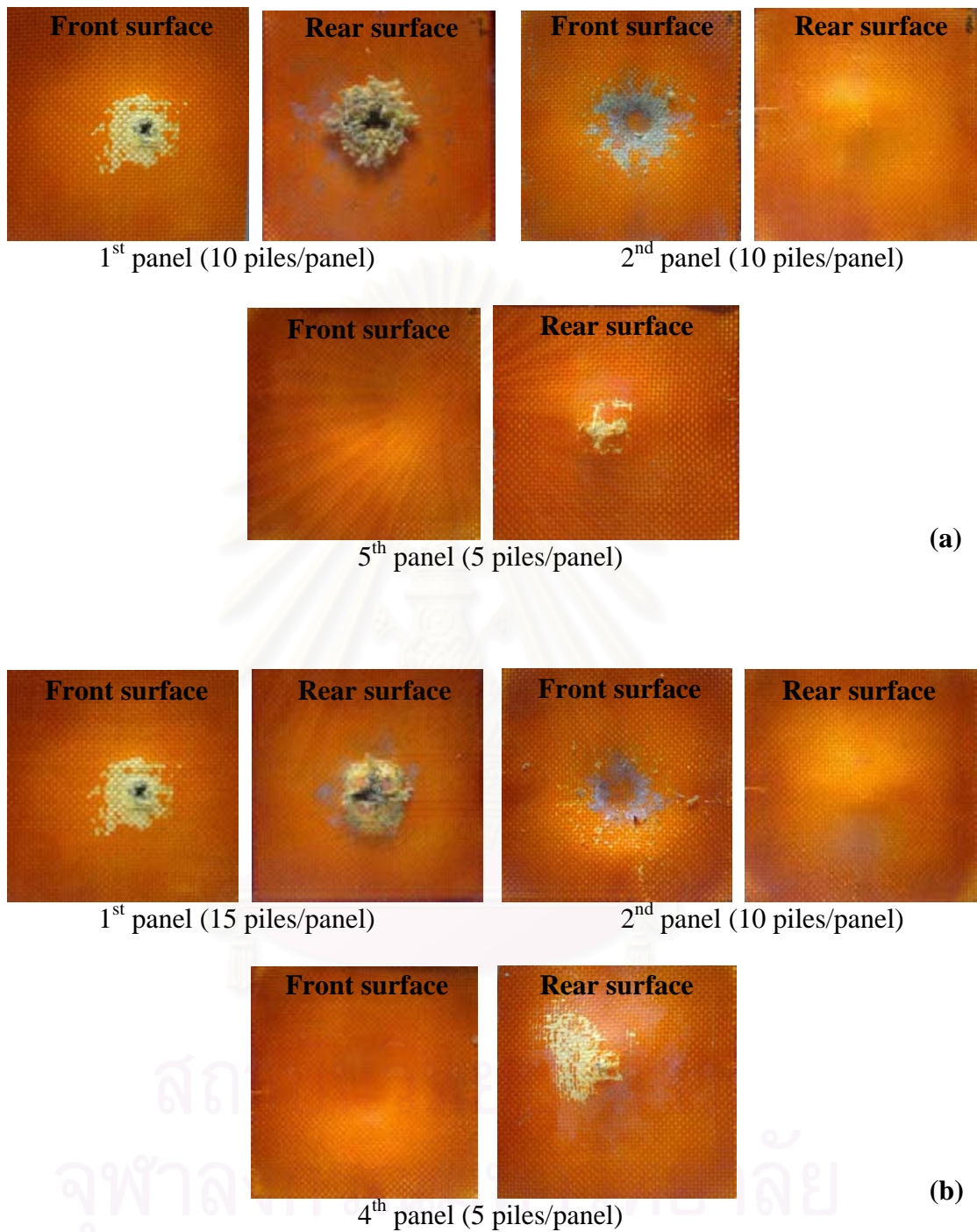
Figure 5.29: Damaged and delaminated area of sample after impact with projectiles velocities which required by NIJ standard, level III-A, (.44 Magnum): (a) 10/10/5/5/5, (b) 15/10/5/5.

Before impact

After impact (PBZ)   After impact (1%SiO$_2$)

(a)

Before impact

After impact (10/10/5/5/5)   After impact (15/10/5/5)

(b)
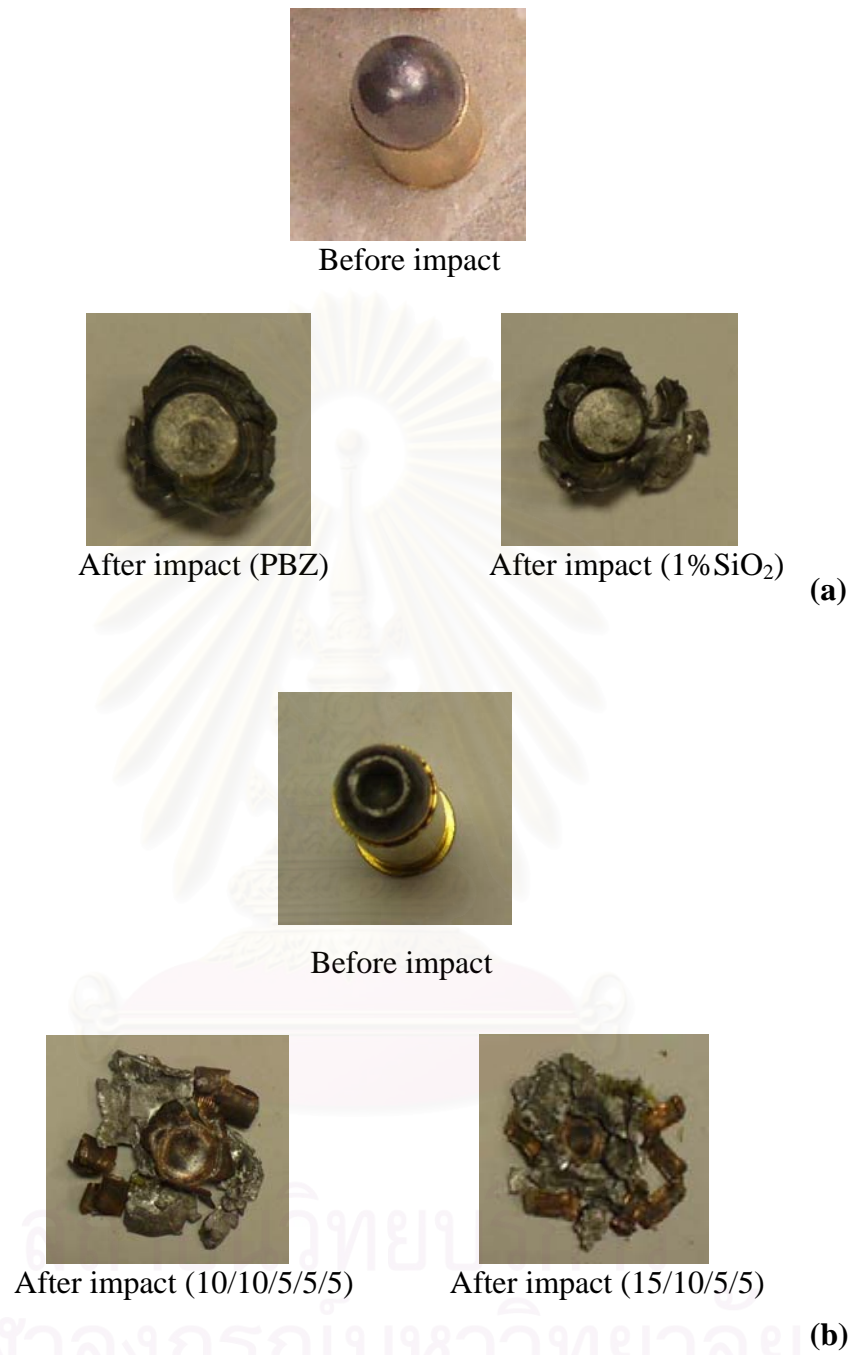
Figure 5.30: Projectiles before and after impact against of the laminate composite: (a) low ballistic test (9 mm handgun), (b) high ballistic impact test of NIJ standard, level III-A (.44 Magnum).

CHAPTER VI

CONCLUSIONS

In the composite of the Kevlar^{TM}-reinforced nano-SiO$_2$-filled polybenzoxazine, the SiO$_2$ content, processing condition and fiber content were investigated to achieve the most effective ballistic properties for ballistic armor applications. The essential characterizations in this study include processability, thermal stability, mechanical properties of the matrices, as well as ballistic impact resistance of the obtained composite materials.

The DSC experiment revealed that the optimal curing condition to obtain the fully-cured specimens of the SiO$_2$/PBZ composites was by heating at 160°C for 2 hours and 180°C for 2 hours (in a hydraulic hot-pressed machine at 25 MPa) followed by post-curing at 200°C for 4 hours (in an oven). The mechanical and thermal properties of nano-SiO$_2$-filled polybenzoxazine composites at different SiO$_2$ contents in the range 0 to 10 wt% tended to increase with increasing SiO$_2$ content. The actual density of composites was measured to be close to the theoretical one suggesting small amount of void was presented in the composite. The glass transition temperature of fumed silica filled polybenzoxazine tended to increase with increasing the SiO$_2$ contents, which was possibly due to the substantial bonding between the polymer and the filler. The degradation temperatures (at 5% weight loss under oxygen atmosphere) of the composites were found to slightly increase with increasing the SiO$_2$ contents. Moreover, the amount of solid residue at 800°C in air indicated the actual weight of the nano-SiO$_2$ in the composite and was consistent with the amount of SiO$_2$ added in the matrix during molding compound preparation.

The flexural modulus of composite was significantly improved by the presence of the SiO$_2$ even at the only few percent of the filler. Furthermore, the flexural strength of composites exhibited a decreasing trend with the addition of the

SiO_2 nano-filler. Additionally, the storage modulus of the composite also exhibited the similar trend with the flexural modulus.

In the fire test of the 10-ply Kevlar[TM]-reinforced SiO_2/PBZ composites, the low level ballistic test (using 9 mm handgun with standard gain of a round lead projectile with lead outer coating) showed that the 7%SiO_2/PBZ as a matrix exhibited the optimum ballistic impact resistance than the other compositions. In addition, the areal density of the composite was 0.24 g/cm^2 (5 piles/panel). The ballistic test results based on NIJ standard (level III-A) suggested that the thickness of composite specimen and the arrangement of the composite panels were important for the ballistic protection. The ballistic impact test results indicated that the suitable thickness of 60 piles of the Kevlar[TM] cloth can successfully protect the ballistic impact at level III-A. Furthermore, the arrangement of composite panels also suggested that at least 15 piles in thickness of the composite panel should be placed as a front plate in order to sufficiently deform the projectile of this impact level and to show the outstanding ballistic performance of the composite.

REFERENCES

Barthel, H.; Heinemann, M.; Stintz, M.; and Wessely, B., "Particle sizes of fumed silica," Part. Part. Syst. Charact. 16 (1999): 169.

Barthel, H., "Fumed silica: Rheological additive for adhesives, resin, and paints," Macromol. Symp. 187 (2002): 73.

Cheeseman, B.A.; and Bogetti, T.A., "Ballistic impact into fabric and compliant composite laminates," Composite Structure 61(2003): 161.

Coppage, Jr.; Edward, A.; and Richard, W., "Anti-ballistic protective composite fabric," U.S. Patent 6,127,291 (2000).

David, S.C., "Armor Systems," U.S. Patent 6,276,254 B1 (2001).

Dickson, L.J.; and Blake, D.I., "Ballistic Armor Laminate," U.S. Patent 5,851,932 (1998).

Ellis, R.L., "Ballistic Impact Resistance of Graphite Epoxy Composites with Shape Memory Alloy and Extended Chain Polyethylene Spectra[TM] Hybridge Components," Virginia, Blacksburg, (1996).

Harper, C.A., "Handbook of Plastics Elastomer and Composites," New York, McGraw-Hill, (1996).

Harry, S.K., "Handbook of Fillers for Plastics," U.S.A.: Van Nostrand Reinhold, (1987).

Hartman, D.R.; Jutte, R.B.; and Ramey, T.W., "Ballistic Material," U.S. Patent 5,215,813 (1993).

Hartman, D.R.; Jutte, R.B.; Beaver, T.R.; and Hill, H.G., "Process for Forming Flat Plate Bllistic Resistant Materials," U.S. Patent 5,006,293 (1991).

Hearle, J.W.S., "High-performance fibres," U.S.A.:Woodhead publishing Ltd., (2000).

Ishida, H.; and Allen, D.J., "Physical and mechanical characterization of near-zero shrinkage polybenzoxazines," J. Polym Sci. 34 (1996): 1019.

Ishida, H.; and Allen, D.J., "Mechanical characterization of copolymers based on benzoxazine and epoxy," Polymer 37 (1996): 4487.

Ishida, H., "Process of benzoxazine compounds in solventless systems," U.S. Patent 5,543,516 (1996).

Ishida, H.; and Rimdusit S. "Very high thermal conductivity obtained by boron nitride filled polybenzoxazine," Thermochim. acta. 320 (1998): 177.

Jacob, M.J.N.; and Dingenen, J.L.J.V., "Ballistic ProtectionM in Personal Armor," J. Mater. Sci. 36 (2001): 3137.

Jana, S.C.; and Jain, S., "Dispersion of nanofillers in high performance polymers using reactive solvents as processing aids," Polymer 42 (2001): 6897.

Jang, J.; and Shin S. "Cure studies of a benzoxazine based phenolic resin by isothermal experiment," Polym. J. 27 (1995): 601.

Kroschwitz, J.L., "High Performance Polymers and Composites," Canada, John Wiley & Sons, Inc., (1991).

Morye, S.S.; Hine, P.J.; Duckett, R.A.; Carr, D.J.; and Ward, I.M., "Modelling of the energy absorption by polymer composites upon ballis impact," Compos. Sci. Technaol. 60 (2000): 2631.

Naik, N.K.; and Shrirao, P., "Composite structures under ballistic impact," Composite Structures 66 (2004): 579.

Ning, X.; and Ishida, H., "Phenolic Materials Via Ring-Opening Polymerization of Benzoxazines: Effect of Molecular Structure on Mechanical and Dynamic Mechanical Properties," J. Polym. Sci., Polym. Phys. Ed. 32 (1994): 921.

Nunes, L.M.; Paciornik, S.; Almeida, J.R.M., "Evaluation of the damage aera of glas-fiber-reinforced epoxy-matrix composite materials submitted to ballistic impacts" Compos. Sci. Technaol. 64 (2004): 945.

Park, A.D., "Lightweight soft body-armor product" U.S. Patent 6,651,543 (2003).

Park, A.D., "Ballistic laminate structure in sheet form" U.S. Patent 5,395,678 (1996).

Park, A.D., "Method for fabricating a ballistic laminate structure" U.S. Patent 5,547,536 (1999).

Pathomsap, S., "The Development of Ballistic Armor from Kevlar[TM] Fiber and Benzoxazine Alloys," Master Dissertation, Graduate School, Chulalongkorn University, (2005).

Perez-Liminana, M.A.; Torro-Palau, A.; Orgiles-Barcelo, A.C.; and Martin-Martinez, J.M., "Modification of the rheological properties of polyurethanes by adding fumed silica: Influence of the preparation procedure," Macromol. Symp. 194 (2003): 161.

Piyawan, T., "Study of Natural Fiber/Polymer Composite from Bamboo," Master Dissertation, Graduate School, Chulalongkorn University, (1998).

Preghenella, M., Pegoretti, A., and Migliaresi, C., "Thermo-mechanical characterization of fumed silica-epoxy nanocomposites," Polymer 46 (2005): 12065.

Reynaud, E.; Jouen, T.; Gauthier, C.; Vigier, G.; and Varlet, J., "Nanofillers in polymeric matrix: a study on silica reinforced PA6," Polymer 42 (2001): 8759.

Rimdusit, S. and Ishida, H. "Development of new class of electronic packaging materials based on ternary systems of benzoxazine, epoxy, and phenolics resins," Polymer 41(2000): 7941.

Rimdusit, S. and Ishida, H. "Synergism and multiple mechanical relaxation observed in ternary systems based on benzoxazine, epoxy, and phenolic resins," J. Polym. Sci. Pol. Phy. 38 (2000): 1687.

Takeichi, T., Zeidam, R., and Agag, T., "Polybenzoxazine/clay hybrid nanocomposites: influence of preparation method on the curing behavior and properties of polybenzoxazine," Polymer 43 (2002): 45.

Tanoglu, M.; McKnight, S.H.; Palmese, G.R.; Gillespie, J.W., "The effects of glass fiber sizing on the strength and energy absorption of the fiber/matrix interphase under high loading rates," Compos. Sci. Technol. 61(2001): 205.

Tyrone, L., and Turbak, A.F., "High-Tech Fibrous Materials," Washington, DC, American Chemical Society, (1991).

Scheirs, J., "Compositional and Faiilure Analysis of Polymers," Australia: Wiley & Sons, Ltd., (2000).

Shirono, H.; Amano Y.; Kawaguchi M.; and Kato T., "Characteristics of alkyltrimethoxysilane-treated fumed silicas and rheological behavior of fumed silica suspensions in an epoxy resin," J. Colloid and Interface Sci. 239 (2001): 555.

Wu, C.L., Zhang M.Q., Rong M.Z., and Friedrich K., "Silica nanoparticles filled polypropylene: effects of particle surface treatment, matrix ductility and particle species on mechanical performance of the composites," Compos. Sci. Technaol. 65 (2005): 635.

Yang, H.H., "Kevlar^{TM} aramid fiber," West Sussex, John Wiley & Sons Ltd., (1993).

Zhang, H.; Zhang, Z.; Friedrich, K.; Eger, C., "Property improvements of in situ epoxy nanocomposites with reduced interparticle distance at high nanosilica content," Acta Materialia 54 (2006): 1833.

Zhang, W.; Blackburn, R.S.; and Dehghani-Sanij, A.A., "Effect of silica Concentration on electrical conductivity of epoxy resin-carbon black-silica nanocomposites," Scripta materialia 56 (2007): 581.

Zheng, Y.; Zheng, Y.; and Ning, R., "Effects of nanoparticles SiO_2 on the performance of nanocomposites," Materials Letters 57 (2003): 2940.

APPENDICES

APPENDIX A

Characterization of Nano-SiO$_2$ filled Polybenzoxazine Composites

Appendix A-1 Glass transition temperature of nano-SiO$_2$ filled polybenzoxazine composites.

SiO$_2$ content	Glass transition temperature (^{o}C)	
	DSC	DMA
0	160	157
1	160	162
3	161	163
5	162	164
7	163	165
10	165	167

Appendix A-2 Degradation temperature of nano-SiO$_2$ filled polybenzoxazine composites.

Resin	Degradation Temperature (^{o}C)		Char Yield (%)
	5% weight loss	10% weight loss	
PBZ	348	376	0.4
1% SiO$_2$/PBZ	352	378	1.1
3% SiO$_2$/PBZ	355	380	3.5
5% SiO$_2$/PBZ	356	382	5.0
7% SiO$_2$/PBZ	358	383	7.8
10% SiO$_2$/PBZ	360	384	9.4

Appendix A-3 Density of the distilled water at the give temperature (g/cm^3).

T (°C)	0.0	0.1	0.2	0.3	0.4	0.5	0.6	0.7	0.8	0.9
10	0.99973	0.99972	0.99971	0.9997	0.99969	0.99968	0.99967	0.99966	0.99965	0.99964
11	0.99963	0.99962	0.99961	0.9996	0.99959	0.99958	0.99957	0.99956	0.99955	0.99954
12	0.99953	0.99951	0.99950	0.99949	0.99948	0.99947	0.99946	0.99944	0.99943	0.99942
13	0.99941	0.99939	0.99938	0.99937	0.99935	0.99934	0.99933	0.99931	0.99930	0.99929
14	0.99927	0.99926	0.99924	0.99923	0.99922	0.99920	0.99919	0.99917	0.99916	0.99914
15	0.99913	0.99911	0.99910	0.99908	0.99907	0.99905	0.99904	0.99902	0.99900	0.99899
16	0.99897	0.99896	0.99894	0.99892	0.99891	0.99889	0.99887	0.99885	0.99884	0.99882
17	0.99880	0.99879	0.99877	0.99875	0.99873	0.99871	0.9987	0.99868	0.99866	0.99864
18	0.99862	0.99860	0.99859	0.99857	0.99855	0.99853	0.99851	0.99849	0.99847	0.99845
19	0.99843	0.99841	0.99839	0.99837	0.99835	0.99833	0.99831	0.99829	0.99827	0.99825
20	0.99823	0.99821	0.99819	0.99817	0.99815	0.99813	0.99811	0.99808	0.99806	0.99804
21	0.99802	0.99800	0.99798	0.99795	0.99793	0.99791	0.99789	0.99786	0.99784	0.99782
22	0.99780	0.99777	0.99775	0.99773	0.99771	0.99768	0.99766	0.99764	0.99761	0.99759
23	0.99756	0.99754	0.99752	0.99749	0.99747	0.99744	0.99742	0.99740	0.99737	0.99735
24	0.99732	0.99730	0.99727	0.99725	0.99722	0.99720	0.99717	0.99715	0.99712	0.99710
25	0.99707	0.99704	0.99702	0.99699	0.99697	0.99694	0.99691	0.99689	0.99686	0.99684
26	0.99681	0.99678	0.99676	0.99673	0.99670	0.99668	0.99665	0.99662	0.99659	0.99657
27	0.99626	0.99623	0.9962	0.99617	0.99614	0.99612	0.99609	0.99606	0.99603	0.99600
28	0.99597	0.99594	0.99591	0.99588	0.99585	0.99582	0.99579	0.99576	0.99573	0.99570
29	0.99597	0.99594	0.99591	0.99588	0.99585	0.99582	0.99579	0.99576	0.99573	0.99570
30	0.99567	0.99564	0.99561	0.99558	0.99555	0.99552	0.99549	0.99546	0.99543	0.99540

Appendix A-4 Density of nano-SiO$_2$ filled polybenzoxazine composite.

SiO$_2$ content (wt%)	Actual density (g/cm^3)	Theoretical density (g/cm^3)
0	1.1879	1.1900
1	1.1916	1.1955
3	1.2022	1.2068
5	1.2130	1.2185
7	1.2320	1.2298
10	1.2430	1.2479

Appendix A-5 Mechanical properties of nano-SiO$_2$ filled polybenzoxazine composite

SiO$_2$ content (wt%)	Flexural modulus (GPa)	Storage modulus (GPa)
0	5.98±0.4	4.82
1	6.47±0.4	5.18
3	6.74±0.1	5.78
5	7.32±0.7	6.61
7	7.52±0.3	7.19
10	7.52±0.2	7.36

Appendix A-6 Vickers microhardness at 100 gf of nano-SiO$_2$ filled polybenzoxazine composite

SiO$_2$ content (wt%)	HV (MPa)
0	368.2
1	377.5
3	396.7
5	437.1
7	462.8
10	481.1

APPENDIX B

Characterization of Kevlar^{TM}-reinforced Nano-SiO$_2$ filled Polybenzoxazine Composites

Appendix B-1 Glass transition temperature of Kevlar^{TM}-reinforced nano-SiO$_2$/PBZ composites (from DMA thermogram)

Nano-SiO$_2$/PBZ System Compositions	Glass Transition Temperature (^{o}C)
PBZ	182
1%SiO$_2$/PBZ	183
3%SiO$_2$/PBZ	184
5%SiO$_2$/PBZ	185
7%SiO$_2$/PBZ	186

Appendix B-2 Mechanical properties of Kevlar^{TM}-reinforced nano-SiO$_2$/PBZ composite as a function of SiO$_2$ content in matrix

SiO$_2$ content (wt%)	Flexural modulus (GPa)	Storage modulus (GPa)
0	17.9±2.5	15.26
1	17.5±2.2	15.06
3	17.1±1.7	13.82
5	16.5±1.1	12.77
7	15.2±0.3	11.01

Appendix B-3 Degradation temperature of Kevlar^{TM}-reinforced nanoSiO$_2$/PBZ
composite as a function of SiO$_2$ content in matrix

SiO$_2$ content (wt%)	Degradation temperature at 5% weight loss (^{o}C)
0	338
1	340
3	344
5	350
7	360

VITA

Ms. Kanokwan Punson was born in Sukhothai, Thailand. She graduated at high school level in 1997 from Udomdarunee School. She received the Bachelor's Degree of Science with a major in Chemistry from the Faculty of Science, Meajo University, Thailand in 2001. After graduation, she has 3-year working experience at Pharmaceutical Technology Service Center, Bangkok. She entered study for a Master's Degree of Chemical Engineering at the Department of Chemical Engineering, Faculty of Engineering, Chulalongkorn University.

Some part of this work was selected for oral presentation in The Second International Conference on Recent Advances in Composite Materials Conference which was held during February 20-23, 2007 at India Habitat Center, Lodhi Road, New Delhi, India.